JOURNAL OF ENVIRONMENTAL GEOGRAPHY
Journal of Environmental Geography 6 (3–4), 1–11.
DOI: 10.2478/jengeo-2013-0001
ISSN: 2060-467X

14th-16th-CENTURY DANUBE FLOODS AND LONG-TERM WATER-LEVEL CHANGES IN ARCHAEOLOGICAL AND SEDIMENTARY EVIDENCE IN THE WESTERN AND CENTRAL CARPATHIAN BASIN: AN OVERVIEW WITH DOCUMENTARY COMPARISON

Andrea Kiss[1,2*], József Laszlovszky[3]

[1]Institute of Hydraulic Engineering and Water Resources Management, Vienna University of Technology, Karsplatz 13, 1040 Vienna, Austria
[2] Department of Physical Geography and Geoinformatics, Department of Historical Auxiliary Science, University of Szeged, Egyetem u. 2-6, H-6722 Szeged, Hungary
[3] Department of Medieval Studies, Central European University, Nádor u. 9, H-1051 Budapest, Hungary
*Corresponding author, e-mail: kiss@hydro.tuwien.ac.at

Research article, received 25 March 2013, accepted 4 June 2013

Abstract

In the present paper an overview of published and unpublished results of archaeological and sedimentary investigations, predominantly reflect on 14th-16th-century changes, are provided and evidence compared to documentary information on flood events and long-term changes. Long-term changes in flood behaviour (e.g. frequency, intensity, seasonality) and average water-level conditions had long-term detectable impacts on sedimentation and fluvio-morphological processes. Moreover, the available archaeological evidence might also provide information on the reaction of the society, in the form of changes in settlement organisation, building structures and processes. At present, information is mainly available concerning the 16th, and partly to the 14th-15th centuries. These results were compared to the available documentary evidence on 14th-16th century Danube floods occurred in the Carpathian Basin.

Keywords: Danube, floods, high flood-frequency periods, 14th-16th century, sedimentary and archaeological evidence, Carpathian Basin

INTRODUCTION

The 16th century has key importance in studying and understanding medieval and early modern Danube floods. It is due to the fact that a great number of large and extraordinary flood events are known from the early, and then from the mid and late 16th century which caused severe damages along several Central European rivers (for the last systematic overview, see Brázdil et al., 1999; for extraordinary 16th-century floods in Austria, see: Rohr, 2007), including the Danube.

Due to the fact that recently a first systematic overview of documentary evidence on 14th-16th-century Danube floods in the Carpathian Basin has become mainly available in publications (for 11th-15th century evidence: Kiss, 2012a, 16th-century: Kiss, 2012b; Kiss and Laszlovszky, 2013; partly related Vadas, 2011), it is possible not only to list and discuss sedimentary and archaeological evidence on flood events, but also to find some connections and provide links between the different types of flood- and high water-level related evidence. The results of archaeological and sedimentary investigations are in good agreement with the information detectable in documentary evidence: the presently available material presumably highlights most of the great flood events of extraordinary magnitude and the most important flood waves.

Documentary evidence is mainly related to individual flood events or the relatively short-term consequences of preceding great flood events and therefore mainly provides high-frequency information. Archaeological and sedimentary evidence is mainly connected to the consequences of great or catastrophic flood events, flood-rich periods and long-term hydrological changes. Since dating of these events, periods and processes, with using natural scientific and archaeological methods, are usually possible on a multi-annual, multi-decadal level, archaeological and sedimentary data on floods are good indicators of medium- and low-frequency changes in flood behaviour. Nevertheless, documentary evidence can provide an important help in the possible more exact dating of flood events or flood peaks whose impacts could be observed in archaeological (and sedimentary) evidence (for presently available data, see: *Fig. 1*).

Beyond the application of documentary evidence, with the help of archaeological and sedimentary evidence the magnitude, long-term impacts and (materi-

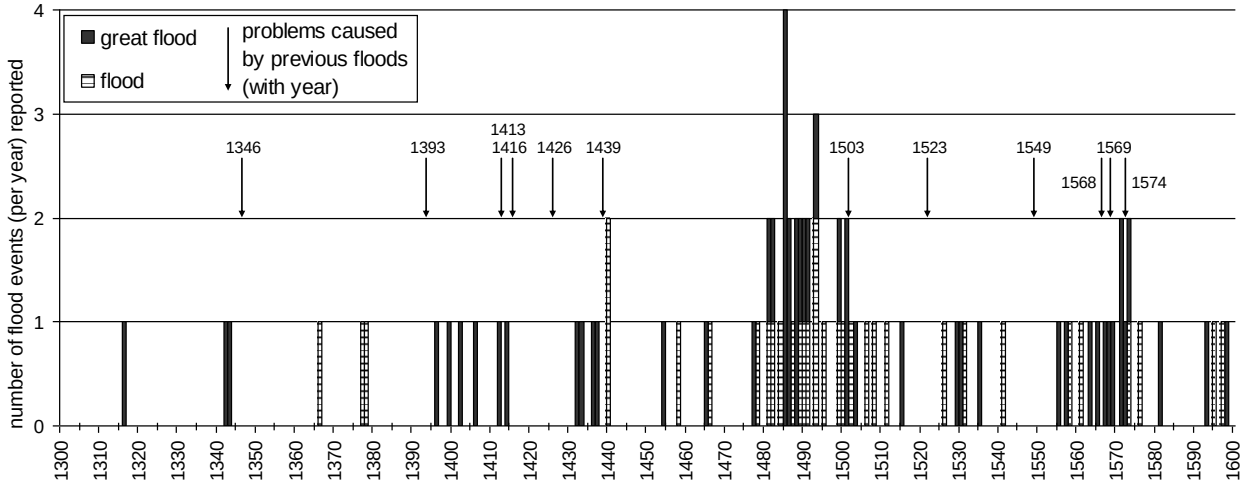

Fig. 1 14th-16th-century Danube floods in the Carpathian Basin, based on presently available documentary evidence (Sources: Kiss, 2012a, 2012b; Kiss and Laszlovszky, 2013)

al) consequences of great flood events as well as general long-term processes can be further studied in more detail.

In the present paper the published materials and scientific literature on findings in the Marchfeld and the Bratislava-Žitný ostrov area (Šamorín), the Danube Bend (Nagymaros, Visegrád, Vác), Budapest (Margit island) either as a source for further investigation (e.g. Dinnyés et al., 1993) or with further environmental interpretations (e.g. Mészáros and Serlegi, 2011) are discussed, and possible connections with documentary evidence are provided. Moreover, unpublished primary results of archaeological excavations, excavation protocols, for example, that of the Visegrád Franciscan friary are also included in the present survey. Most of the archaeological and sedimentary evidence is related to the 16th century: However, most of the processes have started already in the 14th and 15th centuries and therefore these two centuries also form an integrate part of the present discussion.

AVAILABLE SEDIMENTARY-ARCHAEOLOGICAL EVIDENCE: AN OVERVIEW OF SCIENTIFIC INVESTIGATIONS

Mid-16th century: increased Danube sedimentation at Orth – parallel changes on the Lower Morava river?

Due to its immediate vicinity to Bratislava, the available data on 15th-16th-century sedimentation conditions and changes of the Danube has crucial importance in the further understanding of contemporary flood processes. The rapid 16th-century silting-up process of a late medieval harbour, located in a fossil Danube channel, was investigated and results recently published by Fiebing and their colleagues (Fiebig et al., 2009; Thamó-Bozsó et al., 2011). The study area is located south to the town of Orth along the Danube (at the SW edge of the Marchfeld area, a former floodplain), and thus between Vienna and Bratislava (see *Fig. 2*).

Based on the dendrochronology analysis, the wooden remains of the harbour were dated between the 14th-16th centuries. Although some samples date back to the late 14th century (cutting date), most of the construction wood was cut off in the first half of the 16th century (especially between the late 1520s and 1550; see *Fig. 6* in Fiebig et al., 2009). 1550 was defined as a closing date of woods used in the construction of the harbour; the harbour was then covered by flood sediments. Of course, it does not necessary mean that the harbour was immediately given up in 1550 sharp. Nevertheless, the desertion of the harbour must have happened not much later. An interesting additional point is that the Vienna town hospital accounts – which contains information on the Danube floods disturbing or obstructing wood/timber transport – report on a Danube flood in 1548 (WStLA, Bürgerspital Bd. 26; for more source evidence and recent discussion on the consequences in Vienna, see Sonnlechner et al., 2013).

Referring to the age of the deposits (OSL dating) and that of the wooden materials, the authors concluded that a rapid infill (increased sedimentation) of the river branch around the 15th-16th centuries resulted the sudden desertion of the harbour (Thamó-Bozsó et al., 2011). For possible reasons of this rapid infill the authors suggested either the natural process of meander development or the great forest clearances of the late medieval period. In our opinion, a most likely direct factor (for the infill, and in reaching the cut-off of the meander), one or more great Danube floods or high flood frequency of the period, should be also listed among the main reasons of the rapid infill process of the harbour and the Danube channel.

Applying early maps, similar changes from the second half of the 16th-century were also mentioned by hydromorphologists, for example, concerning the cut of a Danube meander at Wolfsthal, probably preceded by a flood event or a series of events (Pišút, 2005; Pišút and Tímár, 2009). The historian, Sándor Takáts (apart from several references on destructive mid and late 16th-century ice flows) also mentioned such a case, namely that a harbour and main toll place, dated from high medieval times, was moved away from its original location

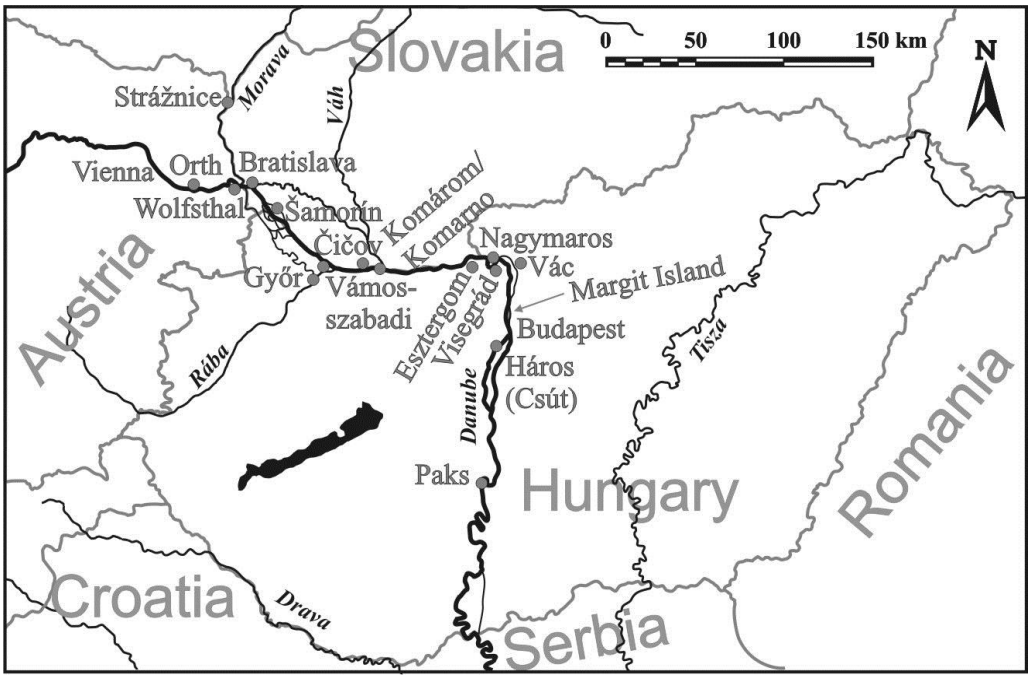

Fig. 2 Locations mentioned in the present paper

to Komárom (from historical Csicsó – today Čičov in Slovakia, in the Žitný ostrov: see *Fig. 1*) in the early 16th century, and its harbour and foreground was filled up with Danube flood sediments (Takáts, 1898).

As a possible parallel, described in an official letter in 1549, short before the Danube at Bratislava also partly changed its bed, and floods were actively damaging the town walls (see Kiss, 1908; for more details see: Kiss, 2012b). Concerning this case, Ortvay (1912) suggested that – similarly to the cases described by Fieber and his colleagues at Orth – an avulsion of the Danube channel occured at Bratislava, and made the town walls (which were anyway in bad condition) more prone to destructive flood events. It is quite probable that this later event had connections to the great 1548 flood in Vienna mentioned above. Moreover, a number of flood events were also reported in contemporary documentation concerning the 1550s, and the great floods occurred practically in each year around the turn of the 1560s and 1570s (see *Fig. 1*).

Another important investigation on river sediments was carried out, practically in the same time, on the lower sections of the Morava River, an important tributary of the Danube, entering the river just before Bratislava. According to the study, a substantial change occurred in the character of flood sedimentation (from clay-dominated layers to layers with more sandy and silty character) around 1550 (and/or the decades around). Prior to this date, the authors also detected another period of increased fluvial activity which, based on the flood catastrophe and its hydromorphological consequences, reconstructed by Bork (1989), they connected to the 14th-century period and the 1342 flood event (Kadlec et al., 2009). In another study concerning the same area it was concluded that two most important changes in river channel structure occurred in the 13th century and in the second half of the 16th century (1550-1600; see Grygar et al., 2011). An interesting additional information might be that, according to Takáts (1898), in 1573 the Morava river left its bed at Ungernsdorf; because of this change, the mills of Marchegg could not be used any more.

Since the Morava River collects the waters in the Moravian Basin, and then enters the Danube close to Bratislava, parallel processes, occurred in the 16th century (especially in the mid 16th century) suggest large-scale changes in the flood behaviour of the river. Moreover, it also suggests that these processes, namely the high flood frequency on the River Morava in the second half of the 16th century, could be detected approximately in the same time on the Danube close to Bratislava (most data in *Fig. 1* is originated from the Bratislava area; see Kiss 2012b) and on its important tributary. Based on documentary evidence, this mid and late 16th-century flood peak was also detected on both the German (e.g. Lech, Isar, partly the Inn; see Böhm-Wetzel, 2006) and the Austrian tributaries of the Danube, and also on the Upper Danube itself (Traun: Rohr, 2006; Danube: Rohr, 2007; Glaser, 2008; Sonnlechner et al., 2013).

It is an interesting, additional information that the importance of the mid and late 16th century in studying historical soil erosion caused by water has not yet been detected in Germany (including Southern Germany). According to the authors of the latest overview, from the high medieval period onwards, only two weak maxima could be traced: one around 1200-1400, with special emphasis on the disastrous 14th-century events culminating around 1342, and another around 2-3 centuries ago, with special emphasis on the late 18th-early 19th century. These interim results, however, might underestimate soil erosion intensity in the medieval and early modern-modern period, due to the low number of dated colluvial layers (see Dreibrodt et al., 2010).

(14th-)16th-century changes in Šamorín: a prosperous town in dangerous location?

In the late medieval town of Šamorín (historical Somorja; see *Fig. 2*) in the Žitný ostrov (historical Csallóköz; island area east to Bratislava, in South-Slovakia) two main building periods were distinguished by archaeological excavations (Urminský, 2005). One of them took place after the destruction of the high medieval wooden structures (in a flood-risk area of Danube branches) in the second half of the 14th century when, together with a change in building material from the wooden-clay structure to brick (at least at the foundations), in the yards of houses (located on a slope descending from the loess terrain) along the main street of the settlement a 0.5 m ground-level rise could be detected. Another turning point occurred around the end of the 15th and beginning of the 16th century. On the main street of the town (Fő utca) new building process was started: in this case the feature of the yards was 'radically' changed: the ground level of the yards was raised with around 1.5 m.

As a documentary parallel, mainly based on the flood-related information preserved in the Bratislava accounts a rather significant flood peak was detected in the late 15th and early 16th century (see *Fig. 1*): starting from the end of the 1470s, in the decades of the 1480s, 1490s and 1500s great and destructive floods and ice flows (and ice floods) occurred at least in every other year, sometimes more than one within a year (e.g. 4 great floods in 1485; for detailed information on documentary evidence, see Kiss and Laszlovszky, 2013). This flood peak, otherwise, quite distinctively appears also on the flood frequency diagrams of the Bavarian Danube tributaries (see Böhm and Wetzel, 2006).

Due to their potential consequences, it is worth to refer to the greatest flood events in particular. In Austria, including the Vienna area, the "deluge" in 1501 (August) was the largest reported flood event on the Danube; it was estimated to be significantly larger than the great flood event of 2002 (e.g. Rohr, 2007; http://www.wien.gv.at), or the ones occurred in 1899 and 1954 (Kresser, 1957). Concerning the Carpathian Basin, a rather clear source refers to this flood event: the inhabitants of Vámos(szabadi – see *Fig. 1*) in the Szigetköz island area, close to Győr (thus, southeast to Šamorín, on the opposite side of the Danube), were allowed to pay half of the tax due on Saint George's Day (24 April) in 1502 because of their need/poorness caused by the "deluge" ("*dilu*(v)*ium aque*"; source: HNA DF 279560). It seems, however, that a significant flood event already occurred on the Danube at Bratislava earlier, in May; while some of the flood damages were reported in late October (HNA DF 240953, 277113). Additionally, a royal charter provides a testimony that the problem of frequent floods caused severe, constant problems for the inhabitants of Bratislava by 1503 (HNA DF 240970; see *Fig. 1*). 1503 in itself is also interesting because, apart from 1501 and 1508, this was another major flood year on the Danube tributaries (see e.g. Rohr, 2007).

The other great (double-)flood event in Austria occurred in 1508. At the moment, information concerning the magnitude of the 1508 flood event in Hungary is available only in indirect evidence: the flood mark of the 1508 flood event (although the newspapers refers to 1509) on a tower of the Győr was still seen and compared to some 18th-century flood marks (1768-referred as 1769 and 1784), in which case the flood level of the 1508 event was above the maximum level of the other two, 18th-century levels (see Magyar Hirmondó 27 March 1784, No. 24; Kiss, 2012b). It is also an interesting question why the 1508 flood mark was reported and no any reference was mentioned on any possible 1501 flood mark.

There is no direct evidence available whether or not these changes were connected to any flood problem. However, it is still an interesting fact that especially the second, 'drastic' ground-level rise occurred – parallel to the building processes and changes observed at the Margit island and also in Visegrád – exactly in the same period when the important late 15th–early 16th-century flood peak and the two catastrophic Danube floods (1501, 1508 and perhaps also 1503) took place. Thus, even if the new building process in Šamorín could also accidentally occur in the same time when large Danube flood events took place – for, example, elevation changes in ground level can be also detected along the Danube in less flood endangered location (e.g. the resettling process of the village of Csöt/Csút at Budafok-Háros; see: Irásné, 2004a and *Fig. 1*) –, the destructive flood events might have had some impact on how the new ground levels, the settlement and building constructions developed. Thus, it is an interesting coincidence or probably more than a mere coincidence that since the second half of the 14th century (when otherwise the wooden structures were also destroyed) exactly around the turn of the 15th–16th centuries arrived the time when significant and extensive earthworks (great rise of ground level of the yards) were carried out.

The question might have some further important aspects: Šamorín is the interesting case which was mentioned in late medieval–early modern documentary evidence concerning early flood protection works. In this respect, both in 1426 and in 1569 the flood danger and damages affecting the town's cultivated lands (and also the entire Žitný ostrov area) were mentioned as a chief problem and the main reason for large-scale flood protection works (Kiss, 2012a,b). However, in these cases, either in the form of a direct royal order or a parliament decision, the damages and losses of the cultivated lands, and not the damages occurred in the town (i.e. buildings, inhabitants) were emphasised. It might also be an interesting parallel that, while a significant rise of ground level occurred in the yards, no elevation change of the main street and the ground level of houses took place around the turn of the 15th and 16th centuries.

Gravel-loess layer as a trace of major 16th century flood(s)? Nagymaros in the Danube Bend

According to András Pálóczi Horváth, a great 16th-century Danube flood left a distinct gravel layer (mixed with loess) over the 15th–16th-century pottery and (early and late) 15th-century coins in the market town of Nagymaros (opposite to Visegrád), in a depth of 110 cm. Regardless of which flood event or events caused this gravel-loess layer, it had to be a

major event or set of events: the appearance and large quantity (dominance) of gravel in the layer may suggest increased sediment-carrying capacity, which is typical for flood events with great discharge (see e.g. Nagyváradi, 2004). Moreover, due to the relatively high level of this significant river sediment, this flood event (or events) could be comparable in height to the great 20th- and early 21st-century Danube floods.

Above the gravel-loess layer, a mixed layer was found with 14th–17th-century remains (report published in: Dinnyés et al., 1993). It has to be noted that the Nagymaros side is the side where Danube sediments (especially rough sediments) are predominantly settled down by the river (it is dependent on the geo- and hydromorphological conditions, and did not fundamentally change up to the present times). Thus, especially rough sediments of Danube floods are much more likely to appear in the Nagymaros area than at Visegrád. As we will see later, several rather interesting features (e.g. fine sediments), presumably related to Danube flood event(s), indeed were identified in Visegrád.

In case of Nagymaros, the predominantly 15th-century archaeological evidence was found as a separate (undisturbed) layer under the gravel-loess layer, which indirectly suggests that the previous layer had enough time to settle down and the following flood event already could not significantly disturb this late medieval layer. Moreover, taking other Danube sedimentary flood investigations into account (e.g. the investigations at Paks, see Nagyváradi, 2004), the gravel-loess layer could develop after a single flood event, or as a result of not only one, but a series of flood events.

As for dating the flood event, applying the parallel observations carried out in Vác and with reference to climatic change, Mészáros and Serlegi suggested that the flood had to occur during the Turkish occupation and thus, not before the mid-16th century (Mészáros and Serlegi, 2011). Since a major flood period occurred on the Danube in the second half of the 16th century (see e.g. Kiss, 2012b), it is possible that this flood layer developed around the mid or late 16th century. Nevertheless, the archaeological dating of the layer located underneath the gravel-loess layer (and so as the mixed 14th–17th-century infill) in itself may also allow an earlier dating for the disastrous flood event(s): this/these could, for example, also happen in the middle of the century, or even before (i.e. 1501, 1508 or 1515, for example, cannot be excluded either).

In documentary evidence, the mid 16th century is characterised by great flood event(s) before 1549 prior to 1549, the consequences of great flood event at Bratislava. Moreover, damaging floods, reported prior to 1555, were probably also mentioned at Komárom together with 1557 and 1558 flood events at Bratislava. Then the flood series of the 1560s has to be considered: the great flood events, especially from 1567 (for Austria, see Rohr 2007), in the late 1560s (1568, 1569) and early 1570s (great flood events occurred almost every year: see Kiss, 2012b) caused long-term, irreversible changes, for example, in the Bratislava and Žitný ostrov area (e.g. lands swept away, reported in 1574: Maksay, 1959) and can be considered as floods of extraordinary magnitude (for destructions in Austria and Vienna, see: Rohr, 2007; Sonnlechner et al., 2013). Moreover, based on documentary evidence, we have to consider another peak of frequent and great flood events in the late 16th and the early 17th century, detectable in the Komárom area (see e.g. HNA, UC 86: 10, Király, 1890; for further overview, see: Kiss, 2012b).

Long-term processes: rising Danube water level at Visegrád in the late medieval–early modern times

A long-term process, affecting settlement and building conditions even in the late medieval–early modern period, was observed at the urban excavations of Visegrád. Here a clear water-level rise of the Danube occurred between the 13th and the 16th centuries, first detected by Miklós Héjj. He also raised attention to large-scale human impact on the Danube catchment area as a potential reason for increased rise of Danube water levels. Miklós Héjj's investigations of settlement development, based on the excavations of the medieval royal centre and civil town of Visegrád, suggested a long-term rise of Danube (high or flood) water levels (in its Danube Bend section) from the 13th century onwards (Héjj, 1988). As a consequence of this process, we have to consider that the (high or flood) level of the Danube might have been lower in the Middle Ages than it is today (Mészáros, 2006). Additionally, due to the extensive excavations of the royal palace complex and the settlement itself, concerning the rise of ground levels in different periods, a more detailed analysis can be provided.

Visegrád town: Late 15th–early 16th-century cellar infill due to floods

Even more specific flood-related evidence has been recently published referring to some of the urban excavation sites: located in the present-day school yard, under the 18th-century features a 14th-century building was excavated. The cellar of this late-medieval building was filled up at the end of the 15th or beginning of the 16th century, presumably due to flood problems. This theory of the excavating archaeologists was supported by the fine sediment (mud) layers settled by flood water, found in the same cellar underneath the artificial infill (Kováts, 2013).

The archaeological data on late 15th–early 16th-century floods is in good agreement with the information detected in documentary evidence: one of the most important (and certainly best documented) medieval flood peaks took place exactly around the decades of the 1480s, 1490s and 1500s (see *Fig. 1*).

All in one? 14th–16th-century flood processes and the Franciscan friary in Visegrád

Excavations carried out in recent years at the site of the medieval Franciscan friary (built in the 1420s), located close to the Danube on a gentle slope, provide us with further evidence (Buzás et al., 1995; Laszlovszky, 2009, 2013). Since some important parts of the excavation results are yet unpublished, and also due to the fact that in this case practically all the 14th–16th-century processes, described in other cases, could be detected, related infor-

mation on the excavation site and the identified processes are discussed here in more detail.

In this case at least two (or three) different processes could be identified. One was the general rise of the ground levels, which process can be clearly detected from the 14th century: the remains of the earlier settlement were located around two meters underneath the friary, but especially under the cloister built in the 1420s (during the late 14th–early 15th-century flood peak: Kiss 2011; for great Danube floods in the Carpathian Basin see *Fig. 1*, and Kiss, 2012a; for the Eastern Alpine Region: Rohr, 2007). When the friary was founded, a big (double-)cellar was built on the western (Danube) side of the cloister: one under the kitchen and the other under the refenctury (*Fig. 3*). In this case, in order to compensate the slope of the terrain, the builders raised the ground level. At the same time, the floor level of the previously mentioned double cellar was roughly the same as the floor level of the houses of the 14th-century settlement, replaced by the building complex of the Franciscan friary (Laszlovszky, 2009, 2013).

Two re-building phases were also detected during the archaeological investigation of the friary. One of them took place during the Matthias-period (1458-1490, with a building activity ca. 1470-80s), while the larger, almost total re-building of the complex happened during the first decade of the 16th century. During this new building phase, another significant rise of the ground level was initiated, which can be clearly detected in the layers of the cloister garth and under the pavement of the cloister walk. Already in this phase one of the two cellars in the western wing, under the newly constructed kitchen has been filled up with earth and a small new cellar was erected in the eastern wing of the cloister, close to the hill slope, behind the building complex (see *Fig. 3*).

The other process detected is related to the cellar under the refectory: during another early 16th-century building process the remaining cellar, located in the western, Danube side of the friary under the refectory, was filled up and a new cellar was built on the opposite (eastern) side of the friary in a safer location, carved into the rock of the slope of the hill and far from the river.

During the building process, in 1511 the Franciscans received permission to use the stones of the Saint George chapel in building the new tower of the friary (Buzás et al., 1995). The re-building process must have been finished by May 1513, when the congregation of the observant province took place in the friary.

One year later (May 1514) another congregation of the observant leaders took place in the friary: in this case with the task of electing the delegates who could go to Assisi for the general chapter. The friary clearly had to be in 'good shape' in 1513 and 1514 when the important personalities arrived and stayed there for the congregations. The next important information is known from 1540: in this year, due to the siege of the lower (royal) castle, the friary was damaged, and then, after the Turkish occupation, by 1544 the Franciscans left the friary forever (Buzás et al., 1995).

Nevertheless, some time between these two dates, namely between 1514 and 1540 something (serious) happened in the environment of the friary, because one part of the building, namely the northern cloister walk (with pavement, pillars, vaulting etc.; for location, see *Fig. 3*) sank down with one meter, and because of this great change, the Gothic vault of the corridor has collapsed. When rebuilt, no vaulted structure was constructed, but most probably a simple horizontal wooden ceiling was used to cover the northern corridor. The infill of the for-

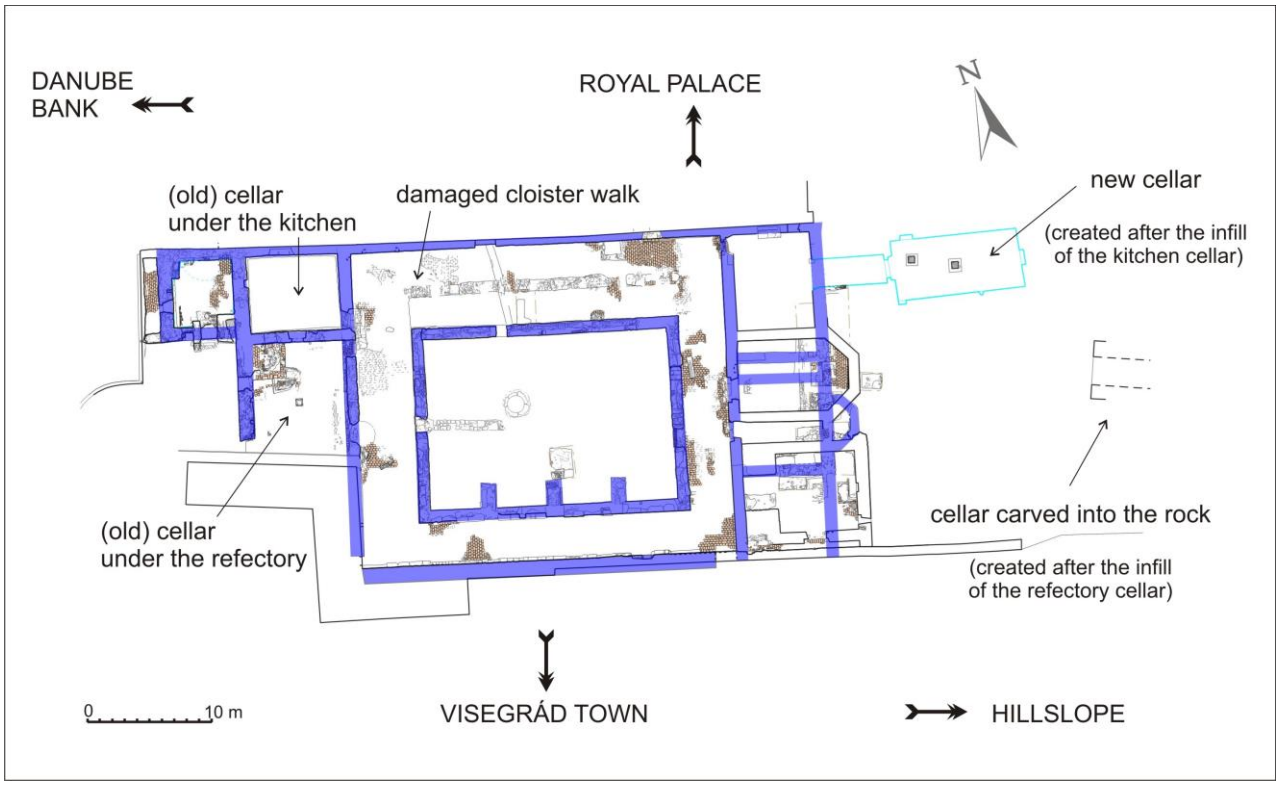

Fig. 3 Layout of the excavated early 15th-century Franciscan friary in Visegrád

mer cellar under the refectory close to the Danube (western side of the friary), and the establishment of the other, new cellar far from the Danube (eastern side of the friary), carved into the rock of the hill presumably occurred in the same time. Based on these features, the location of the friary, the stratigraphy and morphological conditions of the area, the excavators presume that this major damage, occurred some time between 1514 and 1540, had strong connections with Danube floods happened around the same time, and also with the generally rising trend of Danube water levels.

Compared to the palace area and the urban settlement centre, the Franciscan friary was more seriously affected by these floods. Similar situation was observed during the 2002, 2006 and 2013 flood events (e.g. water was standing in the former, medieval cellars). This observation offers an explanation for the major damages of the northern cloister walk, while no similar damages were detected during floods in the palace area.

In case of the Franciscan friary in Visegrád three conclusions were drawn on the basis of the excavated features. The building process of the friary in the 1420s was preceded by a significant ground-level rise compared to the previous ground level of the 14th-century buildings. This ground-level rise was probably necessary because of the long-term rise in Danube (flood) water levels (as described also by Héjj for other parts of the town). The great flood events of the 1500s and/or the floods of the entire late 15th–early 16th-century flood peak as well as the above described long-term water-level rise had a clear impact on the early 16th-century re-building processes in the form of a significant rise of ground level, and also with the infill of the cellars located close to the Danube (Kiss and Laszlovszky, 2013).

Between 1514 and 1540 at least one or more destructive flood events had to have strong impacts in the area which caused considerable damage in the buildings, so that a major reparation had to be carried out. Concerning these decades, as shown in *Fig. 1*, the great 1515 flood event or the series of flood events reported prior to 1523 (see later the case of Margit Island) or the floods around 1529-1531 as well as in the mid-1530s could be responsible for these damages (see *Fig. 1*). All these floods or flood series, otherwise, were also reported either on the Austrian or the Bavarian sections of the Danube (more information: Kiss and Laszlovszky, 2013).

Increasing 14th-16th-century groundwater levels near the Danube? The example of Vác

Related to the late medieval–early modern, long-term Danube water-level rise, interesting observations were recently published concerning the medieval-early modern Vác (Mészáros and Serlegi, 2011). The authors found it possible that already in the 15th century a cellar had to be filled up (by litter) because of the generally rising groundwater-level conditions, which strongly depended on the Danube water levels. In general, a significant increase of groundwater level was detected between the 13th–14th- and the 16th-century situation. Similarly, the bottom of the well, constructed in the second half of the 16th century, was 1.7 m higher than the bottom of the wells constructed one-two centuries before. It is really interesting, however, that the 17th-century well had a bottom ca. 60 cm lower then the late 16th-century one. Same observations were made in case of other, 17th–18th-century wells, which were all somewhat deeper than the late 16th-century one. The bottom of the 19th-century well was 2 m deeper than the 14th–15th-century ones. Nevertheless, in this later, 19th-century case the groundwater level could be already influenced by the increased water take-off due to strong population growth.

Thus, for the 16th-century, with no elevation change of the surface (ground) level, the authors reconstructed rather high average groundwater levels. Based on the observations carried out in wells and cellars, the average groundwater level of the (late) 16th century was much higher than in the Middle Ages, or in other parts of the early modern times, but also much higher than in the 19th century. In general, similarly to the observations of Miklós Héjj (1988) concerning the rising water-level conditions of the Danube between the 14th and 16th centuries, a significant groundwater-level rise, presumably influenced by the water levels of the Danube, was reconstructed by Mészáros and Serlegi (2011) concerning the same period in Vác.

It is also important to note that the highest water level was reconstructed for the second half of the 16th century, and already lower water levels were detected in the 17th century. The second half of the 16th century was also a very important period on the Danube (and also on most of its tributaries), especially because of the unusually great number of extraordinary (summer) floods. Significant floods especially were detected in the late 1560s–early 1570s when almost in each year there were great and extraordinary flood events (see *Fig. 1*); but already the 1550s as well as the 1580s-1590s are important flood decades (Kiss, 2012b; Kiss and Laszlovszky, 2013; for great floods of the Austrian sections: Rohr, 2007; Sonnlechner et al., 2013; for the Danube at Ulm: Glaser, 2008; for major Bavarian tributaries: Böhm and Wetzel, 2006). It could easily happen that these flood events were combined with generally higher water-level conditions on the long-term, detected in the archaeological evidence (e.g. at Vác).

Flood risk, early 16th-century building process and holy bones: the Margit Island (Budapest)

On the Margit Island (a Danube island located between Buda and Pest) before the Turkish occupation of the Buda area in 1541, the last great building process on the Dominican nunnery complex and the royal manor started in the late 15th century, continued in the early 16th century. The early 16th-century re-building of the royal manor, located nearby the monastic church, had some elements which, according to the excavating archaeologist, served the purposes of flood defence: the floor level was raised with 40-60 cm, and buildings were surrounded by large stone sheets in the open spaces (Irásné, 2004b). According to Feuerné (1971), another archaeologist working before in the same excava-

tion area, the tomb of Margit could be emptied years before 1529, because the nuns – referring to the devastations of floods – had previously removed the holy remains. Although without any further reference on the source, the author presumably referred to the charter issued in 1523 which contained the permission for changing the location of Margit's bones due to its flood-endangered place (HNA DL 25312; for a recent overview, see Vadas, 2013). An earlier building process was also detected on the mid 13th-century monastic sites, which started around 1381 and was still going on in 1409 (Feuerné, 1971).

Thus, in case of the Dominican monastery at least two flood-risk periods can be identified: one occurred in the early 16th century (or short before), and the other, occurred in and (short) before 1523. Concerning the available documentary evidence, the earlier, archaeological evidence can be easily connected to the great flood peak of the (late 15th–) early 16th century. Nevertheless, the second (documentary) case referring to significant floods prior to 1523, with currently no available single flood references, might need more explanation. Although in the Carpathian Basin (apart from the great flood in 1515) at the moment no contemporary reference on Danube floods is available, important Danube floods were reported concerning the Austrian and Bavarian sections in 1520 (Melk; see: Pertz, 1851), 1522 and 1524 (Regensburg; see: Heigel, 1878). Moreover, the Traun river, which is a good indicator of the conditions in the Eastern Alpine catchment of the Danube, had a significant flood period at that time: damaging flood events (sometimes three in a year) occurred in each year between 1519 and 1522 (Rohr, 2006).

MAIN FLOOD PEAKS DETECTED IN THE 14th-16th CENTURY: DISCUSSION

As for a conclusion and discussion of results, it is useful to have an overview of the evidence listed above according to main reference periods (see *Fig. 4*).

The 14th-15th centuries

In case of the Visegrád and Vác archaeological investigations, either based on settlement change observations or well depth measurements, a significant increase of water-levels, under the presumable direct influence of the Danube, was suggested concerning the (14th–)15th and 16th centuries (Héjj, 1988; Mészáros, 2006; Mészáros and Serlegi, 2011). In the second half of the 14th century, after the destruction of wooden buildings, the ground-level rise of the yards (accompanied by change to a brick based building structure) was observed in Šamorín (Urminský, 2005). A significant ground-level rise was also detected at the building process of the Franciscan friary in the 1420s, compared to the earlier, 14th-century level of the settlement. In connection to this question, it might be also interesting to see whether or not any change could be detected at such a flood-sensitive location as the Margit Island during the late 14th and early 15th century building process.

As for the Danube flood information preserved in documentary evidence, both in Austria and Hungary a clear increase was detected in the reported number of large flood events in the first decades of the 15th century. Although more Danube flood references could be found in the Carpathian Basin in the 15th than in the 14th centuries, and this is especially true for the first and last decades of the 15th century, this difference can be also caused by the differences in documentation between the two centuries. More floods (also Danube floods) are mentioned in the Carpathian Basin from the end of the 14th century, but especially in the first decades of the 15th century, when long-term problems were as well documented (see *Fig. 1*; and Kiss 2011, 2012a). The increased number of large flood events on the Danube in the early 15th century is also clearly detectable in the contemporary Austrian documentation (Rohr, 2007). Whereas a somewhat increased flood activity can be witnessed in the Upper-Danube flood reconstruction referring to Ulm, not much sign of a high flood frequency period is yet found around the turn of the

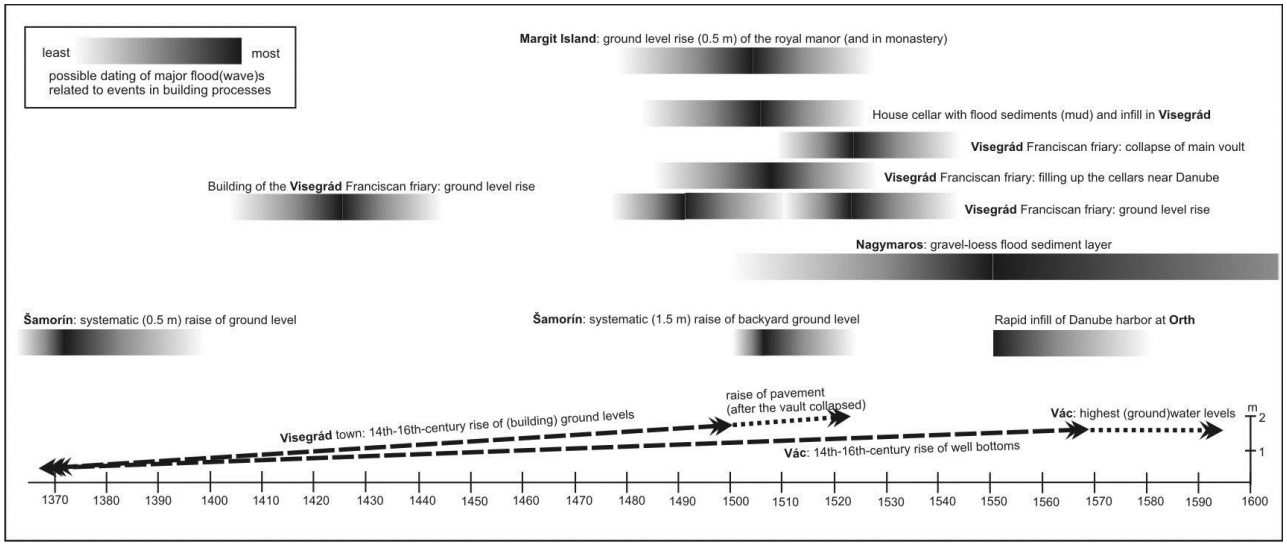

Fig. 4 An overview of 14th–16th-century Danube flood related archaeological-sedimentary evidence in the West and Central Carpathian Basin

14th–15th centuries or in the early 15th century (compared to, for example, the extreme flood peaks of the late 17th or the mid 18th centuries). A moderate increase in recorded flood events are presented concerning the second half of the 15th century (for the Danube flood reconstruction at Ulm, see Glaser, 2008).

Thus, some of the archaeological evidence (e.g. Vác and Visegrád) suggests long-term rising water-level conditions of the Danube between the 14th-16th centuries. Moreover, some late 14th- or early 15th-century changes in building processes (e.g. ground-level rise: Visegrád, Šamorín) were also detected. In case of Visegrad this was explained by the generally rising (flood) water levels, but these processes might be also connected to the flood peak at the end of the 14th, but especially in the first decades of the 15th century. Therefore, further investigations are needed to identify the nature of this relationship. More evidence is available from the late 15th century when new building processes started in a number of places along the Danube: a ground-level rise was clearly detected, for example, in case of the new building process of the Franciscan friary in Visegrád. Since most of related archaeological evidence were dated to the late 15th–early 16th centuries without further specification on timing, the late 15th century is discussed bellow together with the early 16th century.

The (late 15th and the) 16th centuries

The relationship is more straight-forward and easily detectable concerning the late 15th and 16th centuries: the much larger number of archaeological and sedimentary evidence culminate around the late 15th–early 16th century and mid 16th century, as well as around the second half of the 16th century. In all three cases already a significant number of documentary evidence is available for studying the possible relationship between flood peaks, long-term water-level changes and some of the available archaeological and sedimentary evidence.

Considering long-term groundwater-level changes in relation with the Danube, in case of Vác investigations showed clear difference between the late medieval situation of lower water levels, and the highest, late 16th-century water levels. Compared to the late 16th-century high water levels detected in wells, the 17th-century again showed a contrast with its lower water-level conditions. The flood (or floods), marked by a gravel-loess layer in Nagymaros, could have occurred any time between the late 15th and the 17th centuries. While in these two cases no exact dates or decades of flood processes can be detected (except for the very high late 16th-century water levels), in other cases the changes can be more clearly connected to certain decades, and therefore, it is possible to discuss them in time division.

1) The late 15th and early 16th centuries:

As we could see, a significant rise of yard levels (1.5 m) was reconstructed in Šamorín, while an important (over half meter) ground-level rise could be also detected in the early 16th century, both in case of the Visegrád friary and the Dominican nunnery at the Margit Island. The influence of great flood events is probably the most clearly detected in the Visegrád cases. Another clear consequence was the infill of cellars (due to repeated flooding), detected both in Visegrád town centre and in case of the Franciscan friary.

In documentary evidence, primarily based on the information related to Bratislava, a significant flood peak was reconstructed concerning the late 15th and early 16th centuries: starting with 1478, the 1480s, 1490s and 1500s were especially rich in destructive flood events. Moreover, the extraordinary flood events occurred on the Austrian sections of the Danube in 1501 ("millennium flood"), 1503 and also in 1508, which great flood waves presumably also appeared on the Carpathian Basin sections. Observations concerning the early 16th-century significant ground level rise as well as the infill of cellars due to flood danger show parallels to what happened after 1501 along the Austrian sections of the Danube (see Rohr 2005): apart from rising ground levels concerning new building processes, in Engelhartzell after the 1501 flood the toll house had no windows at the ground floor.

Great flood(s) after the early 1510s caused significant damages in the Franciscan friary of Visegrád: based on documentary information, in this case either the great 1515 flood event, the flood series prior to 1523 or the (great) floods around 1530 (1529, 1530, 1531) as well as in the mid 1530s (1535, 1537) might be responsible for the major damage.

2) Mid-16th century and the second half of the 16th century:

As for the upper sections of the Danube, at Orth concerning the rapid in-fill process of a harbour, high intensity sedimentation process (which could as well be connected to a higher number of more intense flood events) was detected around or short after 1550. This event might be a process parallel to the great 1548 flood event or the floods of the 1550s.

In Vác the highest water levels in wells were detected in the second half of the 16th century (Mészáros and Serlegi, 2011); the Nagymaros gravel-loess layer was also dated by the same authors for the mid or late 16th century. Parallel investigations suggest the intensification of fluvio-morphological processes (increased channelling activity and sedimentation) around the same time on the Danube in the Bratislava and Žitný ostrov area as well as at the lower sections of the River Morava.

These processes correspond to the great flood peak, especially documented concerning the second half of the 16th century, culminating around the late 1560s and early (mid) 1570s, characterised by great material damages and long-lasting inundations (e.g. in the Bratislava and Žitný ostrov area in 1574).

CONCLUSION AND OUTLOOK

In a growing number of cases, results of archaeological and sedimentary investigations can be directly or indirectly connected to large Danube flood events, series of floods

events and/or general, long-term changes in water-level conditions. The processes detected in archaeological evidence are partly long-term changes: a general rise of the Danube (flood) water levels were detected concerning the 14th-16th centuries. This water-level might have reached its peak in the second half of the 16th century.

Medium and short term evidence mainly corresponds to the main flood peaks or even to single catastrophic flood events. Such processes may be identified in archaeological evidence concerning the second half of the 14th, early 15th centuries; while most of the cases listed above were connected to the flood peak (and/or generally increasing water-level conditions) of the late 15th and early 16th centuries. In other cases connections between sedimentary/archaeological evidence and the mid- and late 16th-century high flood-frequency period were presumed.

Documentary evidence referring to the same period suggests that higher flood frequency and intensity periods occurred in the early and mid 16th century; a probably more prolonged one took place in the second half of the 16th century, with a peak in the late 1560s-early 1570s and maybe with another at the end of the 16th century. Earlier flood peaks in documentary evidence were detected on the Danube at the turn of the 14th-15th centuries and in the last decades of the 15th century, continuing in the early 16th century.

Comparing the above-mentioned results with the only available, systematic long-term Upper-Danube flood reconstruction (see Glaser, 2008: for Ulm, Germany), some clear similarities and differences can be recognised: based on the available documentary evidence, in Ulm a (smaller) flood peak was reconstructed for the second half of the 14th century, and a moderate increase in the second half of the 15th century. The real increase in flood frequency can be observed on the Ulm series only after the first decades of the 16th century, which tendency more intensively continues from the mid 16th century onwards.

Acknowledgement

The research of the first author was carried in the framework of the ERC project "Deciphering River Flood Change."

References

Bork, H.R. 1989. Soil erosion during the past millennium in central Europe and its significance within the geomorphodynamics of the Holocene. *Catena Supplement* 15, 121–131.

Böhm, O., Wetzel, K.-F. 2010. Flood history of the Danube tributaries Lech and Isar in the Alpine foreland of Germany. *Hydrological Sciences Journal* 51 (5). 784–798.

Brázdil, R., Kotyza, O. 1995. History of Weather and Climate in the Czech Lands I (Period 1000-1500). Zürcher Geographische Schriften 62. Zürich, 114, 115, 168.

Brázdil, R., Glaser, R., Pfister, Ch., Dobrovolný, P., Antoine, J.M., Barriendos, M., Camuffo, D., Deutsch, M., Enzi, S., Guidoboni, E., Kotyza, O. 1999. Flood events of selected European rivers in the sixteenth century. *Climatic Change* 43, 239–285.

Buzás, G., Laszlovszky, J., Papp, Sz., Szekér, Gy., Szőke, M. 1995. The Franciscan friary of Visegrád. In: Laszlovszky, J. (ed.). Medieval Visegrád. Royal Castle, Palace, Town and Franciscan Friary. *Dissertationes Pannonicae* 3.4, Budapest, 26–33.

Dinnyés, I., Kővári, K., Kvassay, J., Miklós, Zs., Tettamanti, S., Torma, I. 1993. Magyarország régészeti topográfiája 9: Pest megye régészeti topográfiája. 13/2. A szobi és a váci járás. Budapest: Akadémiai Kiadó, 218–219.

Dreibrodt, S., Lubos, C., Terhorst, B., Damm, B., Bork H.R. 2010. Historical soil erosion by water in Germany: Scales and archives, chronology, research perspectives. *Quarternary International* 222, 80–95.

Feuerné Tóth, R. 1971. A margitszigeti domonkos kolostor (The Dominican nunnery at the Margit Island). *Budapest Régiségei* 22, 245–268.

Fiebig, M., Preusser, F., Steffen, D., Thamó Bozsó, E., Grabner, M., Lair, G.J., Gerzabek, M. H. 2009. Luminescence Dating of Historical Fluvial Deposits from the Danube and Ebro. *Geoarchaeology* 24, 224–241.

Glaser, R. 2008. Klimageschichte Mitteleuropas. 1200 Jahre Wetter, Klima, Katastrophen. Darmstadt: Primus Verlag, p. 227

Grygar, M., Nováková, T., Mihaljevič, M., Strnad, L., Světlík, I., Koptíková, L., Lisá, L., Brázdil, R., Máčka, Z., Stachoň, S., Svitavská-Svobodová, H., Wray, D.S. 2011. Suprisingly small increase of the sedimentation rate in the floodplain of Morava River in the last 1300 years. *Catena* 86, 192–207.

Heigel, Karl von 1878: Leonhart Widman's Chronik. Die Chroniken der deutschen Städte vom 14. bis ins 16. Jahrhundert. Band 15. Leipzig: Heitzel.

Héjj, M. 1988. Településföldrajzi megfigyelések. Visegrád a 14-16. században (Observations concerning settlement geography. Visegrád in the 14th-16th centuries). In: Köblös, J. (ed.). Visegrád 1335. Budapest: Pest Megyei Levéltár, 63–67.

HNA, DF 240970 = Letter of King Ulászló to the town of Pozsony [Bratislava], Buda 1503.

HNA, DF 279560 = Hungarian National Archives, Database of Archival Documents of medieval Hungary (DF) 279560: A győri káptalan számadáskönyve (Account books of the chapter of Győr). fol. 35.

HNA, DF 277113 = The account books of Bratislava, 1501-1502. fol. 478, 516.

HNA, DF 240953 = The letter of Count Szentgyörgyi to Pozsony [Bratislava]. Óvár 1501.

HNA, UC 86: 10 = Hungarian National Archives, Urbaria et Conscriptiones (UetC) 86: 10(a): 1592/1602 (Komárom) Kürtze Verzaichniß und Beschreibung.

http://www.wien.gv.at/umwelt/wasserbau/hochwasserschutz/donau/katastrophenhochwaesser.html

Irásné Melis, K. 2004a. Régészeti kutatások a budapesti középkori Csöt faluban. II (Archaeological investigations in the medieval Csöt village in Budapest, Part 2). *Communicationes Archaeologiae Hungariae* 2004, 173-222.

Irásné Melis, K. 2004b. A Budapest Margit-szigeti domonkos apácakolostor pusztulása a 16-17. században (Destruction of the Dominican nunnery in the 16th-17th centuries, in Budapest, Margit Island). *Budapest Régiségei* 38, 107–113.

Kadlec, ,J., Grygar, T., Svétlik, I., Ettler, V., Mihaljevič, M., Diehl, J.F., Beske-Diehl, S., Svitavská-Svobodová, H. 2009. Morava River floodplain development during the last millennium, Strážnické Pomoraví, Czech Republic. *The Holocene* 19 (3), 499–509.

Király, J. 1890. Geschichte des Donau- Mauth- und UrfahrRechtes der Kön. Freistadt Pressburg. Pressburg [Bratislava], 81–85.

Kiss, I. R. 1908. *A Magyar Helytartótanács I. Ferdinánd korában és 1549-1551. évi leveles könyve*. (The Hungarian Locotenential Archives in the period of Ferdinand I and the letter book of the years 1549-1551) Budapest, 116-117. letter 99, written on 13 June 1549.

Kiss, A. 2009. Floods and weather in 1342 and 1343 in the Carpathian basin. *J. of Environmental Geography* 2 (3-4), 37–47.

Kiss, A. 2010. Az 1340-es évek árvizei, vízállás-problémái és környezetük, különös tekintettel az 1342. és 1343. évekre (Floods, water-level problems and the environment in the 1340s, with special emphasis on the years of 1342, 1343). In: Almási,T., Szabados, Gy., Révész, É. (eds.). *Fons, skepsis, lex*. Szeged: SZTE Történet Segédtudományok Tanszék–Szegedi Középkorász Műhely, 181–193.

Kiss, A. 2011. Árvizek és magas vízszintek a 13-15. századi Magyarországon az egykorú írott források tükrében: Megfoghatók-e és mi alapján foghatók meg rövid, közép és hosszú távú változások? (Floods and high water levels in 13th-15th-century Hungary, in the light of contemporary documentary evidence. Is it possible to detect short-, medium- and long-term changes?). In: Kázmér, M. (ed.). Környezettörténet 2 (Environmental history 2). Budapest: Hantken Kiadó, 43–55.

Kiss, A. 2012a. Dunai árvizek Magyarországon a középkori írott források tükrében: 1000-1500. Esettanulmányok, forráskritika és elemzési problémák (Danube floods in Hungary in medieval documentary evidence: 1000-1500. Case studies, source critics and analysis problems). In: Kiss, A., Piti, F., Szabados, Gy. Középkortörténeti tanulmányok 7 (Research in medieval studies 7). Szeged: Középkorász Műhely, 339–355.

Kiss, A. 2012b. "Nam per saepissimas inundationes Danubii maior pars periit." Documented 16th-century Danube floods in the Carpathian Basin I. In press: *Chronica* (12).

Kiss, A., Laszlovszky, J. 2013. Sorozatos árvízhullámok a Dunán? Egy 16. század eleji árvízsorozat hatása a Dunakanyar településeire és épületeire (Series of flood waves on the Danube? The impact of an early 16th-century flood series in the settlements and buildings of the Danube Bend). *Korall* 3, 48-80.

Kováts, I. 2013. 18. századi temető Visegrád központjából / 18th century cemetery in Visegrád centre. *Magyar Régészet* / *Hungarian Archaeology* 3, 1–9.

Kresser, W. 1957. *Die Hochwässer der Donau*. Wien: Springer Verlag.

Laszlovszky, J. 2009. Crown, Gown and Town: Zones of Royal, Ecclesiastical and Civic Interaction in Medieval Buda and Visegrád. In: Keene, D., Nagy, B., Szende, K. (eds.). Segregation – Integration – Assimilation. Religious and Ethnic Groups in Medieval Towns of Central and Eastern Europe. Farnham: Ashgate, 179–203.

Laszlovszky, J. 2013. The Royal Palace in the Sigismund Period and the Franciscan Friary at Visegrád. Royal Residence and the Foundation of Religious Houses. In: Buzás, G., Laszlovszky, J. (eds.). The Medieval Royal Palace at Visegrád. Archaeolingua, Budapest, 207–218.

Maksay, F. 1959. Urbáriumok, XVI-XVII. század (Urbaria. 16th-17th centuries). Budapest 1959. 179–187.

Mészáros, O. 2006. Késő középkori ház Visegrád polgárvárosában – Fő utca 32. (Birkl-telek). Héjj Miklós és Parádi Nándor ásatása, 1963 (Late medieval house in the civil town of Visegrád – Fő utca 32. Birkl-yard. The excavation of Miklós Héjj and Nándor Parádi). *Archaeologiai Értesítő* 131 (1), 145–168.

Mészáros, O., Serlegi, G. 2011. The impact of environmental change on medieval settlement structure in Transdanubia. *Acta Arch.Academiae Scientiarum Hung.* 62, 199–219.

Nagyváradi, L. 2004. Klímaváltozások következményeként fellépő extrém árvizek kimutatása árvízi üledékekkel a Dunán és magyarországi mellékfolyóin (Detecting extreme floods by flood sediments as a consequence of climate changes on the Danube and its Hungarian tributaries). In: Füleky Gy. (ed.). A táj változásai a Kárpát-medencében (Landscape changes in the Carpathian Basin. Water in the landscape). Gödöllő: Környezetkímélő Agrokémiáért Alapítvány, 241–248.

Ortvay, T. 1912. Pozsony város története (History of Pozsony town). 4. Pozsony [Bratislava]: Pozsonyi Első Takarékpénztár (Stampfel), 330.

Pertz, Georgius Henricus 1851: Continuatio Mellicensis. Monumenta Germaniae Hist. Scriptores 9, Hannover: Hahn.

Pišút, P., Tímár, G. 2009. A csallóközi Duna-szakasz folyódinamikai változásai a középkortól napjainkig (Changes of the dynamics of the Danube River in Žitný ostrov, Slovakia). In: Kázmér, M. (ed.). Környezettörténet. Az utóbbi 500 év környezettörténeti eseményei történeti és természettudományos források tükrében (Environmental history. Events of the last 500 years in the light of the historical and natural scientific evidence). Budapest: Hantken Kiadó, 55–70.

Pišút, P. 2005. Príspevok historických máp k rekonštrukcii vývoja koryta Dunaja na uhorsko-rakúskej hranici (16.-19. storočie)(Historical maps for the reconstruction of the river chanelling of the Danube on the Hungarian-Austrian border area (16-19th centuries). In: Pravda, J. (ed.). Historické mapy (Historical maps). Bratislava: Kartografická spoločnosť SR–Geografický ústav SAV, 167–181.

Rohr, Ch. 2005. The Danube Floods and Their Human Response and Perception. (14th to 17th C.) *History of Meteorology* 2, 71–86.

Rohr, Ch. 2006. Measuring the Frequency and Intensity of Floods of the Traun River (Upper Austria), 1441–1574. *Hydrological Sciences Journal* 51 (5), 834–847.

Rohr, Ch. 2007. Extreme Naturereignisse im Ostalpenraum. Naturerfahrung im Spätmittelalter und am Beginn der Neuzeit. Köln–Weimar–Wien: Böhlau Verlag, 231–273.

Sonnlechner, Ch., Hohensinner, S., Haidvogl, G. 2013. Floods, flights and fluid river: the Viennese Danube in the 16th century. *Water History* 5, 173–194.

Takáts, S. 1898. Komáromi harminczadosok dolga a XVI. és XVII. században (The obligations of border tax officers in Komárom, in the 16th-17th centuries). *Magyar Gazdaságtörténelmi Szemle* 5 (2), 421–453.

Takáts, S. 1900. A dunai hajózás a XVI. és XVII. században (Danube shipping in the 16th and 17th centuries). *Magyar Gazdaságtörténelmi Szemle* 7 (2), 97–122.

Thamóné Bozsó, E., Fiebig, M., Preusser, F., Steffen, D., Grabner, M., Lair, G.J., Gerzabek, M.H. 2011. Duna menti fiatal üledékképződés és egy kikötő 16. századbeli feltöltődése a lumineszcens és dendrokronológiai adatok tükrében (Young sedimentation along the Danube, and the 16th-century infill of a harbour in the light of luminescens and dendrochoronological data). In: Kázmér, M. (ed.). Környezettörténet 2 (Environmenta history 2). Budapest: Hantken Kiadó, 194–202.

Urminský, J. 2005. A középkori Somorja a régészeti leletek tükrében (The medieval Somorja in the light of archaeological findings). In: Strešňák, G., Végh, L. (eds.). Fejezetek Somorja város történetéből (Chapters from the history of Somorja town). *Disputationes Samarienses* 4. Somorja-Dunaszerdahely [Šamorín-Dunajská Stredá]: Fórum Kisebbségkutató Intézet, 9–19.

Vadas, A. 2011. Floods in the Hungarian Kingdom as Reflected in Private Letters (1541–1650) – Sources and Possibilities. In: Toader, N. (ed.). Anuarul Scolii Doctorale. „Istorie. Civilizaţie. Cultură“ V. Cluj-Napoca: Accent, 77–101.

Vadas, A. 2013. Long term perspectives on rover floods. The Dominican nunnery on Margaret Island (Budapest) and the Danube River. *Interdisciplinaria Archaeologica* 4/1 (2013): 73-82.

WStLA, Bürgerspital = Wien Staat- und Landesarchiv, Bürgerspital B 11- Spitalmeisterrechnung; Spitalmeisteramtsrechnung, Bd. 26 (1548).

JOURNAL OF ENVIRONMENTAL GEOGRAPHY
Journal of Environmental Geography 6 (3–4), 13–20.
DOI: 10.2478/jengeo-2013-0002
ISSN: 2060-467X

ESTIMATION OF SOIL MATERIAL TRANSPORTATION BY WIND BASED ON IN SITU WIND TUNNEL EXPERIMENTS

Andrea Farsang[1*], Rainer Duttmann[2], Máté Bartus[1], József Szatmári[1], Károly Barta[1], Gábor Bozsó[3]

[1]Department of Physical Geography and Geoinformatics, University of Szeged, Egyetem u. 2-6, H-6722 Szeged, Hungary
[2]Department of Geography, Division of Landscape Ecology and Geoinformatics, Christian-Albrechts-University Kiel, Germany
[3]Department of Mineralogy, Geochemsitry and Petrology, University of Szeged, Egyetem u. 2-6, H-6722 Szeged, Hungary
*Corresponding author, e-mail: farsang@geo.u-szeged.hu

Research article, received 10 June 2013, accepted 21 August 2013

Abstract

25% and 40% of territory of Hungary is moderate to highly vulnerable to deflation. However, precise estimates about the soil loss and related losses of organic matter and nutrients due to wind erosion are missing in most cases. In order to determine magnitudes of nutrient masses removed at wind velocities that frequently occur in SE Hungary, in-situ experiments using a portable wind tunnel have been conducted on small test plots with an erosional length of 5.6 m and a width of 0.65 m. The wind tunnel experiments have been carried through on a Chernozem which is typical for this region. In order to compare the effects of soil coverage on the masses of blown soil sediment and adsorbed nutrients, two soil surface types have been tested under similar soil moisture und atmospheric conditions: (1) bare soil (dead fallow) and (2) bare soil surface interrupted by a row of maize plants directed downwind along the center line of the test plots.

The results of our experiments clearly show that a constant wind velocity of 15 m s^{-1} (at a height of 0.3 m) lasting over a short time period of 10 minutes can already cause noticeable changes in the composition and size of soil aggregates at the top of the soil surface. Due to the grain size selectivity of the erosive forces the relative share of soil aggregates comprising diameters > 1 mm increased by 5-10% compared with the unaffected soil. Moreover it has shown that short time wind erosion events as simulated in this study can result in erosion rates between 100 and 120 g m^{-2}, where the erosion rates measured for bare soils are only slightly, but not significantly higher than those of the loosely vegetated ones. Soil samples taken from sediment traps mounted in different heights close to the outlet of the wind tunnel point to an enrichment of organic matter (OM) of about 0.6 to 1 % by mass referred to the control samples. From these findings has been calculated that the relocation of organic matter within short term wind erosion events can amount to 4.5 to 5.0 g OM m^{-2}. With the help of portable field wind tunnel experiments we can conclude that our valuable, high quality chernozems are struck by wind erosion mainly in drought periods.

Keywords: deflation, wind tunnel experiment, nutrient transport

INTRODUCTION

It is well-known that among other processes of soil degradation, wind erosion can cause enormous damages on the regional as on the global scales. For this reason, research on this topic has started early (Chepil 1942, 1955; Chepil and Woodruff 1963; Woodruff and Siddoway, 1965). However, for a long time attention was mainly given to the physical mechanisms and to the measurement of wind erosion under field and lab conditions (Gillette, 1978; Bódis and Szatmári, 1998). Since the 1980s research focused on the modeling of wind erosion processes including the calculation of soil erosion rates at different spatial and temporal scales and, especially, the estimation of the losses of organic matter and nutrients caused by deflation (Zobeck and Fryrear, 1986; Zobeck et al., 1989; Sterk et al. 1996; Larney et al. 1998; Bach, 2008). The amount of nutrient loss per hectare varies within a broad range, depending on the soil type, the physical properties and the organic matter content. For stronger wind erosion events Neemann (1991) reports about nutrient losses of about 150 kg N ha^{-1}, 200 kg P_2O_5 ha^{-1}, 200 kg K_2O ha^{-1}, 200 kg MgO ha^{-1} and 600 kg CaO ha^{-1} (Neemann, 1991, Charles et al., 2002, Sankey et al., 2012).

In Hungary, the deflation preferentially occurs in regions covered with sandy soils (e.g. the Danube-Tisza Interfluve, Nyírség). Hence, these areas form the recent center of soil erosion research (Borsy, 1972; Harkányiné and Herkó, 1989; Lóki and Schweitzer, 2001; Mezősi and Szatmári, 1998; Mucsi and Szatmári, 1998; Szatmári, 1997, 2005) although the vulnerability of Chernozem soils to wind erosion has been already emphasized in earlier research (Bodolayné, 1966; Bodolayné et al., 1976). The vulnerability assessment of the Hungarian soils to deflation has been made possible after finalizing the 1:100.000 soil maps, which have a special focus on physical diversity (Várallyay et al., 1979, 1980). The assessment of wind erosion risk indicates that 26% of the total area of Hungary is covered with highly

vulnerable sandy soils, another 40% of the country has been classified as medium vulnerable, corresponding with the wide spreading areas composed of sandy loam and loam (Lóki, 2003). As stated by Baukó and Beregszászi (1990) in their case study in Békés County, these soils bear large economic potential, which increases the need for sustainable land use practices.

To-date only little is known about the quantities of wind-driven soil and nutrient losses from Chernozems as they are typical for the south eastern parts of the Great Hungarian Plain (Apátfalva). In order to gain knowledge about the magnitudes of deflation rates of mineral soil, organic matter and nutrients, wind tunnel experiments have been performed under controlled conditions. Although wind tunnel experiments have been widely used in many other regions (e.g. Maurer et al., 2006; Bach, 2008; Fister and Ries, 2009), this paper describes the first applications of an in-situ wind tunnel experiment in Hungary. The major objectives of this study are (I) to compare the rates of soil loss caused by winds of frequent velocity on uncovered and loosely covered soil surfaces as they are typical for most of the wind erosion events in this area, (II) to analyse the changes of the above-ground soil structure and (III) to calculate the magnitudes of humus- and of the nutrient losses during wind storm events of defined intensity.

STUDY AREA

The study area is located in the Csongrád-plain micro region (*Fig. 1*). The elevation of the area ranges between 79.5 and 107.6 m forming nearly a perfect plain. The clayey, loamy subsurface sediments are covered by infusional loess of various depths. The climate of the area is warm and dry with an annual average temperature of 10.3 °C and an annual precipitation of around 560–570 mm. The aridity index (ratio of the potential maximal evaporation and the annual precipitation) is around 1.3, and may have a considerable effect on the deflation of the soil. The prevailing wind direction is NW, but winds from SE are also frequent (Dövényi, 2010). The synops data, which provide mainly hourly data, measured in Szeged weather station (WMO Index 12982). In the cases of all wind velocity data 160° is dominant, but the strongest winds come from 320°, so this direction is chosen to set the model (*Fig. 2*).

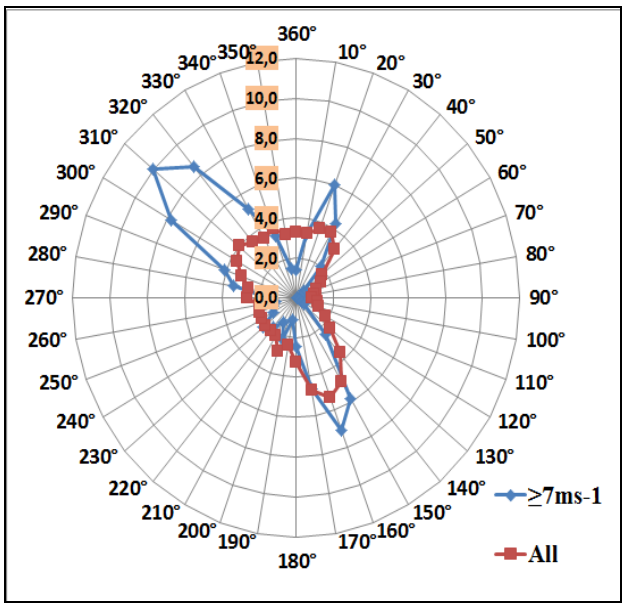

Fig. 2 Wind direction change at Szeged in aspect of wind velocity (March-April, 2000-2011)

The typical soil type is a Chernozem according to WRB, 2006, having a loamy, at some places clayey loam texture (*Fig. 3*) and high humus contents in the A-horizons (4.5-4.8%). The carbonate content varies between 4-12% by weight. During the experiments, the water content of the soil was 7–8 v/v%.

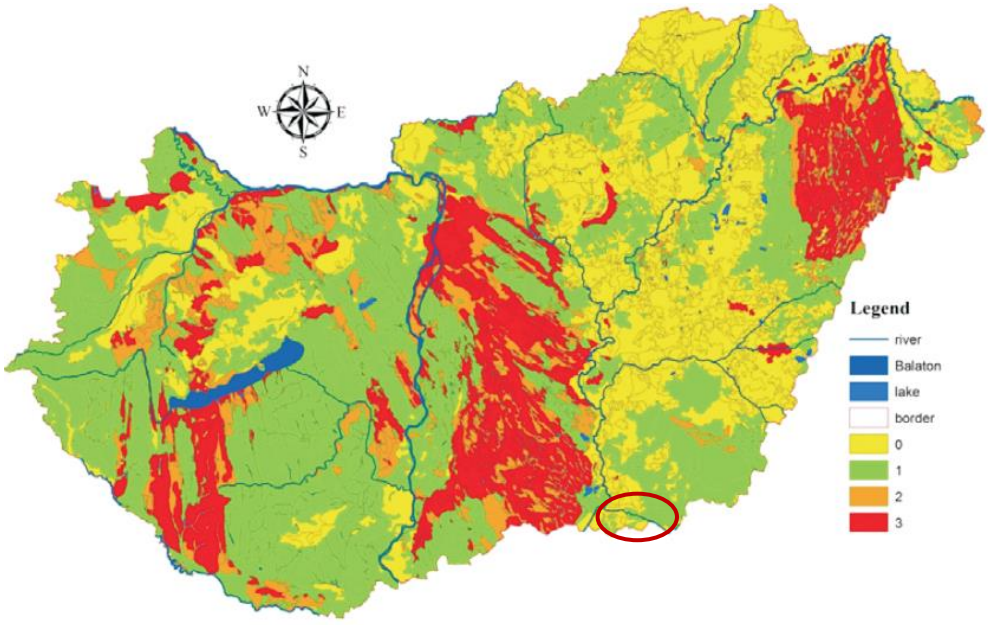

Fig. 1 Potential wind erosion map of Hungary with the studied area (0: insignificant, 1: slight, 2: moderate, 3: severe) (Lóki, 2000)

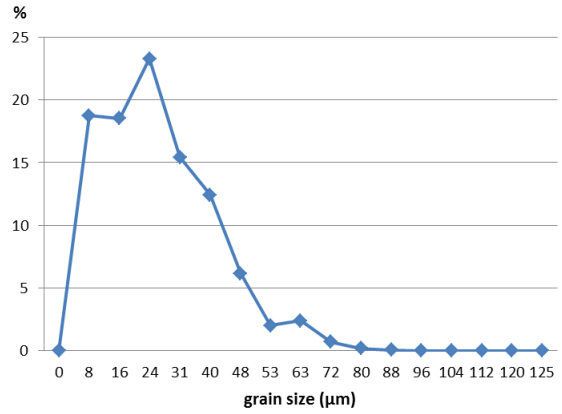

Fig. 3 Grain size distribution of the chernozem soil in the study area

METHODS

The undisturbed surface soil was measured in a portable and adjustable 12 m long field wind tunnel (*Fig. 4*) in situ on the study plot in the summer of 2011. Experiment "A" was conducted upon a non-cultivated, plant-free surface. The "B" series simulate the effects of a loosely vegetated surface. For this purpose a row of maize plants with a height of 25-30 cm and a spacing of 10 cm was placed in the center of the wind tunnel (*Fig. 5*). For both series three parallel deflation experiments where carried through each one with a duration of 10 minutes and approximately 15 ms^{-1} wind speed.

Wind velocity has been measured along horizontal and vertical profile lines during all experiments (*Fig. 7*) using a Lambrecht Jürgens 642 anemometer. The ground area blown within the wind tunnel covers 3.36 m^2. Measurements of wind velocity confirmed the existence of a logarithmic shaped boundary layer of a thickness of about 35.1 cm.

The threshold wind velocity in both experiments was observed at 13 ms^{-1}. Following each wind experiment both the surface soil and the rolling soil fractions were sampled. The latter were collected in boxes positioned at the end of the tunnel. The MWAC (Modified Wilson and Cook) traps at 5, 15, 25, 35, 45 and 55 cm heights at the end of the tunnel were emptied (*Fig. 6*).

The samples were air dried, and after the appropriate preparation, the following parameters were determined: distribution of aggregates by sieving, "Arany" yarn test according to the MSZ-08-0205:1978

Fig. 4 The portable wind tunnel

Fig. 5 Surface soil of the two experiment series: "A" series with an undisturbed surface soil, "B" series on a maize field

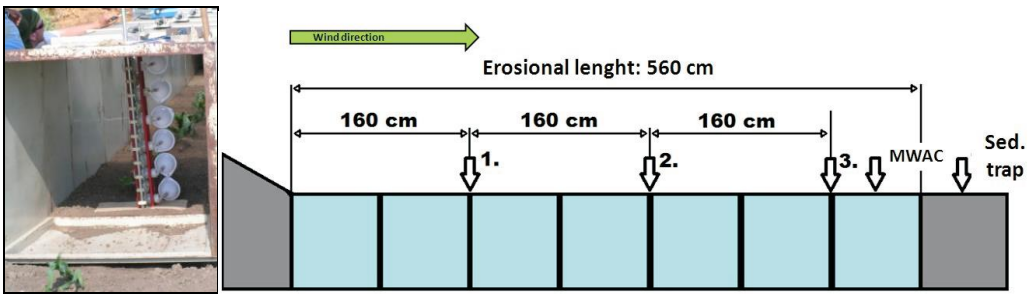

Fig. 6 The location of the soil sample points, the MWAC traps and the sediment traps at the end of the tunnel about 15 ms^{-1} with

specification, pH(H_2O), carbonate content according to the MSZ-08-0206/2:1978 specification, and the organic matter content according to the MSZ 21470/52:1983 specification.

The total element content of the soil and the captured sediment was determined by XRF HORIBA Jobin-Yvon XGT-5000. The particle size distribution was measured by Fritsch Analysette 22 Microtel Plus.

RESULTS AND DISCUSSION

Analyses of the wind profiles reveal significant differences between the "A" series (bare soil) and the "B" ("maize") series. Figure 5 clearly shows the influence of a different surface roughness and surface structure on the changes of the wind velocity over the whole cross-section of the wind tunnel.

The isotache profile of the “A” series, expectedly reveals a decrease of wind velocity close to the ground, depending on the soil roughness cause by the coarser aggregate on top of the soil. The Z_0-value has been calculated at 0.25 mm.

At a height of 10 cm the wind velocity increases up to 13 m s^{-1} while it reaches its original velocity of 15 ms^{-1} in a height of 20 cm. Surprisingly, the isotache profile of the “B” series shows a different behaviour. In contrast to other studies (Bolte, 2008) that show a strongly reduced wind velocity behind wind breaking obstacles, we found only a minor decrease in wind velocity within and behind the row of maize plants, and even a higher wind speed compared with the same heights of the series "A" experiments (*Fig. 7*). This fact suggests the occurrence of vortex movements around the single maize plants causing an increase in wind velocity up to 16-17 m s^{-1} which might contribute to higher deflation rates along plant rows oriented in downwind direction at this stage of growth.

The 10 minutes wind event had a significant impact on the relative percentage of aggregate sizes in the surface soil (*Fig. 8*, *Table 1*). The experiments show that the dust fraction was reduced, and therefore the proportion of larger aggregates increased in the top 5 cm of the soil. It is noteworthy that during the “B” experiment series, the ratio of 1< mm aggregates in the surface layer increased by 5 – 10% compared to the original soil (*Fig. 8.*).The largest saltation movement was caused by the increase of the wind velocity along the outer sides the maize row. Comparing the original surface soil and the aggregate composition of the material collected in the traps (mass%, n = 3) afterwards the “A” series experiment, it is obvious that 58% of the soil material trapped in the recessed traps consisted of aggregates with a diameter of 1 to 4 mm (*Table 1*). Compared with the aggregate composition of the original surface soil, in both experiment series the diameter of the soil crumbs increased significantly in the trapped soil material (7%). During the 16-17 ms^{-1} wind speeds of the “B” experi-

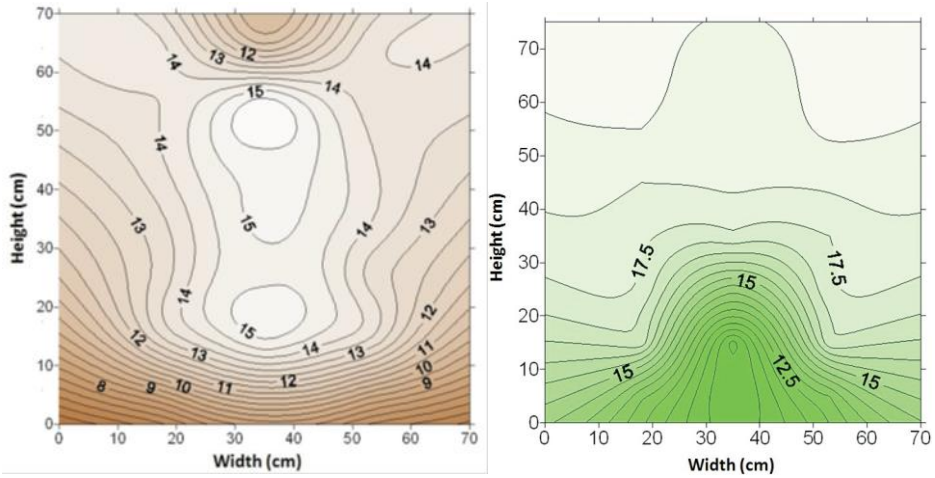

Fig. 7 The wind profiles (ms^{-1}) of the two experiment series (left: “A” series, right: “B” series)

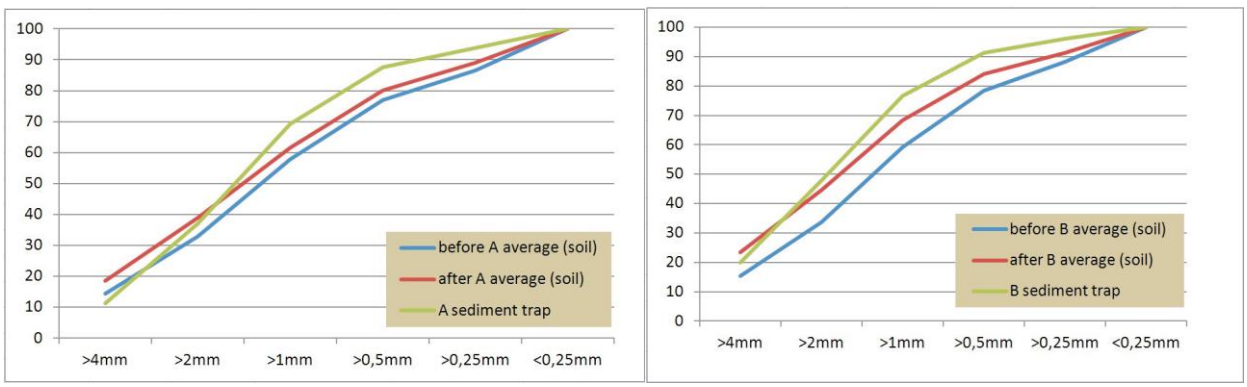

Fig. 8 Change of the aggregate structure (%) of the surface soil (left: “A” experiment series, right: “B” experiment series)

Table 1 The aggregate composition of the original surface soil and the, in the traps accumulated, soil material (Mass%, n=3)

mm	„A" series surface m/m%	Standard deviation	„A" series trap m/m%	Standard deviation	„B" series surface m/m%	Standard deviation	„B" series trap m/m%	Standard deviation
>4	14.4	3.9	11.3	0.2	15.4	1.7	19.9	9.2
2–4	18.4	1.7	25.7	1.5	18.3	0.5	27.8	3.6
1–2	25.1	1.2	32.3	1.8	25.4	1.04	28.8	4.9
0.5–1	19.0	1.4	18.2	0.6	19.3	0.6	14.7	1.6
0.25–0.5	9.7	1.3	6.3	0.5	9.8	0.6	4.8	0.5
<0.25	13.4	2.6	6.1	0.9	11.8	0.9	3.9	0.2

ment series, more 4 mm and larger aggregates where moved. On average 20% of the trapped soil material in the traps had an aggregate diameter larger than 4 mm.

The organic matter (OM) content of the accumulated material in the traps increased (*Fig. 9*). By dividing the OM content of the material captured in the MWACs trap, by the OM content of the original surface soil, an enrichment factor of 1.1 to 1.2 - depending on the strength of the wind - can be found for the traps at a height of 15 and 25 cm. The material taken from the traps at a height between 0.15 m and 0.55 m, the OM content showed an increase of 0.6 – 1% compared to original soil (*Fig. 10, Table 2*).

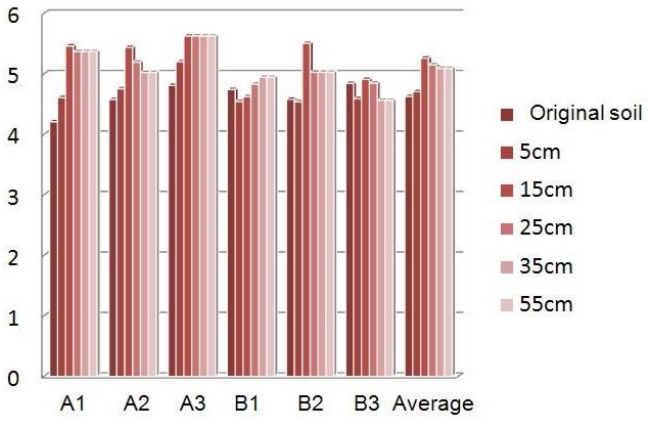

Fig. 9 Amount of the humus

The effect of the soil movement during the 10 minute wind events on the amount of accumulated soil material in the trap has been quantified, given the area of the surface exposed to the wind and the size of the surface of the MWAC traps (*Table 2*). The majority of the soil movement consist of rolling soil material.The amount of trapped soil material not show significant differences; in case of the "A" series 97 g m^{-2} of rolling soil material was registered while during the "B" series 59 g m^{-2} was recorded. In the first place, the soil with aggregates smaller than 0.25 mm (soil dust) was collected in the MWAC traps, which was in case of the "A" series 10.7 % of the total transported material, while during the "B" series this was 17.4 %. The average soil movement during the "A" measurement series was 107 g m^{-2}, and during the "B" measurements series 115 gm^{-2}. From the total amount of transported soil, just the suspended fine fractions are accumulating in the MWAC traps at larger distance; during the 10 minutes 15 ms^{-1} wind event, an amount of 15 g m^{-2} was registered.

The amount of relocated humus **(**g m^{-2}**)** movement was calculated based on the total amount of soil material that was transported during the wind event and the humus content of the accumulated sediments in the traps. The OM content in the sediment traps (above 0.15 m) was 0.6–1% higher than that of the original surface soil (*Fig. 9-10*). The amount of relocated OM content caused by deflation could reach up to 4.5–5.0 g m^{-2} (*Table 2*).

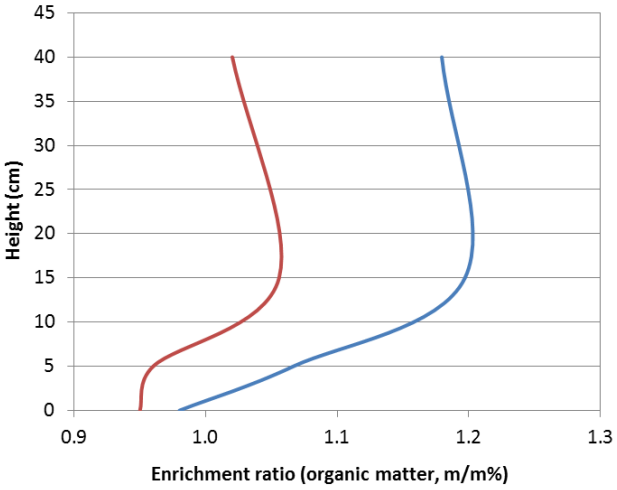

Fig. 10 Variation of the amount of humus enrichment ratios in the sediment collected with MWAC traps at 5, 15, 25, 35 and 45 cm height (red: "A" experiment series, blue: "B" experiment series

Macro elements (P, Ca, K) do not show any increase in the transported soil fraction, their enrichment ratios vary between 0.95 and 1.09 (*Table 3-5*). The 10 minute long wind experiment with 15 ms^{-1} wind speed transported 0.1 g m^{-2} of P, 1.6 g m^{-2} of K and 2.9 g m^{-2} of Ca.

Comparisons between the amount of relocated nutrients calculated in this study and those amounts reported from other studies –are complicated, because of differing wind tunnel characteristics, differing initial conditions and varying soil properties.

Table 2 Amount of the transported soil (g m^{-2}), the relocated humus (g m^{-2}) and the humus enrichment ratios during the two experiment series (A and B) (wind speed 15 m s^{-1}, 10 minute long single experiments)

.	Amount of transported soil (average) (g m^{-2})	OM (%)		Enrichment ratios	Amount of relocated humus (g m^{-2})
		(average)	standard deviation	OM% $_{eroded}/_{original\ soil}$	
The rolling soil fraction collected in recessed boxes at the end of the tunnel					
A - box	97.0	4.47	0.08	0.98	4.34
B - box	95.0	4.44	0.17	0.95	4.22
The suspended soil fraction collected with MWAC traps					
A - 5 cm	5.53	4.86	0.31	1.07	0. 27
A - 15 cm	2.35	5.45	0.12	1.20	0.13
A - ≥25 cm	2.12	5.37	0.12	1.18	0.11
B - 5 cm	8.51	4.56	0.03	0.96	0.39
B - 15 cm	5.24	5.01	0.45	1.06	0.26
B - ≥25 cm	6.25	4.85	0.11	1.02	0.303
Total transported humus (A series): 4.85 g m^{-2}					
Total transported humus (B series): 5.17 g m^{-2}					

Table 3 Amount of the transported soil (g m^{-2}), the relocated P (g m^{-2}) and the P enrichment ratios during the experiments (wind speed 15 m s^{-1}, 10 minute long single experiments)

	Amount of transported soil (average) (g m^{-2})	P (ppm)		Enrichment ratios	Amount of relocated P (g m^{-2})
		(average)	standard deviation	P $_{eroded}/_{original\ soil}$	
The rolling soil fraction collected in recessed boxes at the end of the tunnel					
Box	96.0	1004.2	249	1.07	0.096
The suspended soil fraction collected with MWAC traps					
5 cm	5.53	887.8	63.2	0.95	0.005
15 cm	2.35	903.3	107.5	0.97	0.002
≥25 cm	2.12	861.6	63.4	0.92	0.002
Total transported P/experiments: 0.106 g m^{-2}					

Table 4 Amount of the transported soil (g m^{-2}), the relocated K (g m^{-2}) and the K enrichment ratios during the experiments (wind speed 15 m s^{-1}, 10 minute long single experiments)

	Amount of transported soil (average) (g m^{-2})	K (ppm)		Enrichment ratios	Amount of relocated K (g m^{-2})
		(average)	standard deviation	K $_{eroded}/_{original\ soil}$	
The rolling soil fraction collected in recessed boxes at the end of the tunnel					
Box	96.0	15018	2072	1.00	1.44
The suspended soil fraction collected with MWAC traps					
5 cm	5.53	16167	1916	1.06	0.089
15 cm	2.35	16374	2204	1.08	0.039
≥25 cm	2.12	16493	929	1.09	0.035
Total transported K/experiments: 1.605 g m^{-2}					

Table 5 Amount *of* the transported soil (g m^{-2}), the relocated Ca (g m^{-2}) and the Ca enrichment ratios during the experiments (wind speed 15 m s^{-1}, 10 minute long single experiments)

	Amount of transported soil (average) (g m^{-2})	Ca (ppm)		Enrichment ratios	Amount of relocated Ca (g m^{-2})
		(average)	standard deviation	Ca $_{eroded}/_{original\ soil}$	
The rolling soil fraction collected in recessed boxes at the end of the tunnel					
Box	96,0	26961	5925	0.9	2.59
The suspended soil fraction collected with MWAC traps					
5 cm	5.53	29253	5862	0.97	0.162
15 cm	2.35	31753	5900	1.04	0.075
≥25 cm	2.12	31983	1848	1.08	0.068
Total transported Ca/experiments: 2.89 g m^{-2}					

Bielders et al. (2002) calculated nutrient balance of sandy soil triggered by three natural storms in Sahel. They measured a soil loss of about 0.3-1.9 kg m^{-2}. Because of the low nutrient content of the native soil, total nutrient losses remained very low: P loss was calculated at 9-65 mg m^{-2}, K 20-128 mg m^{-2} and Ca loss 7-62 mg m^{-2}. The study of Sterk et al. (1996) was conducted to quantify nutrient losses by saltation and suspension transport. During two convective storms mass fluxes of wind-blown particles were measured in Niger on sandy soil. The trapped material was analysed for total element content (K, P, C, N). The following nutrient losses were estimated: 5.7 g m^{-2} K and 0.61 g m^{-2} P. In the study of Sankey et al. (2012) the nutrient concentrations by Mehlich3 extraction (P, K, Mg, Cu, Fe, Mn, Al) in wind-transported sediment were determined. The soils were collected from burned and unburned soil surfaces in Idaho, USA. They estimated 0.256 g m^{-2} y^{-1} P mobilization and 1.451 g m^{-2} y^{-1} K mobilization.

Nutrient transport determined by us are congruent to the values measured by Sterk et al. (1996) because their experiments also focused on wind events and the total element was investigated from captured sediment, as well.

CONCLUSION

During this research measurements with a field wind tunnel were executed on the chernozem soils on the southern part of the Great Hungarian Plain. The experiments were repeated three times with two different types of surface cover . They make obvious that already short-time wind events of a wind velocity of 15 ms^{-1}, can erode more than 100 g m^{-2}.

If one hypothetically assumes that the simulated conditons would be true for a complete field this would equalize a loss of 1 ton of treasurous and highly fertile agricultural soil per hectare that would have been lost

From this material, the main part is transported on or close to the surface. Only 10 to 15% is moved in suspended form. This material can be transported over a much larger distance, and this way losing permanently its significantly higher humus content than the original soil, which is crucial for the agriculture.

Acknowledgements

This research has been financially supported by the OTKA K 73093 and OTKA IN 83207 and TÁMOP-4.1.1. C-12/1/KONV-2012-0012 ”ZENFE” projects.

References

Bach, M. 2008. Aolische Stofftransporte in Agrarlandschaftem. PhD Dissertation. Christian-Albrechts Universitat, Kiel.

Baukó, T., Beregszászi, P. 1990. Egyszerűsödő agrár-térszerkezet – fokozódó szélkárosodás Békés megyében (Simplifying spatial struture of agricultural lands – increasing wind erosion in Békés county). Környezetgazdálkodási Évkönyv 1989. Békéscsaba, 87–95.

Bielders, C.L., Rajot, J.L., Amadou, M., 2002. Transport of soil and nutrients by wind in bush fallow land and traditionally managed cultivated fields in the Sahel. *Geoderma* 109, 19–39.

Bódis, K., Szatmári, J. 1998. Eolikus geomorfológiai vizsgálatok DDM felhasználásával (Eolic geomorphological investigations using DEM). In: VII. Térinformatika a felsőoktatásban szimpózium. Budapest, 102–107.

Bodolay, I.-né, 1966. A széleróziót befolyásoló változó talajfizikai tulajdonságok (Physical properities influencing wind erosion). *Agrokémia és Talajtan*, 15, 372–383.

Bodolay, I.-Né, Máté, F., Szűcs, L. 1976. A szélerózió hatása a Bácskai löszháton (Effect of wind erosion on Bácsa Loess Plateau). *Agrokémia és Talajtan* 25, 96–103.

Bolte, K. 2008. Untersuchungen zur feuchteabhangigen Dynaik des bodespezifischen Erosionwiderstandes bei Bewindung unter Windkanalbedingungen Schriftenreihe des Institut für Pflanzenernahrung und Bodenkunde Universitat Kiel. 146 p.

Borsy, Z. 1972. A szélerózió vizsgálata a magyarországi futóhomok területeken (Investigation of wind erosion on sandland areas of Hungary). *Földrajzi Közlemények* 20 (2–3), 156–160.

Chepil, W.S. 1942. Relation of wind erosion to the water-stable and dry clod structure of soil. *Soil Science* 55, 275–287.

Chepil, W.S. 1955. Factors that influence clod structure and erodibility of soil by wind: V. Organic matter at various stages of decomposition. *Soil Science* 80 (5), 413–421.

Chepil, W.S., N.P. Woodruff 1963. The Physics of Wind Erosion and Its Control. Advances in Agronomy 15, New York: Academic Press Inc., 302 pp.

Dövényi, Z. (ed.), 2010. Magyarország kistájainak katasztere (Microregion cathaster of Hungary). MTA FKI, Budapest, 285–289.

Farsang, A., Szatmári, J., Négyesi, G., Bartus, M., Barta, K., 2011. Csernozjom talajok szélerózió okozta tápanyag-áthalmozódásának becslése szélcsatorna-kísérletekkel (Estimation of soil organic matter transportation due to wind erosion in case of chernozem soils). *Agrokémia és Talajtan* 60 (1), 87–102.

Fister, W., Ries, J.B. 2009. Wind erosion in the central Ebro Basin under changing land use management. Field experiments with a portable wind tunnel. *Journal of Arid Environments* 73 (11), 996–1004.

Gillette, D. 1978. A wind tunnel simulation of the erosion of soil: Effect of soil texture, sandblasting, wind speed, and soil consolidation on dust production. *Atmospheric Environment* 12 (8), 1735–1743.

Harkányiné Székely, Zs., Herkó, D. 1989. Magyarország homokveréses kártérképe (1977-1986) (Damages due to sand blast in Hungary (1997-1986). I. M=1:100 000. ICA Nemzetközi Térképészeti Társulás XIV. Világkonferenciája Budapest

Larney, F.J. et al. 1998. Wind erosion effects on nutrient redistribution and soil productivity. *Journal of Soil and Water Conservation* 53 (2), 133–140.

Lóki, J. 2003. A szélerózió mechanizmusa és magyarországi hatásai. (The process of wind erosion and its effects in Hungary). MTA doktori értekezés. Debrecen.

Lóki, J., Schweizer, F. 2001. Fiatal futóhomokmozgások kormeghatározási kérdései– Duna–Tisza közi régészeti feltárások tükrében. *Acta Geographica Geologica et Meteorologica Debrecina*. XXXV, 175–183.

Maurer, T., Herrmann, L., Gaiser, T., Mounkaila, M., Stahr, K., 2006. A mobile wind tunnel for wind erosion field measurements. *Journal of Arid Environments* 66 (2) 257–271.

Mezősi, G., Szatmári, J. 1998. Assessment of wind erosion risk on the agricultural area of the southern part of Hungary. *Journ. Hazardous Materials* 61, 139–153.

Mucsi, L., Szatmári, J., 1998. Landscape changes of a blown sand surface on the Great Hungarian Plain. The problems of landscape ecology. III. Warsaw, 215–222.

Neemann, W. 1991. Bestimmung des Bodenerodierbarkeitsfaktors für winderosionsgefahrdete Böden Norddeutschlands – Ein Beitrag zur Quantifizierung der Bodenverluste. Geologisches Jahrbuch 25,. Hannover.

Sankey, J.B., Germino M.J., Benner S.G., Glenn N.F., Hoover A.N. 2012. Transport of biologically important nutrients by wind in an eroding cold desert. *Aeolian Research* 7, 17–27.

Sterk G., Herrmann L., Bationo A. 1996. Wind-blow nutrient transport and soil productivity changes in southwest Niger. *Land degradation and Development*, 7, 325–335

Szatmári, J. 1997. Evaluation of wind erosion risk on the SE part of Hungary. *Acta Geographica Szegediensis.* XXXVI, 121–135.

Szatmári, J. 2005. The evaluation of wind erosion hazard for the area of the Danube–Tisza Interfluve using the revised wind erosion equation. *Acta Geographica Szegediensis*. XXXVIII, 84–93.

Várallyay Gy., Szűcs L., Murányi A., Rajkai, K., Zilahy, P. 1979. Magyarország termőhelyi adottságait meghatározó talajtani tényezők 1:100 000 méretarányú térképe I (Map of pedological factors determining the site conditions in Hungary I). *Agrokémia és Talajtan* 28, 363–384.

Várallyay, Gy., Szűcs, L., Murányi, A., Rajkai, K., Zilahy, P., 1980. Magyarország termőhelyi adottságait meghatározó talajtani tényezők 1:100 000 méretarányú térképe II. (Map of pedological factors determining the site conditions in Hungary II). *Agrokémia és Talajtan* 29. 35–76.

Woodruff, N.P., Siddoway, F.H. 1965. A wind erosion equation. *Soi. Sci. Soc. Am. Proc.* 29, 602–608.

Zobeck, T., Fryrear, D.W. 1986. Chemical and physical characteristics of windblown sediment. *Transaction of the ASAE* 29, 1037–1041.

Zobeck, T., Fryrear, D.W., Petit, R. D., 1989. Management effects on winderoded sediment and plant nutrients. *J. Soil and Water Conservation.* 44, 160–163.

JOURNAL OF ENVIRONMENTAL GEOGRAPHY
Journal of Environmental Geography 6 (3–4), 21–29.
DOI: 10.2478/jengeo-2013-0003
ISSN: 2060-467X

INVESTIGATION OF DAILY NATURAL AND RAPID HUMAN EFFECTS ON THE AIR TEMPERATURE OF THE HAJNÓCZY CAVE IN BÜKK MOUNTAINS

Beáta Muladi*, László Mucsi

Department of Physical Geography and Geoinformatics, University of Szeged, Egyetem u. 2-6, H-6722 Szeged, Hungary
*Corresponding author, e-mail: muladi@geo.u-szeged.hu

Research article, received 28 August 2013, accepted 7 October 2013

Abstract

The aim of this study the authors measured and analyzed the effect of the exterior daily temperature change on the interior temperature in a dripstone cave visited by cavers exclusively. The measurement was carried out in the Hajnóczy Cave located in the southern part of Bükk Mountains in Hungary. Although only one entrance is known, there are more evidences for the strong effect of exterior conditions on the interior processes like temperature fluctuation and dripstone development. Using high resolution wireless digital thermometer sensor network the air temperature and air humidity were measured in 32 points in every 10 minutes for long time but now the data of a 8-days period were analyzed. Based on these data different zones of the cave could be separated and during summer conditions the climatic variability of the entrance transitional and deep cave zone was described. Based on statistical analysis of spatial information significant correlation was found between the exterior temperature fluctuation and that of such a cave chamber, which is relatively far from the cave entrance. This fact proves that existence of a fissure system which is permeable for air but not passable for cavers. During the measurement the human effect was also analyzed and 0.3-0.6 °C temperature rising was recognized for a short time. Because of the surface vicinity the effects of the environmental change can have sensible impact on the cave and its natural phenomena. Among others temperature rising, air humidity decreasing were detected in present study.

Keywords: cave temperature, wireless sensor network, Hajnóczy Cave

INTRODUCTION

The macroclimate is the determining factor for karst development and formation of surface and subsurface processes. Beside the general macro scale processes, however the microclimate factors have important effects on ecological mechanism and other natural processes like corrosion, erosion, dissolution. Generally it can be stated, that the microclimate has an impact on cave morphology, biology (flora and fauna), and management. The scientific research started mainly in mid 20th century with the investigation climate of caves and its influence upon cave organisms (Poulson and White, 1969). Jakucs (1977) investigated the connection between microclimate factors and chemical processes in soil and limestone layer. de Freitas and Littlejohn (1987) analysed the impact of cave microclimate upon sensitive cave fauna and cave management. The 3-zone model has been developed to describe the general zones of climatic variability within a cave (Cropley, 1965; Poulson and White, 1969; Fodor, 1981). According to this 3-zone model, a twilight zone exists near the cave entrance with greatest variability in microclimate parameters. Moving from the entrance towards the interior of the cave, the influence of exterior climatic conditions diminishes and a middle zone exists in complete darkness with some variability in cave microclimate. Further in the cave, at the rear, a deep cave zone exists with constant microclimatic conditions (Gamble et al., 2000).

The great improvement achieved in the last decades are mainly due to the new technology and particularly to the inexpensive data loggers which record unattended a great number of data. At the same time, the financial support of some show caves to carry on environmental researches and to evaluate the visitors' capacity was instrumental in the development of cave climatology (Hoyos et al., 1998; De Freitas et al., 2006; Lario and Soler, 2005). The high resolution microclimate study can give very useful spatial information about the air mass movement not only in the show caves but in such caves which are used and investigated only by researchers (Cigna, 2002). New entrances, new interior passages can be found according to the analysis of detailed spatial information based on microclimate measurement.

STUDY AREA

The Hajnóczy Cave is located on the South-Western part in Bükk Mountains (*Fig 1*). The cave was formed in Middle Triassic Ladinian and Upper Triassic Karnian cherty grey limestone. The cave entrance can be found on the Odorvár hill slope at 475 m above the sea level.

Odorvár (574 m) is a limestone hill situated in the western side of the valley of the Hór creek. The "odor" word means area with hollows. The total length of its corridors is cca. 4257 m, the vertical difference between the highest and deepest points is 125 m (*Fig 2*.).

Fig. 1 Bükk Mountains (Mucsi L.)

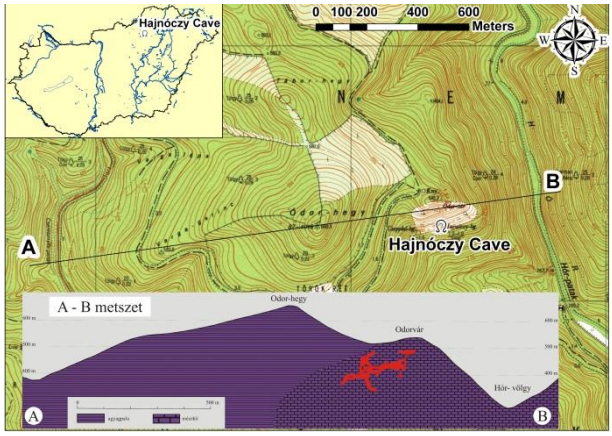

Fig. 2 Hajnóczy Cave location on topographical map (Muladi B.)

The air temperature measurement was carried out in the two morphologically distinguishable parts of the cave (Varga, 2003).

The first investigated area was the entrance part of the cave, which can be characterized by narrow corridors. After this part the cave halls were formed along bedding planes by karstic corrosion. This kind of passage system, which is rich in narrow corridors, continues from the cave entrance through The House-top (Háztető) and Ruin hall (Rom-terem) to the Great hall (Nagyterem). This part can be described as a labyrinth, in which the distance between the bottom and ceiling of the halls is continuously increasing.

Further part of the cave can rather be described as part of large halls formed by erosional processes and by small corridors which connect these halls. This part contains the Leyla, and the very narrow passage Almond (Mandula) called after its cross section shape. After the Almond passage the Gallery of 10-15 m high hall follows. This is one of the most beautiful halls of the cave because of the uncountable stalagmites. The largest hall of the cave called as The Giant hall is the last hall on this west-eastern part of the cave. The horizontal dimension of this hall is 62*16 m, while the vertical dimension is 10-12 m. The ceiling of the Giant hall is very near to the surface as shown by the tree roots that can be seen on the walls. The western part of the cave can be found in limestone layers which are covered by older dark grey shale.

The Hajnóczy Cave was discovered in 1971, and the mapping and the scientific investigation started immediately after its discovery. The first air temperature measurement campaign was executed by Miklós, G. and Városi, J. from 1975 to 1977. According to their measurements the air temperature ranged from 8.5 °C to 10.5 °C. The relative humidity was higher than 98% on average, but there were wetter and drier halls in the cave. Up to now is observable the fact that the halls near to the surface are drier, while the halls and corridors deep under the surface are more wet.

If the difference between the cave and surface air temperature is about 10 °C, then the amount of the moving air is cca. 0.4 m^3/s. The velocity of the air ranges from 5 to 25 cm/s, and at the entrance part it was 20-40 cm/s, while the air flow impulsion reached 50 cm/s (Miklós, 1978).

DATA AND METHODS

Present research activity started in December 2011. Almost 2 years of continuous measurements have resulted in detailed information about the annual trend of the cave air temperature and main features of cooling and warming processes (Muladi et al., 2012). Aim of our study was to determine the spatial profile of air temperature of the cave developed during summer air circulation period in July 2012. Horizontal air movement and vertical lamination could be identified because digital equipment was installed in the cave at the same time, in different halls and corridors. The air humidity was also measured beside the air temperature.

Fig. 3 UC Mote Mini (Muladi B.)

UC Mote Mini low power wireless sensor module developed at the University of Szeged was used for our measurements (*Fig. 3*). This device promotes IEEE 802.15.4/ZigBee wireless communication protocol in order to realize a low data rate. The radio module can operate at a data rate of 250Kbps in ISM 2.4Ghz band. The control is regulated by 16 MHz Atmel ATmega128RFA1 microprocessor with 128kB RAM. Several types of sensors are integrated into this device.

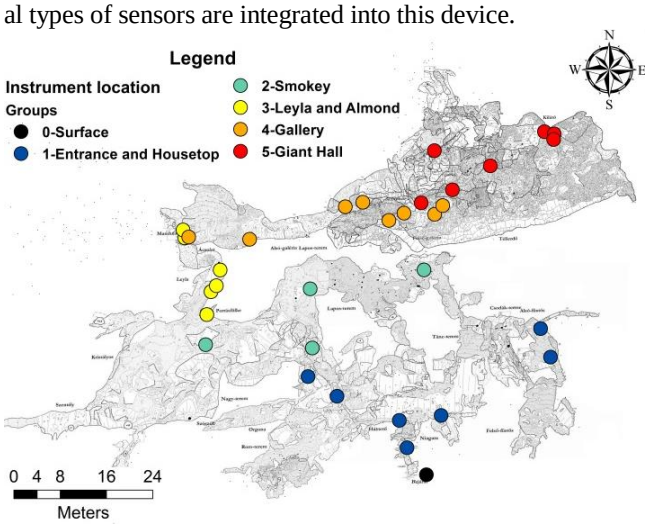

Fig. 4 Hajnóczy Cave map and devices location

The accuracy and the scale of SHT21 temperature and the humidity sensor are ± 0.3 °C, 0.01 °C and ± 2.0% RH, 0.04 % RH, respectively. Data collection can be realized with 2MB external flash TinyOS, which is a small open-source energy-efficient software operating system, supporting large scale self-configuring sensor networks. The device is powered by LIR2450 battery (Senirion, Datasheet SHT21). During our study, data were recorded in every 10 minutes. The sensors could be used for more than 3 months without battery replacement.

The data obtained every 10 minutes were evaluated using a matrix of correlation coefficients. First, data were averaged according to hour and day, resulting in a new dataset. Then these data were processed with pair wise correlation coefficients in order to investigate the direct and indirect relationships among cave airflows.

The temperature and relative humidity of cave air were detected using 32 sensors (14 of them can also measure air pressure) in Hajnóczy Cave. In each case one of the sensors was placed near the cave entrance to measure surface temperature *(Fig. 4).*

RESULTS

According to the direction of the air movement the Hajnóczy Cave is rather a through cave then a big cave, apart from the fact that it has only one known entrance. One part of the main halls is situated in relatively higher position to the entrance and these halls are near to the radiated southern hill slope. So during summer meteorological conditions, when the exterior air mass is always warmer than the air in the cave, the cooler and heavier air mass of the cave is continuously flowing out through the cave entrance. At the same time warmer exterior air moves to the cave through the fissure system in the limestone layers. In this case 3-4 °C difference can be measured in the air temperatures in different parts of the cave.

The minimum air temperature was 8.2 °C during the summer measuring period which is equal to the annual mean temperature of this hilly region. Because of the insulating effect of the buried limestone layer (in some places its thickness is less than 4-5 m) the maximum air temperature was higher than 11.2 °C. In 1975-77 the air temperature measurement was carried out by analogue instruments but the results can be compared to our data which were collected by digital thermometers. The air temperature ranged from 8.5 to 10.5 °C that time, which means that there is no significant difference between the data of these two datasets.

The 0.7 °C difference between the maximum values can be the reason for the higher monthly mean temperature on July 2012 (24.1 °C) compared to the lower monthly temperatures measured in 1975-77 (20.6-22 °C).

The results of the analysis of air mass movement and the effect of the exterior air to the air temperature of the cave is presented in this paper. The results are based on the data which were collected from 01st July to 09th July 2012.

Surface, Entrance and Housetop, Smoky

One thermometer was installed near to the cave entrance to measure the temperature of the exterior air mass. During the measuring period the maximum values ranged between 33 and 35 °C, while the minimum values changed between 13 and 23 °C (*Fig. 5b*).

During the summer air circulation period the air mass is flowing out from the cave through the total section of the entrance. The passages near the entrance are sink-like, because the surface conditions have an effect on the air temperature just within the first few meters from the entrance. The influence of the convection is so intensive in this part of the cave, that the effect of a visiting group could not be measured. After the entrance part, where 3-4 smaller halls are located, the velocity of the air mass decreases, so vertical lamination of the air mass can be proved by the decreasing air temperature. The sensor located very near to the entrance measured 10.8-10.9 °C with slightly traceable daily fluctuations (No. E1 on *Fig. 5b*). The following sensor detected almost with 2 °C lower air temperature about 5 m from the entrance. The graph of this data also show daily fluctuation, but the difference between the minimum and maximum values is less than 0.1 °C. At the Housetop the air temperature was changed between 8.2 and 8.3 °C without any daily fluctuation (No. E3 on *Fig. 5c).*

The Lower and the Upper Smoky halls are located east to the Housetop in the labyrinth-like part of the cave near to entrance. They called after the black colour walls, which might be the results of the manganese content of the stalagmite coverage.

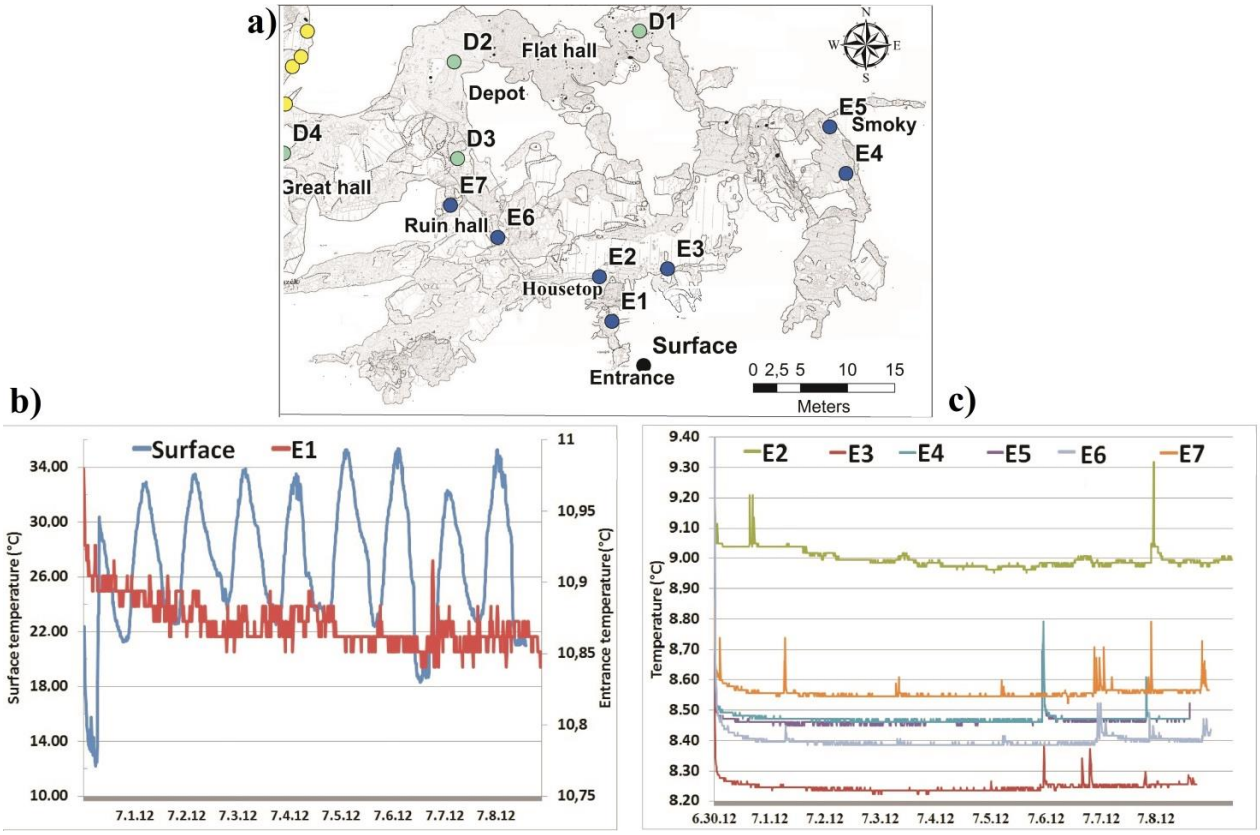

Fig. 5 Sensors location (a) Surface and entrance (b), Housetop, Smokey and Ruin hall (c) temperature data (°C)

The Upper Smoky hall is relatively dry because of its closeness to the surface. The Lower Smoky hall has a narrow connection to the Upper Smokey hall, and it is a "bag-like" place, where constant air temperature (8.4 °C) was measured (No. E4, E5 on *Fig. 5c*).

The Ruin hall is situated west to the Housetop-between entrance zone and Depot hall as transitional zone between them. Two sensors were installed in this hall (No. E6, E7 on *Fig. 5a*), and the air temperature ranged from 8.4 to 8.55 °C in the analysed period without any daily fluctuation. The sensors were located near to the cavers pathway so human heat radiation sometimes increased the air temperature with 0.1-0.2 °C (No. E6, E7 on *Fig. 5c*). The position of the Ruin hall is similar to the Lower Smokey hall; both are big-like room in which the air temperature does not change in a short period.

The Ruin chamber is connected with the Great chamber by the Depot. The Depot is the first room in which the cavers can deposit their measuring and research equipment onto a horizontal surface safely. From the Depot the pathways forks, one path leads to the Great chamber, the other one goes back to the Lower Smoky room through the Flat chamber.

The Depot steeply leads down from the Ruin chamber to the Great chamber. Few years ago the cavers climbed out a chimney-stack over it. This almost vertical passage was called White fox chamber.

During the summer measurement 2 sensors were deposited in Depot (No. D2, D3 *Fig. 6a*), one on the top and one on the bottom. A third sensor was hanged in the middle part of the Flat chamber (No. D1 *Fig. 6a*). Cold air mass (8.3 °C) was in stable situation on the bottom without any daily fluctuation (see graph labelled D2 on *Fig. 6b*), while the warmer air temperature was measured on the top of this chamber (8.8 °C).

The Flat hall (Lapos-terem) is located further on the entrance but the temperature data of the sensor situated in this hall (D1 on *Fig. 6b*) show very strong influence of surface. The daily fluctuation of the air temperature is not so high (ΔT=0.12 °C) but it was detectable by the sensor.

Peaks on the graphs are the effects of the visiting groups on air temperature. For a short period the air temperature was higher with 0.1 and 0.3 °C in the Lower Smokey hall after visits of 3 cavers on 6th and 8th July 2012 (*Fig. 7*). The Flat hall has smaller air volume because the average height of this hall is about 70 cm so the human effect on air temperature was more significant ((ΔT=0.2-0.4 °C) after the visiting of 4 persons on 7th July (*Fig 7*).

It was very surprising to observe clear daily temperature fluctuation during summer air circulation condition in the Flat hall which is located far from the cave's entrance. Miklós and Városi supposed that the air mass is moving from the Giant hall toward the entrance (Miklós, 1978). The distance between the Giant hall and the Flat hall is large and the air mass velocity in the cave is low consequently air convection from the Giant hall would not have an effect on the air temperature of the Flat hall. Subsequently, there has to be a connection between the surface and the Flat hall through an unknown entrance or through the fissure system and cave passages.

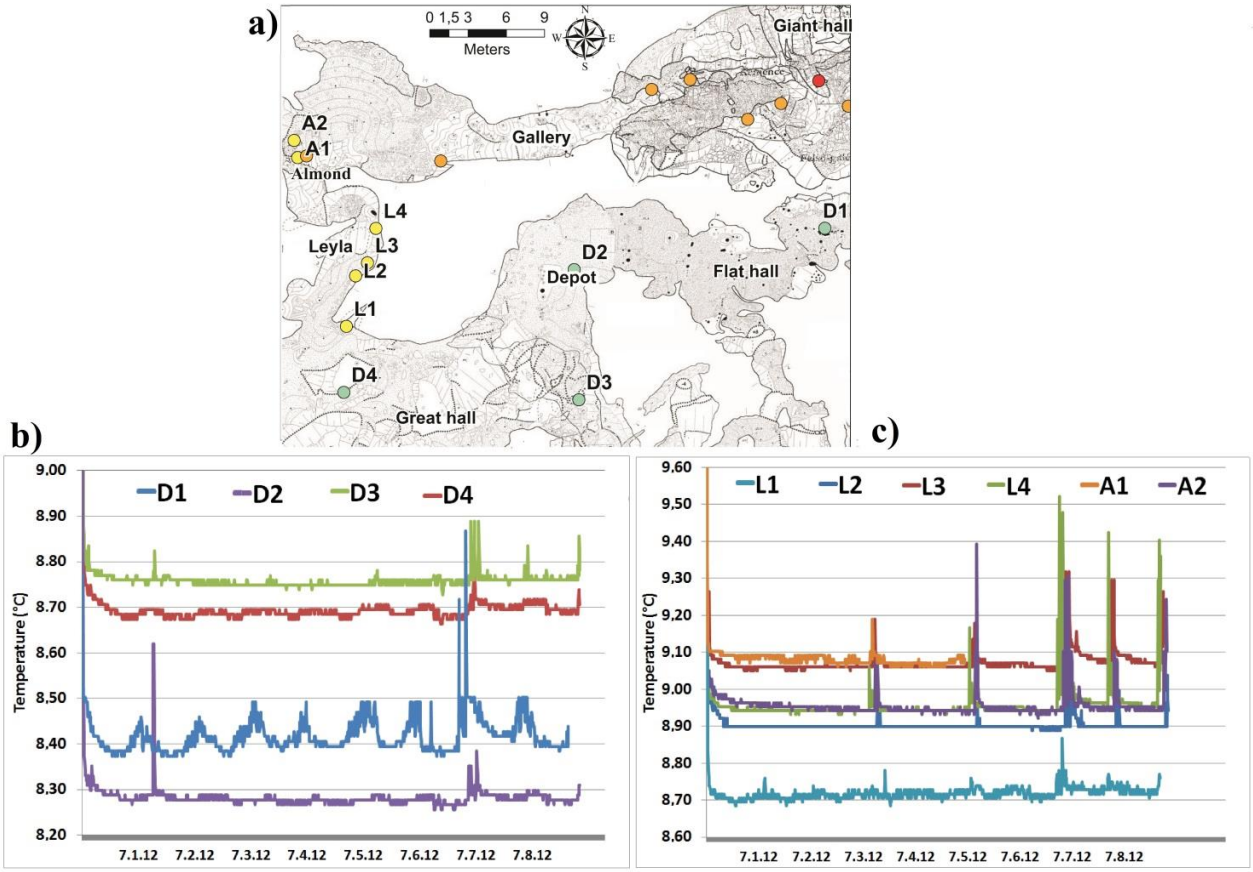

Fig. 6 Sensor location (a) Depot and Great Hall (b) and Leyla and Almond (c) temperature data (°C)

To prove our assumption first of all the correlation between the surface and Flat hall's temperature was calculated. Foremost the graphs were smoothed using following equation:

$$T_i=(\text{sum } T_{i-j})/11 \qquad j=-5,\ldots,5$$

where

T_i = average temperature in a given time (i)

The daily maximum temperature value in the Flat hall was reached at a later time than the maximum value of surface temperature. This time-lag was fluctuating daily as a function of the difference between the daily maximum and minimum surface temperature. The minimum delay was 1.3 hour, and the maximum delay was 4.8 hour.

The correlation between for the daily temperature values of the Flat hall and surface was calculated using the sliding cross correlation method. The correlation coefficient (r) expresses the strength of the relationship between the two variables.

$$r=\frac{\sum(x-M_x)\cdot(y-M_y)}{\sqrt{\sum(x-M_x)^2\cdot\sum(y-M_y)^2}},$$

where

M_x is the mean of the x, and M_y is the mean of the y variable.

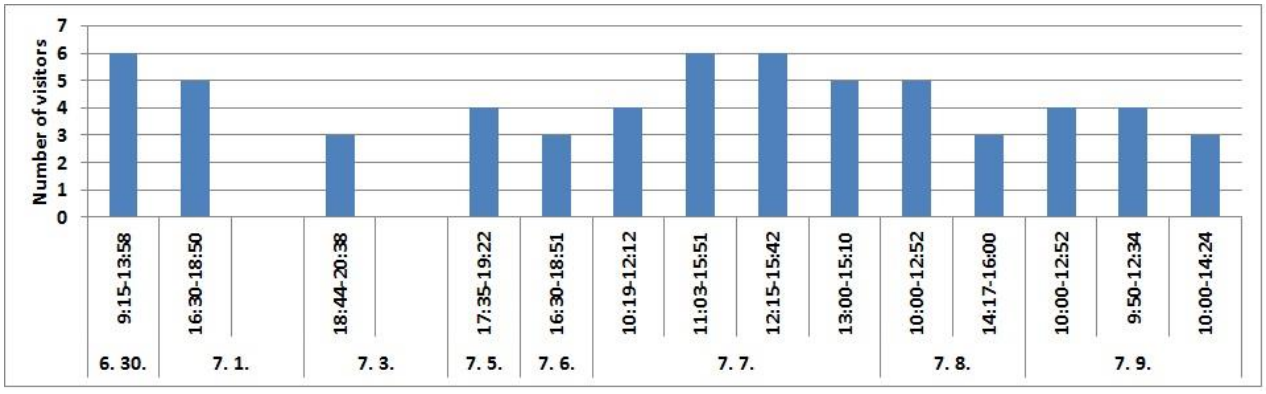

Fig. 7 Number of cavers in the cave (Source: Leader of the Hajnóczy József Speleological Research Group)

Table 1 The differences of the time and temperature

Date	1-Jul	2-Jul	3-Jul	4-Jul	5-Jul	6-Jul	7-Jul	8-Jul
Time difference based on sliding correlation	2.5	4.8	4.1	2.1	4.5	1.3	1.7	1.3
Daily surface temperature difference	11.3	10.6	10.2	9.8	12.1	15.9	13.4	14.4
Maximum sliding correlation	0.90	0.94	0.86	0.85	0.89	0.85	0.96	0.88

The correlation coefficient (r) can be ranged between -1 and 1. If the value is close to -1 or one there is a strong connection between the values, if it is close to 0 the connection is random. A positive value indicates a positive connection, while a negative value indicates a negative relationship (Péczely, 1979).

The 8 day analysing period was divided into 8 segments considering the measured time-lags, and then the correlation coefficient was calculated for the daily values. According to the cross-correlation method, the maximum value of the daily correlation coefficient ranged between 0.85 and 0.96 (*Table 1*), consequently there is a significant connection between the daily temperature values of the Flat hall and that of the surface.

The highest correlation coefficient was shown at different time-lags in this period. Miklós and Városi stated 35 years ago that there can be strong connection between the highest outer air temperature value and the value of the cavern air velocity. According to our statistical analysis a strong opposite relationship exists between the difference of the maximum and minimum surface air temperature (ΔT) and the length of time-lags (LTL). The following function defines the numerical connection between time-lag (dependent variable) and ΔT. (*Fig. 8*)

$$LTL = -0{,}4279\ \Delta T + 8{,}0142$$

The correlation coefficient r is equal to -0.64, which shows negative correlation between these parameters.

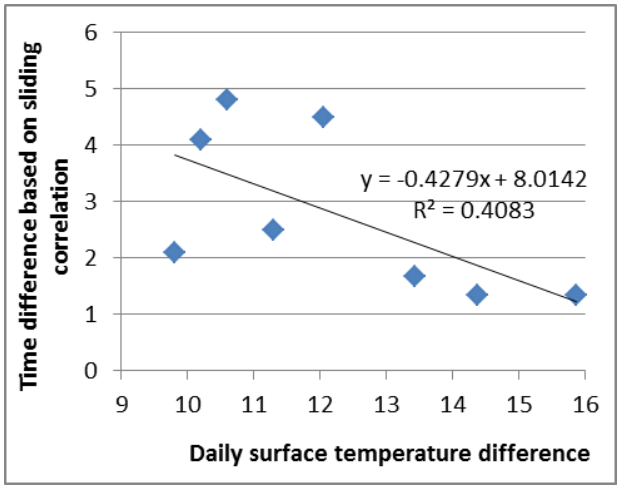

Fig. 8 Time difference based on sliding correlation and daily surface temperature difference

We proved that the air temperature is affected by the outer air mass in the Flat hall, which is located far from the entrance. If the air is moving out from the cave through the entrance there has to be one or more paths in which the outer air masses can reach into the cave. One of these paths might be the passages which connect the Upper Smokey hall with the Flat hall. The other more probable pathway is the White fox chamber, which is a vertical passage above the Depot hall. During the discovering of this chamber, the researchers found animal bones. These bones were washed into the cave many years ago, indicating that there has to be an open fissure system somewhere above the currently known entrance. The thickness of the limestone layers has to be less than 5-6 m. This value is based on the data of the cave map of high accuracy and digital elevation model calculated from stereo aerial imageries. The spatial distance between the supposed end of the fissure system on the surface and the sensor location is cca. 40-50 m, therefore the velocity of the passing air has to be cca.0.5-1 cm/s if we calculate by the known time-lags (1.3-4.8 hours) (*Fig. 9*).

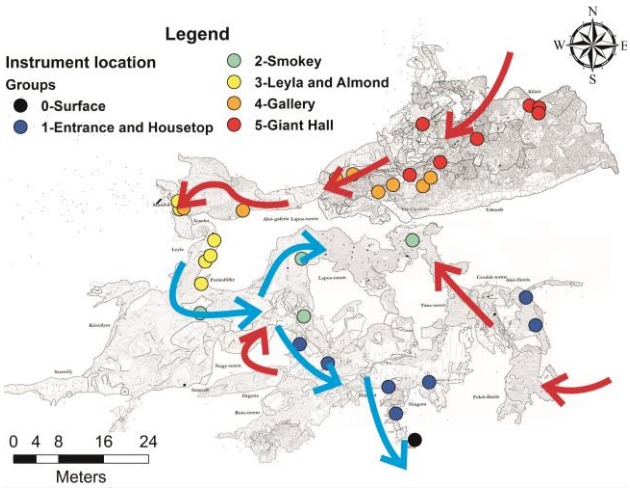

Fig 9 Hajnóczy Cave atmospheric circulation

The Great chamber is the largest chamber in the cave's first zone (48 m long, 14 m wide and 5-8 m heigh). There are few stalagmites in it and calcite crystals on the wall of a dried out pond (*Fig. 10*).

Daily fluctuation of air temperature can be seen on the graph belongs to the data measured in this chamber (No. D4 *Fig. 6b*), so we can take it that the exterior air can directly reach this chamber through the fissures above it.

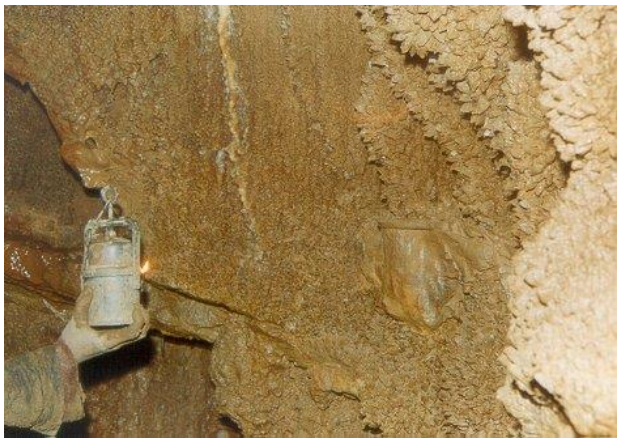

Fig. 10 Great chamber calcite crystals on the wall (Mucsi L.)

The Leyla and the Almond passage are found on the north eastern part of the Great chamber. This is the way to the main section of the cave, what contains the for example the Grand Canyon and the Tsitsogó on its western part and Gallery and Giant chamber on the eastern part of it. The Almond passage was closed by limestone and shale agglomerate for thousands years until 1977, when the cavers broke through that (*Fig. 11).*

The highest value of the velocity air convection can be measured in the Almond passage in the Hajnóczy Cave, because large volume of air mass has to move through on a tunnel whose cross section is less than 0.25 m^2.

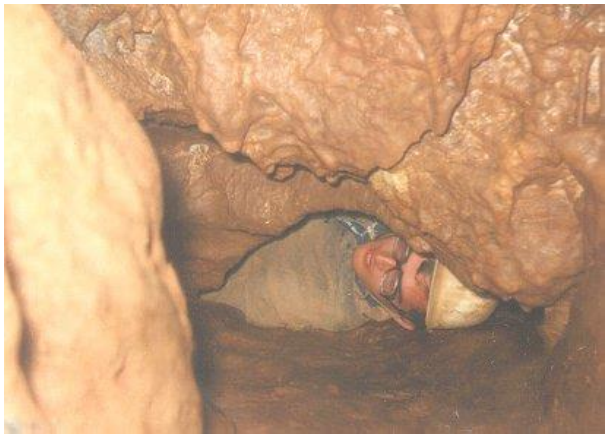

Fig 11 Almonds passage (Miklós G.)

Miklós and Városi measured 20-40 cm/s air velocity in Almond in 1977. The air is flowing from the Gallery toward the entrance in summer. The air temperature ranged between 8.7 and 9,1 °C in July 2012 with a fine daily fluctuation. Because of the tight cross section of the Almond passage the temperature increasing effect of the visitors (cavers) can be measured and the rate of temperature rising is 0.5-0.6 °C.

Gallery

The Gallery is one of the most beautiful parts of the cave. Its dimensions are: 70 m long, 1-8 m wide and 4-13 m high (*Fig. 12*). The reason for the stalagmite formation is the vertical position of thin limestone layers. Large amount of infiltrating saturated karst water can get into the cave along the limestone layer and after the dropping from the ceiling to the bottom of the hall the stalagmites (columns) grow bigger. Miklós and Városi measured a little bit higher air temperature in the Gallery in 1975 than in the entrance part, but the position of the measuring equipment is unknown. Therefore 7 sensors were utilized in our measurement in 2012 and vertical lamination of the relatively calm air mass was detected (*Fig. 13*). The measured air temperature values are higher than that of the deeper parts of the cave, because upper part of this chamber is not so far from the eastern slopes of Odorvár.

Fig. 12 Gallery stalagmite formation (Mucsi L.)

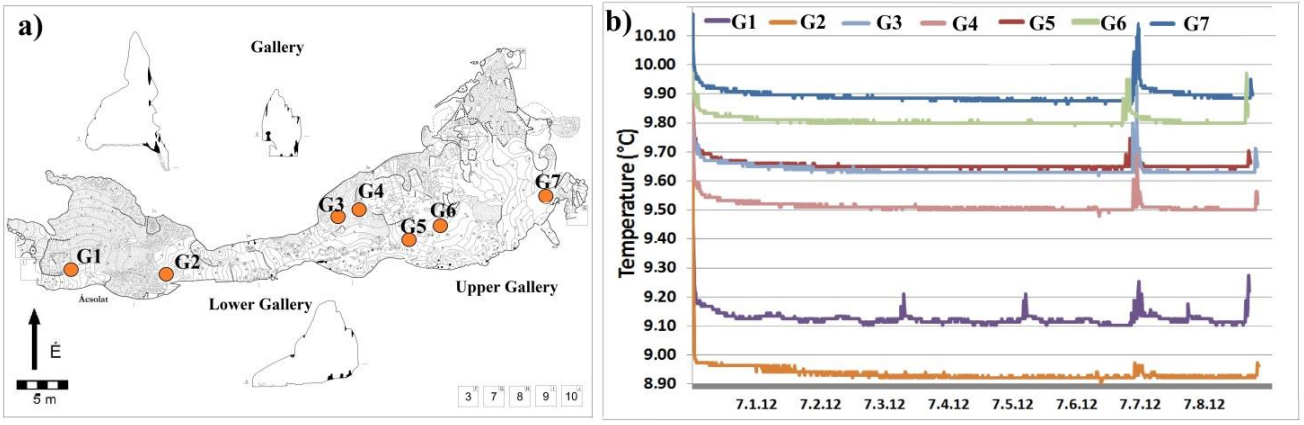

Fig. 13 Gallery's sensors location (a) and temperature data (b) (°C)

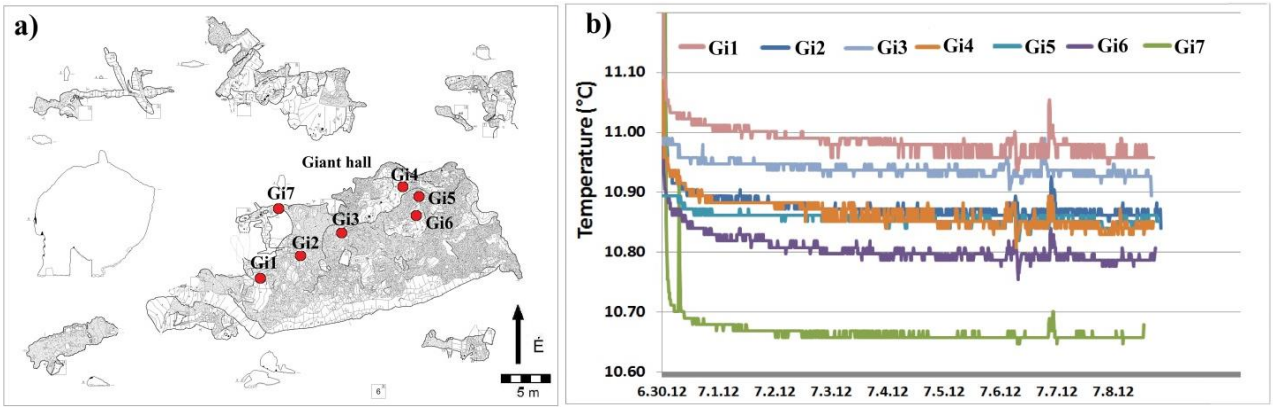

Fig. 14 Giant Hall's sensors location (a) and temperature data (b) (°C)

Giant Hall

The entrance to the Giant chamber can be reached from the eastern end of Gallery through huge collapsed rock blocks. Almost whole skeleton of Ursus deningeri was found near to these blocks in the Upper Gallery under a 3-5 cm thick dripstone layer. This fact also proves the vicinity of the surface. The Giant chamber is the largest chamber of the Hajnóczy Cave (63 m long, 16 m wide and 14 m high).

The Giant chamber is the driest part of the cave because it has very small catchment area, and the air humidity is lower because of the relatively high air temperature (10.67-11 °C). This is the reason of the thin limestone layer. The tree roots can reach the ceiling of the Giants hall (*Fig 14*).

The reason of this is that there is a thin limestone layer above this cave chamber proved by the tree root hanging from the ceiling. About 4 m^2 area was covered with bat's guano in 1980's, when this chamber was discovered and few flying and hanging bat can be seen in this part of the cave which is also the evidence of the surface vicinity. Because of the low air humidity and few seeping water some of the formerly "living" dripstone phenomena died now. According to the maximum temperature values (11 °C) measured in 2012 compared to the data from 1975 (10.4 °C) the temperature rising can be recognized. Because of the proved strong connection with the surface the cause of this temperature rising is the effect of very hot summers of last decades. Unfortunately due to the lack of the long term temperature measurement the potential effect of the global warming can be hardly proved.

CONCLUSION

Temperature observations were collected inside the Hajnóczy Cave in order to characterize microclimate of a temperate zone cave system in summer condition. The applied wireless sensor system operated well. Cavers affected rapid temperature rises were detected and small scale daily fluctuation was also revealed. Some general characteristics of cave system can be drawn from these observations that concur with existing temperate cave microclimate theory. The first characteristic is that external atmospheric disturbances can affect temperatures of cave system. The daily fluctuation can be observed far from the entrance, which proves new unknown connection of this chamber with the surface. The former air circulation system described on min 1970's by Miklós and Városi was updated according to the measurement carried out in 2012.

The second characteristic is that interior air mass is laminated on bigger chambers of the cave where the natural ventilation does not work. Thirdly it has been recognized that the exterior warm air can reach the upper passages of the cave through the fissures in limestone layer and rises the mean air temperature of the cave (8.5 °C) with 2.5 °C in the Giant chamber.

Therefore the air circulation of the cave system is rather similar to the air circulation of a multi-entrance system. Because of this open system the cave is very sensitive to the effect of the rapid climatic processes and to global climate change in long term.

Acknowledgement

We would like to express our appreciation to all those who contributed to our work. Special thanks goes to Dr. Miklós Maróti, Zoltán Csépe, Csaba Varga, Ákos Mező and Károly Barta for their help.

The instruments were provided by the TÁMOP-4.2.2/08/1/2008-0008 supported by the European Union and co-financed by the European Social Fund

This research was supported by the European Union and the State of Hungary, co-financed by the European Social Fund in the framework of TÁMOP 4.2.4. A/2-11-1-2012-0001 'National Excellence Program'.

References

Cigna A.A. 2002. Modern trend in cave monitoring, *Acta Carstologica* 31 (1), 35–54.

Cropley, J.B. 1965. Influence of Surface Conditions on Temperatures in Large Cave Systems. *NSS Bulletin* 27 (1), 1–10.

De Freitas, C.R., Littlejohn, R.N. 1987. Cave climate: assessment of heat and moisture exchange. *International Journal of Climatology*, 7, 553–569.

De Freitas C.R., Littlbjohn R.N., Clarkson, T.S, Kristament, I. S. 2006. Cave climate: Assessment of airflow and ventilation *Journal of Climatology* 2 (4), 383–397.

Fodor, I. 1981. A barlangok éghajlati és bioklimatológiai sajátosságai (The climatic and bioclimatological

characteristics of the caves), Akadémia Kiadó, Budapest, 168–169.

Gamble, D.W., Dogwiler, J.T., Mylroie, J.E., 2000. Field assessment of themicroclimatology of tropical flank margin caves. *Climate Research*, 16, 37–50.

Hoyos, M., Soler, V., Can˜ averas, J.C., Sa´nchez-Moral, S., and Sanz-Rubio, E., 1998. Microclimatic characterization of a karstic cave: human impact on microenvironmental parameters of a prehistoric rock art cave (Candamo Cave, northern Spain): *Environmental Geology*, 33, 231–242.

Hoyos, C.D., Agudelo, P. A., Webster, P. J., Curry, J. A. 2007. Deconvolution of the factors contributing to the increase in global hurricane intensity, *Science* 312, 94–97.

Jakucs, L. 1977. Morphogenetics of karst regions: variants of karst evolution, Akadémia Kiadó, Budapest, 16–19.

Jakucs, L. 1999. Tüdő asztma és szpeleoklimatológia (Lung Asthma and Speleoclimatology) IN Tóth, J., Wilhelm, Z. (ed.) Változó környezetünk Pécs, 165–181.

Miklós, G. 1978. A Hajnóczy-barlang mikroklímája (The mikroclimate of the Hajnóczy Cave), *Karszt és Barlang* I-II. füzet, Budapest, 11–18.

Mucsi, L. 1992. Karsztmorfológiai vizsgálatok Orvár környékén, Különös tekintettel a különböző kőzetadottságú felszínekre (Investigation of karst morphology in Odorvar, Specific reference to difference surface rocks), Szeged, 18–22.

Muladi, B., Csépe, Z., Mucsi, L., Puskás, I. 2012. Application of wireless sensor networks in Mecsek mountain's caves IN Proceedings of the 13th National Congress of Speleolgy, Moutathal, Schweiz, 131–137.

Poulson, T.L., White, W.B. 1969. The cave environment. *Science* 165, 971.

Senirion, Datasheet SHT21. Humidity and Temperature Sensor IC http://www.sensirion.com/en/products/humidity-temperature/download-center/

Varga, Cs. 2003. Hajnóczy-barlang (Hajnóczy Cave) In Székely, K. (ed.) Magyarország fokozottan védett barlangjai Mezőgazda Kiadó, Budapest, 200–204.

JOURNAL OF ENVIRONMENTAL GEOGRAPHY
Journal of Environmental Geography 6 (3–4), 31–37.
DOI: 10.2478/jengeo-2013-0004
ISSN: 2060-467X

INLAND EXCESS WATER PROJECTION BASED ON METEOROLOGICAL AND PEDOLOGICAL MONITORING DATA ON A STUDY AREA LOCATED IN THE SOUTHERN PART OF THE GREAT HUNGARIAN PLAIN

Károly Barta*

Department of Physical Geography and Geoinformatics, University of Szeged, Egyetem u. 2-6, H-6722 Szeged, Hungary
*Corresponding author, e-mail: barta@geo.u-szeged.hu

Research article, received 2 February 2013, accepted 5 June 2013

Abstract

The research investigated the process of excess water formation. Complex measurement stations were developed in order to determine the most important hydro-meteorological and soil factors contributing to the formation of excess water. The stations measure the amount of precipitation, evapotranspiration, evaporation from water surface, soil moisture in 3 different depths; soil temperature in 5 different depths; furthermore, soil water level. The study area is located in the southeastern part of Hungary, near Szeged, in the flood plain of Tisza and Maros with extremely clayey soils. The former soil data were completed by new soil survey to determine several soil parameters (e.g. bulk density, porosity, field capacity, saturated hydraulic conductivity). Infiltration was calculated from the measured parameters and water budget elements of bigger rainfall event were analyzed between March 2010 and August 2011. Genetic types of excess water can be separated based on the data.

Keywords: excess water, infiltration, water budget, soil

INTRODUCTION

The two most frequent type of inland excess water formation are the upwelling (or vertical) type (due to the increasing groundwater table) and the accumulative (or horizontal) type (the water accumulates under gravity in the lowest areas due to limited infiltration and/or runoff, independent from the groundwater table or communicating by capillary system). This type of inland excess water is often caused by inadequate agrotechnic methods which can lead to soil structure degradation, e.g. soil compaction. These degradation processes can be noticeable all over the world where you can find any agricultural activities. Based on data of JRC IES (Joint Research Centre Institute for Environment and Sustainability, Ispra) the soil compaction affects 94 million ha only in Europe, almost 10% of the continent. Several studies deal with this problem (Hamza and Anderson, 2005; Ndiaye et al., 2007) mentioned both the effects of agricultural machines and overgrazing as well. Clayey soils are particularly sensitive to compaction that can step up the probability of inland excess water (Birkás, 2011; Birkás et al., 2009).

In the last years a lot of methods were developed to determine the spatial extent of inland excess water hazard, as a result of which maps with small spatial resolution were born (Thyll and Bíró, 1999; Körösparti et al., 2009). There is an increased need in humid years for a detailed projection of the extent and location of inland excess water formation in a better resolution. The projection and the monitoring require an elevation model of high resolution and the exact data of groundwater level. Furthermore, the projection of accumulative inland excess water needs the monitoring of water budget parameters (precipitation, infiltration, evapotranspiration, soil moisture etc.) in a high spatial resolution apart from the knowledge about the basic soil parameters.

A complex monitoring system was developed firstly to get detailed knowledge about the formation of the phenomenon, furthermore, to project the future inundations based on the measured data series. A further question was if the method is able to distinguish the upwelling and accumulative types, and to determine the weight of the affecting factors in the formation of groundwater and the rise of the groundwater table (the role of local infiltration, vertical groundwater flow, soil frost etc.). The method was tested on study areas in the Marosszög microregion. The paper focuses on the technical and methodological development of the monitoring system and the results of the monitoring.

TECHNICAL PARAMETERS OF THE MEASUREMENT STATIONS

The complex measuring unit was set up using 1 precipitation measuring unit, 2 lysimeters, 1 soil temperature measuring unit, 3 soil moisture measuring unit and 1 groundwater-table measuring unit.

The certain units are determined by the following parameters:

- Precipitation measuring unit: the precipitation is measured with 0.1 mm precision by Reed switch and buckets.
- Lysimeters: the equipments work as weighting lysimeters; PVC trays of 20 cm diameter and 5 cm depth are connected to the scales. In one of the equipment, undisturbed soil monolith with vegetation is placed, the other is filled by water. The former one measures the evaporation of the vegetation of the sampled area (usually crops or meadows), the latter is able to simulate the evaporation of opened water surfaces (and excess water inundations). The weight loss on the scales refers to the evaporation that is counted by the measured data in mass unit compared to the surface of the trays.
- Soil temperature measuring unit: a tube of 50 cm that measures the temperature of the soil in 5 different depths. This unit measures the temperature profile of the soil. Its importance increases in winter and early spring time when the formation or the termination of a soil frost can be monitored.
- Soil moisture measuring unit: TDR soil moisture meters are used that are able to measure over not only the field capacity, but around saturation with a reliable precision. With this method the depth of infiltration can be monitored, the capacity of water intake can be calculated from the unsaturation of the soil, furthermore, the detection of a soil layer, where soil moisture is below the moisture of the capillary zone around the groundwater table and the soil moisture of the (almost-saturated) near-surface layers. The latter has a crucial role in the formation of the accumulative type of inland excess water. The changes in the soil moisture make the estimation of the infiltrated water in mm possible.
- Groundwater-table measuring unit: DATAQUA measuring sensors are implemented to control the level of the groundwater. The exact groundwater data levels control the independence of inland excess water formation from the groundwater.

The sensors measure in an hour interval, and the measured data are transferred to a central server by GPRS connection. The data of the measurement stations are managed online and delivered to PC-s in .xls format.

STUDY AREA AND METHODS

Two measurement stations were set up in the inundated areas between the Tisza and Maros in Maroslele settlement. Measurement station 1 was installed in a meadow called Tápai-rét, Measurement station 2 is located westwards from Batida to monitor an area determined by accumulative inland excess water (*Fig. 1-2*). The investigated areas are located at the boundary of the micro-regions South-Tisza-valley and Marosszög. It is a lowly elevated backswamp area around 78-85 m a. s. l. with an extremely variable precipitation around 530-570 mm/year (Dövényi, 2010). The subsoil horizons are the recent sediments of Maros and Tisza, determined by clay, sandy or silty clay, only the ancient point bars are determined by coarser fractions. The mechanical composition of the upper 50-90 cm of the soils became more extreme due to the soil formation, as a result of which a low permeability layer formed, promoting the formation of inland excess waters. The characteristic soil types are humic Fluvisols and Gleysols, in some places Vertisols, on highly elevated areas Solonetz soils occur (AGROTOPO, 1985-86). The relief of the area is small; due to the fluvial origin remnants, point bars occur in the mostly plain area. In the backswamp areas many close depressions of high extent occur that contribute to the formation of accumulative inland excess water. These factors are further strengthened by anthropogenic facilities: roads covered by asphalt, dirt roads and the levees along the channels (Kozák, 2011).

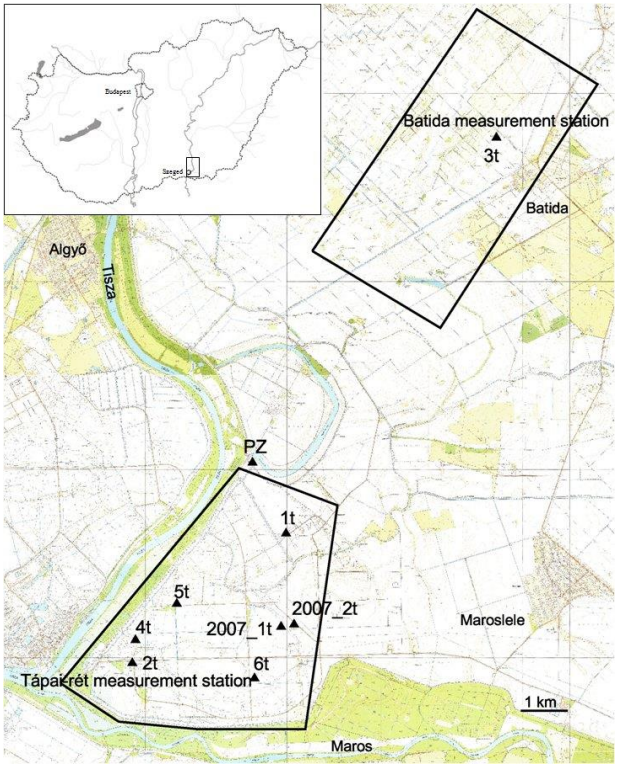

Fig. 1 Measurement stations in Marosszög (2t: Tápai-rét, 3t: Batida). Other marks show the other soil sampling points

Databases and detailed soil measurements were used for the allocation of the measurement stations. The characteristic soil/sediment layers were sampled in a 2 m depth. The main soil parameters (pH, soil plasticity according to Arany, carbonate-, salt- and humus content) and the particle size distribution were measured. In case of the compacted layers (B horizon or plough pan layer) bulk density, porosity, field capacity, actual soil moisture and saturated hydraulic conductivity were determined from undisturbed samples. Based on the particle size distribution, the bulk density and the humus content the characteristic pF values (pF 0; 2.5; 4.2; 6.2) and saturated hydraulic conductivity were determined using pedotransfer functions.

Fig. 2 Installation of the measurement stations

The water surplus on the soil surface can be calculated from the measured and calculated parameters using the following water regime function:

$$R = P - ET - I$$

where:
R: water surplus (mm)
P: measured precipitation (mm)
ET: evapotranspiration (mm)
I: infiltration (mm) (generally calculated from the saturated hydraulic conductivity of the soil horizon with the lowest water infiltration capacity, however, the changes in the soil moisture give more exact estimations from the infiltrating precipitation)

These point measurements can be extended only until the soil patch of the measurement stations, further values of *I* have to be estimated by using available soil maps. In spring and summer of 2010 a more detailed pattern of precipitation measurements would have been needed due to the spatial distribution of weather events (rainstorms, thunderstorms etc.), thus, the measured data of the dike-reeve's houses were implemented in the estimation of the spatial pattern of precipitation.

The calculated water surplus map using the data series of the measurement stations and the digital elevation model of the area allows the projection of the occurrence and extent of the inundations. Although, measurements are made in every hour, due to the temporal dynamics of the process, the method can be used only in the autumn and winter period with low evapotranspiration, and only in areas where almost impermeable (clayey) soil horizons can be found near the surface. In other cases, the spatial projection of the accumulation process will have significant errors.

Data series between March 2010 and August 2011 were used. Due to technical problems, evapotranspiration data are available for short intervals, thus, the water regime calculations are made only for low-temperature-periods.

RESULTS

Analysis of the soil parameters

The most relevant soil parameters effecting the formation of inland excess water were analysed. Using former results of soil measurement, 9 soil profile were investigated altogether. The number of the analysed points was not enough to compile a detailed soil map, however it allowed to outline the overall description of the area. Heavy, non-calcic clay and clay loam soil are characteristic. Salt content of these soils are not signifi-

Table 1 Characteristic soil parameters of the study area (Perneki, 2010; Galbács, 2011)
A: soil sample, K_A: plasticity index according to Arany, TFT: bulk density, P: porosity, vk_{sz}: field capacity, F: saturated hydraulic conductivity

A	B	C (g/cm^3)	D (v/v%)	E (v/v%)	F (m/s)
2007_1t/50-70 cm	51	1.67	37.2	17.1	1.20E-08
PZ/0-30 cm	60	1.55	40.4	17.0	1.60E-06
1t/50-70 cm	51	1.67	37.2	34.8	1.20E-08
2t/50-55 cm	63	1.61	28.4	21.5	8.00E-10
3t/0-40 cm	50	1.65	37.9	33.9	6.00E-09
4t/50-55 cm	81	1.46	31.8	24.3	9.00E-10
5t/55-60 cm	61	1.65	32.4	24.3	9.00E-10
6t/50-55 cm	95	1.32	31.2	22.8	9.00E-10

cant, only in the deeper layers was detected more than 0.05% salt content. The humus content of the top-soil varied between 1 and 2% in the samples. The soil forming alluvial sediments are characterised by high clay content and low carbonate content in the analysed profile. The only exception is the Batida area, where loess also occurs under the young sediments.

In most of the soil profiles there is a compacted layer, considering as impermeable, which affects the water management properties of the soil (*Table 1*).

There were only a few soil samples, which water permeability was better than 10^{-9} m/s. The evolution of this extreme low water permeability was caused by the extreme soil texture and also by the degrading effect (compaction, texture degradation) of the tillage and the inadequate cultivation technics. These soil properties have important effect on inland water formation, because only a small part of the area is suitable for infiltration. Thus probably the inland excess waters are accumulative type in this area and water can be infiltrated to the ground water on areas where the soils have the better water permeability, on the so-called "hydrological windows", and the water increase the level of the ground water table delayed. Beside these good water permeability soils, the ground water level is controlled by the adjacent Tisza River and the drainage channel network.

On the basis of the analysis, in the Batida area and in the Tápai-rét area the water permeability is very low, thus the *'I'* parameter in the water regime function can considered as 0, practically. Nevertheless, at intensive precipitation events few mm infiltrations can be detected, on the basis of the measurement dataset.

Analysis of data series of the complex measuring station

Soil moisture and groundwater table data are compared in three different depths in case of both measuring stations to analyse the relation of infiltration and groundwater – excess water. The measured data confirmed the previous experiences. In case of Tápai-rét study area, only excess water inundations of groundwater origin occurred in the investigated 1.5 year-period.

In case of Batida study area, accumulative inland excess water was found in spring 2010 (*Fig. 3*). Here, the groundwater table was below 2.5 m at the time of the installation, because the measuring station is located on a 40-50 cm higher elevation compared to its environment, where continuous inundations were observed from autumn 2009. The soil moisture decreased from up to down, thus the infiltrating water surplus hardly reached the 35 cm depth, confirming the presence of the accumulative inland excess water. During the spring 2010, the

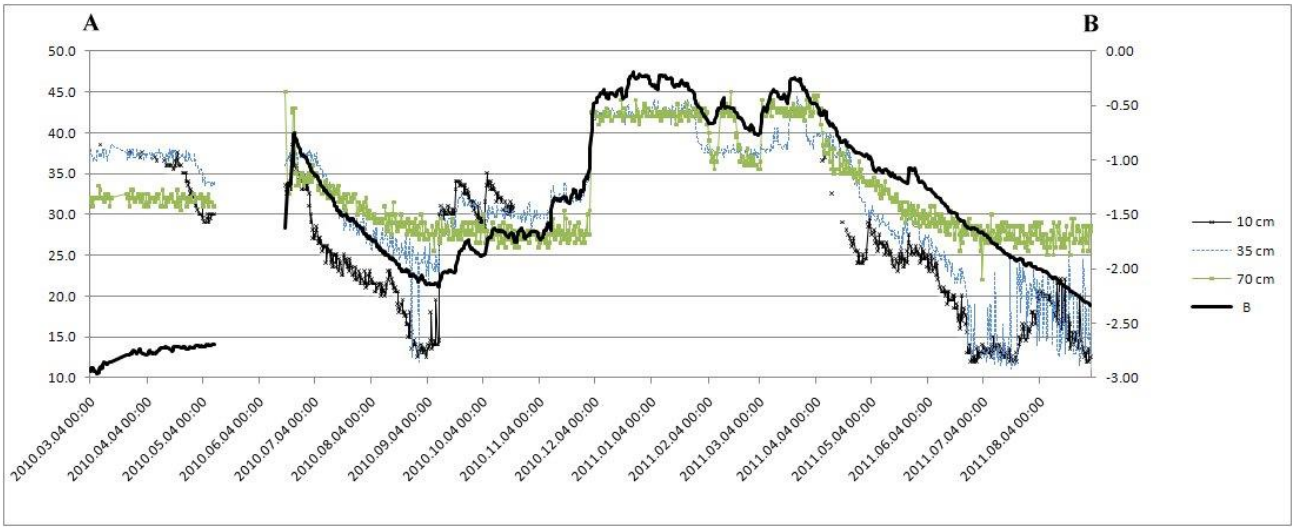

Fig. 3 1.5-year-long data series from Batida measurement station
A: soil moisture in depths 10, 35 and 70 cm (v/v%), B: soil water level below surface (m)

Table 2 The most important rainfall events in Batida
RQ: precipitation, T: temperature, ΔSM1, ΔSM2: soil moisture growth in depths 10 and 20 cm, I: infiltration rate
* the high value is caused by capillary lifting

Date	RQ (mm)	T (^{0}C)	ΔSM1 (v/v%)	ΔSM2 (v/v%)	I (mm)
11.03.2010	8.9	0.5	-	-	0
31.03.2010	7	8-9	-	-	0
05.04.2010	6.6	9.5	-	-	0
19.04.2010	15.4	10-11	-	-	0
10.09. 2010	37.6	17-18	15	5.5	36
16.09.2010	35.8	14-15	3.5	2	11
06.10.2010	41.6	11-12	5	-	10
16-20.10.2010	20.6	9-10	-	-	0
25-28.11.2010	17.1	3-5	2	1.5	7
01-02.12.2010	39.9	2-3	8.5	14.5	46 mm*

increase of the groundwater table was not due to the locally infiltrating water surplus, but the hydrological windows of higher water infiltration capacity in higher distances. Later, due to the humid spring of 2010, the groundwater level was increasing above 1 m below surface for summer, and helped the soil being saturated by the capillary rise. In autumn, the groundwater was decreasing again and the former situation occurred again. After the intensive precipitation of 1st December, the accumulative inland excess water and groundwater level has reached each other. Only the changes of soil moisture due to the precipitation was involved in the calculation of infiltration, thus, the March-April in 2010 and October-November in 2010 were taken into consideration, when groundwater-table was deep enough not to influence the soil moisture by the capillary rise (*Fig. 3*).

The more significant precipitation events, the temperature values influencing evapotranspiration and the increase of the soil moisture in the depths of 10 and 35 cm were selected (the effect of the precipitation events can not be detected in 70 cm depth). The moisture content of the soil is shown to be the most important influencing factor of infiltration among the affecting factors. The spring precipitation events were determined by lower precipitation, small evapotranspiration, but no infiltration occurred (*Table 2*). On the contrary, in case of early autumn precipitation events, infiltration was high in spite of the warmer weather conditions due to the low values of soil moisture (below 15-20 v/v%). Thus, due to the increased water infiltration capacity of the soil, accompanying by soil cracking due to the drying-out of the surface, rapid infiltration of water occurs.

When precipitation events are taken into consideration from March until November (191 mm), the infiltration of 64 mm occurred. If the precipitation, fallen below 10°C temperature, is regarded (40 mm), only 7 mm got into 10 cm depth, thus, by minimal evapotranspiration approx. 31 mm water surplus formed, meaning more than 300 m^3 potential inland excess water in every hectacres.

In case of the study area Tápai-rét, the inland excess water originated from groundwater in the whole investigation period. It is confirmed by the fact that inland excess water formation was not found when the groundwater-table decreased below 70 cm (2010 autumn, from May 2011). Therefore, infiltration can be concluded from soil moisture data series only in dry periods. Table 3 confirms that capillary rise plays an important role in the alteration of soil moisture, since the calculated data from soil moisture changes resulted in the same or higher estimated infiltration than the total precipitation amount. In case of Tápai-rét study area, a synergistic effect can also be observed. Due to the closeness of Tisza and Maros, the waters also influence the

Table 3 Calculated infiltration from soil moisture changes in Tápai-rét, 2010
RQ: precipitation, ΔSM1, ΔSM2: soil moisture growth in depths 10 and 20 cm, I: infiltration rate

Date	RQ (mm)	ΔSM1 (v/v%)	ΔSM2 (v/v%)	I (mm)
21-22.06.2010	12	6	5.5	11.5
03.07.2010	34.3	11	9	20
28.07.2010	17	5.5	6.5	12
06.08.2010	12	5	6.5	11.5
30-31.08.2010	15.1	8	16.5	24.5
10.09.2010	27.2	11	12	23
19.09.2010	20.4	12.5	11	23.5

groundwater-level. The previous correlation analyses confirm this additional effect only above a certain water level. However, further statistical analysis is required to determine the characteristic of the relation. In the investigated 1.5-year-long period, no soil frost was detected.

DISCUSSION

Differentiation of the upwelling (or vertical) type (due to the increasing groundwater table) and the accumulative (or horizontal) type (the water accumulates under gravity in the lowest areas due to limited infiltration and/or run-off, independent from the groundwater table or communicating by capillary system) of inland excess water important not only in scientific point of view, however because they demand different prevention and protection strategies. The accumulative (or horizontal) type of inland excess water is mainly topographic and agro technological problem, while upwelling (or vertical) type of inland excess water is more difficult problem and it can only be managed by ground water level decrease on large area, meaning large amount of water should be transported and/or stored (Kozák, 2003).

On the basis of the soil analysis the studied area is susceptible for the formation of accumulative) type inland excess water, but in very humid periods the ground water table can increase to the level of the surface. The dataset of the vertical and temporal changes of the soil moisture and the changes of ground water level, collected by the measurement station enables to clearly differentiate the two type of inland excess water.

On the Batida study area, the formation 'pure' accumulative type inland excess water could be analysed and the results show that the soil parameters had positive feedback on the inland excess water formation. At the time of the huge autumn precipitation and spring precipitation (snow melt) the soil become nearly impermeable, the gravitational pore volume is extremely decrease and exactly the same time when more infiltration capacity is needed due to the low evapotranspitation the soil retail the total surface water. However in summer periods, when the evapotranspiration is higher and decrease the potential of inland excess water formation, the dry soil has higher infiltration capacity. In this case the inland excess water formation can be delayed by better agrotechnics, which increasing the water holding and infiltration capacity of the soils (Birkás 2011), while the prediction of inland excess water occurrence can be achieved by continuous monitoring of the soil moisture in several depth. By the presented measurement stations, the amount of inland excess water on an exact location can be estimated. By the integration of these point measurements and a high resolution elevation model, the prediction of the real inland excess water inundation would be the next step in the research.

SUMMARY

The aim of the research was to investigate the formation of inland excess water in detail. A complex station for the monitoring of the hydro-meteorological and pedological factors influencing the formation of inland excess water was developed, which measures the precipitation, the evapotranspiration of the soil surface and opened water surfaces, the soil moisture in 3 different depths and the soil temperature in 5 depths. The study area was allocated the back-swamp area at high inland excess water hazard in the micro-regions of the South-Tisza-valley and Marosszög, northeast from Szeged. From the measured data, the estimation of infiltrating water was highlighted. Furthermore, soil samplings were repeated in the neighbouring areas, where pedological parameters (pH, soil plasticity according to Arany, carbonate-, salt- and humus content), and characteristic water regime parameters (bulk density, porosity, field capacity, hydraulic water conductivity) were determined.

The results described an area where due to the low elevation and the extreme particle size distribution, accumulative and upwelling-type inland excess water (of groundwater origin) both occur. The developed stations were able to differentiate the two types of inland excess water, furthermore in case of the accumulative type, the rate and temporal progress of infiltration, its extreme values in relation to soil saturation were estimated. The accumulation of potential inland excess water, the formation of the inundations can be determined by the detailed digital elevation and runoff models.

Acknowledgements

This research was supported by the IPA Cross-border Cooperation Programme of the European Union under the project HUSRB/1002/121/088 MERIEXWA entitled, MEasurement, monitoring, management and RIsk assessment of inland EXcess WAter in South-East Hungary and North Serbia (Using remotely sensed data and spatial data infrastructure)

References

Agrotopgráfia Map Series, Sheet 27, 1985-86

Birkás M. 2011. A klímaváltozás hatása a növénytermesztési gyakorlatra. (The effect of climate change on agricultural practices) In. Rakonczai, J. (ed.) Környezeti változások és az Alföld. A Nagyalföld Alapítvány kötetei 7. Békéscsaba. 257–269.

Birkás, M., Stingli, A., Farkas, Cs., Bottlik, L. 2009. Összefüggés a művelés eredetű tömörödés és a klímakárok között (Relation between compaction due to tillage and climate caused damages). *Növénytermelés* 58 (3), 5–26.

Dövényi Z. (ed.), 2010. Magyarország kistájainak katasztere.(Microregion cathaster of Hungary) MTA FKI, Budapest, 187–194.

Galbács, A. 2011. Belvíz veszélyeztetettség vizsgálata 2010-ben marosszögi mintaterületen (Inland excess water hazard in 2010 on a study area in the Marosszög). Szakdolgozat. Szeged. 48 p.

Hamza, M.A., Anderson, W.K. 2005. Soil compaction in cropping systems. A review of the nature, causes and possible solutions. *Soil & Tillage Research* 82, 121–145.

Kozák, P. 2003. Az alföldi belvizek elvezetése. (Drainage of inland excess water inundations in the Great Hungarian Plain) *Hidrológiai Közlöny* 83 (1), 51–61.

Kozák, P. 2011. Belvízi jelenségek az alsó-tiszai vízgyűjtőkön az 1955-2010 közötti időszakban. (Inland excess water inundations on the Lower-Tisza catchments between 1955 and 2010) In. Rakonczai, J. (ed.): Környezeti változások és az Alföld. A Nagyalföld Alapítvány kötetei 7. Békéscsaba, 127–136.

Körösparti, J., Bozán, Cs., Pásztor, L., Kozák, P., Kuti, L., Pálfai, I. 2009. GIS alapú belvíz-veszélyeztetettségi térképezés a Dél-Alföldön (GIS-based inalnd excess water hazard mapping in the southern part of the Great Hungarian Plain). Magyar Hidrológiai Társaság XXVII. Vándorgyűlése. Konferencia Proceedings CD-ROM (ISBN 978-963-8172-23-5). 2009. július 1-3., Miskolc, 1–14.

Ndiaye, B., Molénat, J., Hallaire, V., Gascuel, C., Hamon, Y., 2007. Effects of agricultural practices on hydraulic properties and water movement in soils in Brittany (France). *Soil & Tillage Research* 93, 251–263.

Perneki, Z., 2010. Talajdegradáció belvízfoltok alatt (Soil degradation below excess water inundations). Master Theses. Szeged. 35 p.

Thyll, Sz., Bíró, T. 1999. A belvíz-veszélyeztetettség térképezése (Mapping of inland excess water inundations). *Vízügyi Közlemények* 81 (4), 709–718.

JOURNAL OF ENVIRONMENTAL GEOGRAPHY
Journal of Environmental Geography 6 (3–4), 39–47.
DOI: 10.2478/jengeo-2013-0005
ISSN: 2060-467X

THE ADVANTAGES OF USING SEQUENTIAL STOCHASTIC SIMULATIONS WHEN MAPPING SMALL-SCALE HETEROGENEITIES OF THE GROUNDWATER LEVEL

László Mucsi [*1], János Geiger[2], Tomislav Malvic[3,4]

[1]Department of Physical Geography and Geoinformatics, University of Szeged, Egyetem u. 2-6, H-6722 Szeged, Hungary
[2]Department of Geology and Palaeontology, University of Szeged, Egyetem u. 2-6, H-6722 Szeged, Hungary
[3]Faculty of Mining, Geology and Petroleum Engineering, University of Zagreb, Pierottijeva 6, 10000 Zagreb, Croatia
[4]INA Plc
*Corresponding author, e-mail: mucsi@geo.u-szeged.hu

Research article, received 21 June 2013, accepted 15 September 2013

Abstract

In the environmental risk assessment of oil fields, a detailed knowledge of the heterogeneity of groundwater surfaces is absolutely indispensable. Based on theoretical considerations, in order to analyse small-scale heterogeneities, we decided that the Sequential Gaussian Simulation (SGS) approach seemed to be the most appropriate one. This method gives preference to the reproduction of small-scale heterogeneities at the expense of local accuracy. To test whether this kind of heterogeneity of the groundwater level corresponds to sedimentological variability, a point bar of the River Tisza (South-Hungary) was chosen. In variograms, the longest range was derived from the large-scale sedimentological heterogeneity of the point-bar, the medium range was in accordance with the radius of the meander and its direction coincided with the depositional strike of the meander, while the shortest range corresponded to the lateral heterogeneity of the deposits where the ground water level was measured. The similarities and differences of the realizations of SGS express the uncertainty of the map representation of the ground water surface. The E-type estimates of 100 equiprobable realizations resulted in a very detailed surface. The hydraulic gradient map obtained from the E-type estimates can provide us with a better understanding of the local flow characteristics.

Keywords: groundwater level, point bar, sequential Gaussian simulation, sedimentology, heterogeneity, geoinformatics

INTRODUCTION

The environmental risk assessment of oil fields highly requires a detailed knowledge of the heterogeneity of groundwater surfaces (Vaanlocke et al., 2010; Balderacchi et al., 2013). In many cases the contamination caused by leaks can only be identified after it has appeared in the groundwater or on the surface. Therefore, the spatial-temporal analysis of the surface of chemically aggressive groundwater could help one pinpoint the most probable location of a natural pipeline leak.

In order to monitor a particular environmental system, we chose the kind of methods suitable for data gathering and analysis. The primary goal of any monitoring activity is partly to locate the source of contamination, and partly to analyse its lateral and vertical dispersion. The ground water surface can be measured only in groundwater monitoring well, therefore the database can contain real data for these points. The groundwater level has to be estimated for other point.

In the "traditional" gridding or triangulation method, the numerical inter/extrapolations are formulated according to the method of least squares estimation. The aim of such methods is to improve the local accuracy and demonstrate the regional tendencies (Journel, 1987; Deutsch and Journel, 1998). In this case, the traditional estimation approaches act as "low-pass filters", filtering out the small-scale heterogeneities affecting the principal tendencies. Kriging has become a very popular estimation method (Theodossiou, 1999; Theodossiou and Latinopoulos, 2006), and it has this filtering property. The kriged surfaces (i.e. surfaces with different geological attributes) appear unnaturally smooth, and the resulting flow and transport dispersion are systematically underestimated (Deutsch, 2002).

The stochastic simulations differ from kriging approaches in the following ways (Carr and Myers, 1985):

In most interpolation algorithms (e.g. kriging) the goal is to find the "best" local estimate of the variable without specific regard to the resulting spatial statistics of the estimates taken together. In the solution, the reproduction of global features and statistics (histogram, variogram) take precedence over the local accuracy.

Based on the simulated groundwater surface, the analysis of contaminant dispersion could also be improved. Hence knowledge of the actual position of the groundwater level as well as its flow path may reduce the environmental risk associated with the joint (combined?) effects of a high groundwater level and other natural corrosives.

STUDY AREA

The largest mining and industrial area of the south-eastern part of Hungary is the Oil and Gas Plant of MOL (Hungarian Oil and Gas Co.). Here almost every aspect of hydrocarbon exploitation, pipeline transportation and oil processing is carried out (*Fig. 1*).

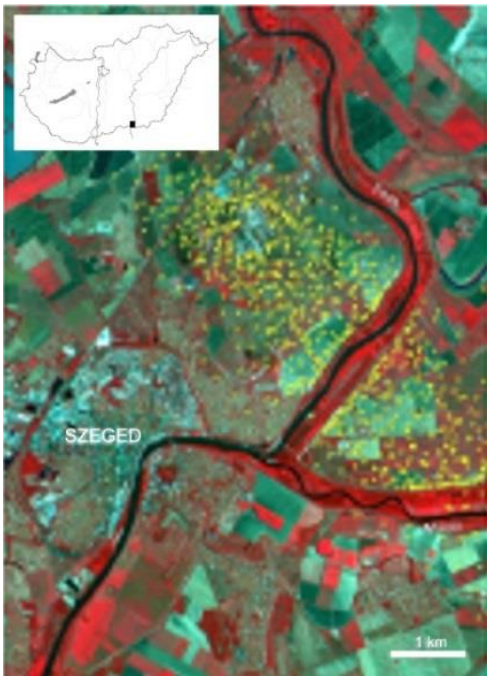

Fig. 1 The area surveyed on a Landsat TM 453 (RGB) color composite. The oil, gas and thermal water wells labeled by yellow circles (Mucsi et al., 2004)

Within the area surveyed, 100 or even 1000 km long oil and gas plant pipeline networks have been installed below the surface. In the neighbourhood of a pipeline leak, the environmental damage caused can be quite serious. For networks that were built a few decades ago, systematic pipeline monitoring should be performed due to frequently occurring natural leaks.

In the area surveyed, a fairly dense pipeline network links the production wells with tank farms. This area is part of the recent valley of the River Tisza. The oil and gas production here, which began in the 1960's, has significantly altered the former agrarian landscape (*Fig. 2*).

However, agricultural activity has continued in parallel with mining and oil processing (see *Fig. 3*). Therefore the risk of a pipeline leak is not just real for MOL, but also for farmers. For the latter group, lower harvest yields due to poorer soil and groundwater quality may be two great causes for concern.

At the end of the last century and beginning of this century, the repeated occurrence of a record high water level of the River Tisza, a high groundwater level (see *Fig. 4*) and the extremely dry summers may actually be the consequences of a changing global climate, and justify the need for a more conscious use (pro-active stewardship?) of our environment.

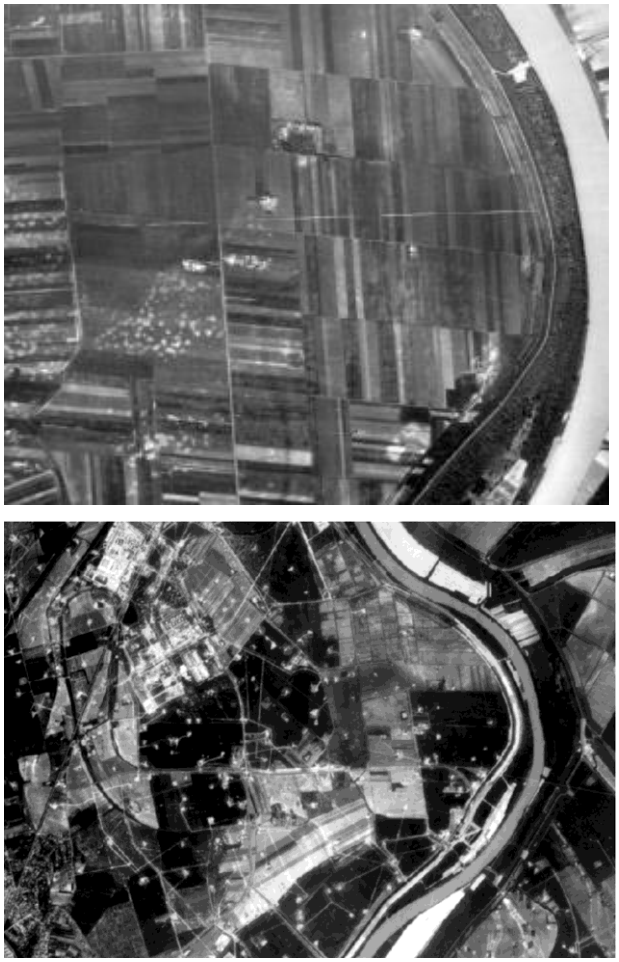

Fig. 2 The alteration of the former agrarian landscape of an aerial photography (1950) and a spy satellite (Corona – KH-4B) image from 1972 (Hungarian Military Archive, USGS)

Fig. 3 Ikonos satellite image from 2004 (INTA SPACETURK)

On the surface, Holocene sand, silt and clay can be found owing to fluvial sedimentation. Based on sediment profiles obtained from the wells below the upper silty sandy lens-like series, a laterally extended silt layer appears 4-5 metres beneath the surface, which can be regarded as a flood plain deposit. Under this series, Late Holocene fluvial sand dominates.

Originally the monitoring system consisted of 25 wells. Since they are located in a cluster, we decided to supplement the original monitoring system with 17 new wells (*Fig.*5).

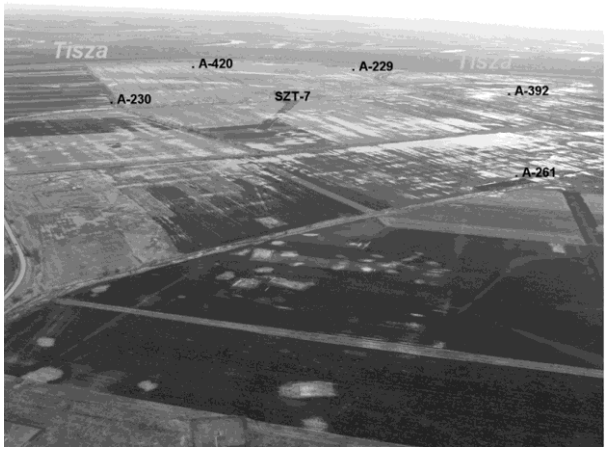

Fig. 4 High groundwater level (aerial photography, Mucsi et al, 2004)

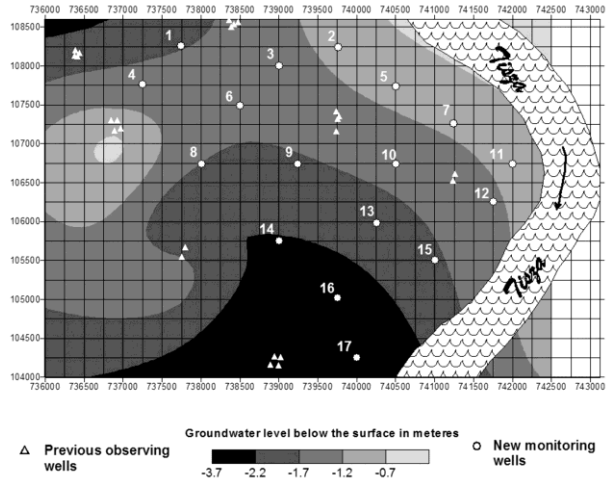

Fig. 5 Location map with the new and old monitoring wells

THEORETICAL CONSIDERATIONS

In general, the ground water level is determined by hydrological processes like precipitation (more precisely, its annual and long-term distribution), evaporation, transpiration, and pedological-sedimentological and topographical conditions.

Here, the heterogeneity of pedological or sedimentological factors may be the biggest two factors among the processes of this multivariate system. Unfortunately, this heterogeneity is not properly reflected in the maps of the groundwater surfaces.

The purpose of this study is to demonstrate a mapping process of the groundwater level that is in consistent with small and medium scale sedimentological heterogeneity by using Sequential Gaussian Simulation (SGS, Deutsch and Journel, 1992). For this purpose a recent point bar sedimentary body of the River Tisza (Hungary) was chosen.

The scales of sedimentological heterogeneity in a point bar

In the idealized cross section of a point bar, the following four basic units can be identified: (1) channel lag deposits, (2) laterally accreted bar deposits with accretion surfaces, (3) a natural levee, and (4) a flood plain series (*Fig. 6*). The bar sequence itself can be subdivided into (a) a lower point bar and (b) upper point bar series (*Fig. 6*).

It is well known that the effective porosity and permeability of a sediment are partly determined by sedimentary textures and structures that permeate the pore space distributions. The influence of sedimentary structures and textures on permeability is very significant, not just for the absolute values but also for the anisotropy. A quite trivial consequence of this fact is that the steady state level of a groundwater surface can vary according to the sedimentary structures and textures of the actual deposits. According to the basic rule of sedimentology (Walter's facies law), lateral facies also occur superposed upon one another. It means that the vertical heterogeneity depicted in *Fig. 5* can also horizontally affect the spatial position of the groundwater level. The lateral scale of this heterogeneity can vary from a few metres to tens or hundreds of metres (Pryor, 1987; Mial, 1996). However, according to the GPR images, there is a textural variability that has a range of a few hundred metres to a few kilometres.

Summarizing the points above: in the point bar sedimentary bodies, the lateral variability of sedimentary features can manifest itself on two different scales. They range (1) from several metres to tens or hundreds of metres and (2) from several hundred metres to several kilometres. The basic unit associated with this scale (1) is the scale of the principal sedimentary structure, while for scale (2) the basic unit is the distance between two neighbouring accretion surfaces.

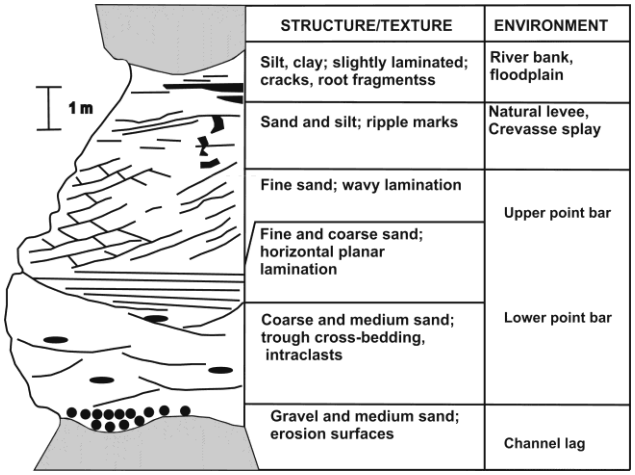

Fig. 6 Idealized cross-section of a point-bar sequence (modified after Brunner et al, 2001)

The ground water level treated as a regionalized variable

When viewed mathematically, two statements can be derived from the above description. They are: (1) The ground water level is a spatial property that can be regarded as a random variable at each data point; (2) There is a spatial relationship associated with these random variables. The first statement follows from the variability of the textural characteristics of the sedimentary body

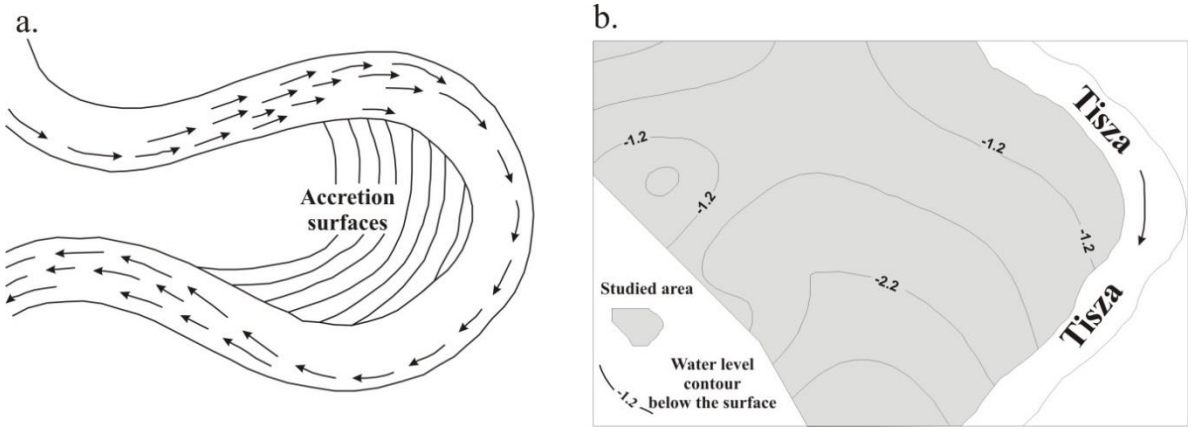

Fig. 7 Appearance of the lateral accretion surfaces on the water table contours

containing the initial water table. The second statement is a consequence of the fact that a point bar is the result of spatially interacting processes. That is, according to the definition given by Cressie (1991), the water table level is a regionalized variable.

A map of absolute position of a ground water level fixes the water table in the real spatial position. This kind of map is a plot of a three-variable function, which gives an estimate of the real position, or more precisely one realization of the several existing estimates.

By continuing this process, the "smooth" surface in Fig. 7 tells us that the variability of hydrological elements affecting the water table is "not too large". This then leads us to ask the following question: "Is the smooth surface simply the result of the gridding technique we applied?" Thus, traditional methods like kriging are really appropriate for describing large-scale heterogeneities. For point bars the latter ranges from a few hundred metres to a few kilometres. The small-scale heterogeneities are simply filtered out via these estimations. In fact the traditional gridding techniques honour the large-scale features quite well. For example, in *Fig. 7* the lateral accretion surfaces are clearly recognizable.
To overcome the above drawbacks, several methods for stochastic simulation have been developed and they have been regularly used in the mapping of reservoir properties in the oil industry since the mid 1980's, but they have been widely applied in the environmental sciences as well (Webster and Oliver, 2001).

THE APPROACH WE ADOPTED

SGS in general

Let us define a regionalized variable (RV) and call it z(u). Stochastic simulations are methods in which alternative and equally probable high resolution models of spatial distribution of the z(u) are generated. The realizations obtained from them are called stochastic images. If the realizations honour the input data (the data points), the simulation is called conditional.

For the local set of data and conditional statistics, kriging is used as an interpolation technique which provides a simple numerical method that is the "best" in the sense that it is accurate locally. Simulation provides several alternative but equally probable models, all of which are the "best" reflection of reality in a certain global sense. The differences between the realizations offer an opportunity for measuring the spatial uncertainty.

The Gaussian simulations honour the covariance model of the data points. This is why they are suitable for modelling processes with an extremely large continuity.
Let us define the common distribution of an RV by Zi (i=1,2,..,N). That is, according to the above theory, let us take the data of all available points and consider the conditioning of this N RV for each type of n data sets. The corresponding conditional cumulative distribution function (CCDF) for this is:

$$F(N)(z1, \ldots, zn|(n))=P\{Zi\leq zi, i=1, \ldots, N|(n)\}$$

If the ground water table is treated as regionalized variable, this variable must be a random variable for any given data point. That is, in the infinitesimally small neighbourhood of any data point it will have a random value. Hence the data-point value is nothing else than a random value of the corresponding RV derived from the distribution function of the infinitesimally small neighbourhood. If processes controlling the ground water table are homogeneous in the region being analysed, then the cumulative distribution function (CDF) surrounding any set of data points can be assumed to be the same as that of over the whole given region. By applying a normal score transformation on the data set, this distribution can be represented in analytical form as well. As is well known, the first two moments determine the normal distribution. This fact was incorporated in the implementation of SGS (Carr and Myers, 1985).

SGS is a widely used simulation technique for extreme continuous data (e.g. porosity). Details of the various implementations are given in Deutsch and Journel (1998), and in Deutsch (2002).

In essence, SGS models the method of iteration, since the estimation of a grid point is done based on the result of the previous step. This view corresponds to the fact that a contour map is unbiased only after the grid estimation method has been fixed (Brooker, 1979).

The expected value (more precisely, the "expected surface") of the series of realizations is the most characteristic spatial distribution that describes "reality".

The difference between the realizations reflects the uncertainty of the mapping of the property being studied - in our case, the surface of the water table. This uncertainty is independent of the accuracy of the measurement of the

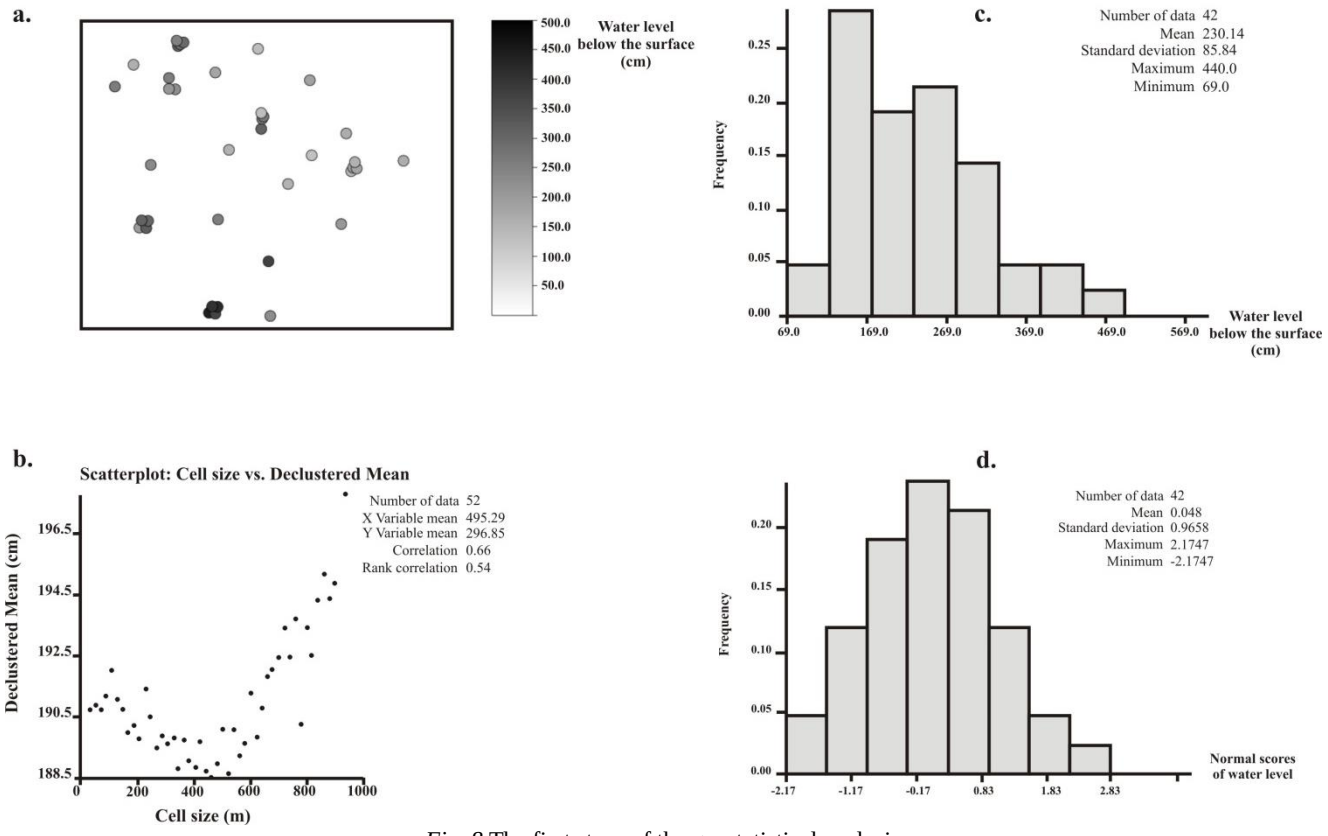

Fig. 8 The first steps of the geostatistical analysis

water table taken from each well. In fact, this uncertainty depends just on the heterogeneity of hydrological factors and the way in which this heterogeneity can be described using available well geometry.

Pre-processing: the steps involved

The first phase was an analysis of the lateral distribution and probability distribution of the data (*Fig. 8a-b*). In the second phase, two things became immediately apparent: (1) the peculiar clustering of data points; (2) the observation that there are many wells in each cluster, and these have significantly different data values (*Fig. 8a*). However, the probability distribution of data is quite symmetrical (*Fig. 8b*). This clustering appearance of wells is fairly common around artificial objects, where small distant wells serve the purpose of environmental protection while the larger distance wells were built for water table observations. However, this may cause problems in mapping, because the clustered wells will shadow the nearby grid points with their own values. Hence the contours will not reveal the true situation. At the same time, this geometry will also affect the relative frequency histogram of the water table values. However, applying a special declustering technique can resolve this problem (Deutsch and Journel, 1998). With this method an appropriate grid system is placed over the area where (in such a way that?) the clustered wells can be sepa-

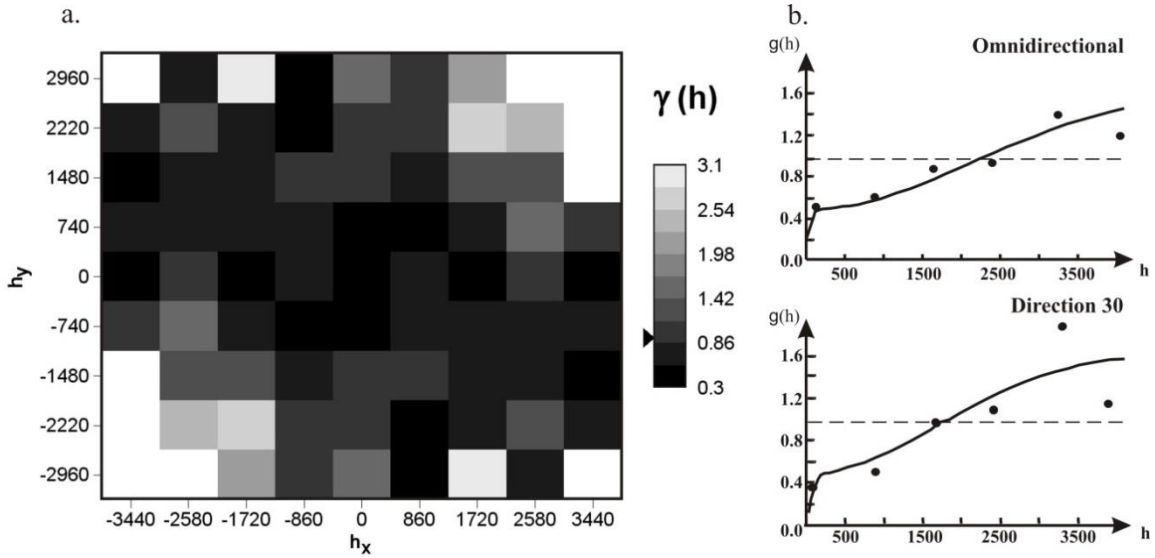

Fig. 9 The variogram surface and the variogram model

rated into individual wells. Then some weighting factors can be derived which are small for the very close wells and become larger with increasing distance. In this way the shadow effect of closer wells can be eliminated. In our case the declustering method gave 500 m as the most appropriate cell distance (*Fig. 8c*). The result of the normal score transformation is shown in *Fig. 8d*.

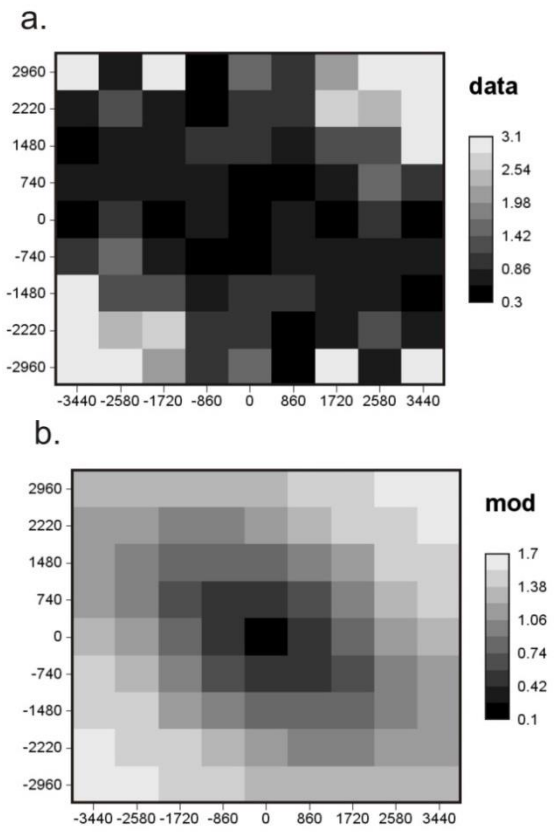

Fig.10 The empirical (a) and model variogram surfaces (b)

Variography

Our analysis of the spatial continuity of the water table was aided by variography. A variogram surface was used for the visual examination of continuity directions (*see Fig. 9a*). This method identified a principal direction of NE-SW. The smallest continuity may be identified in the NW-SE direction (*Fig. 9b*). These directions appear on the smooth surface of the water table as well (see *Fig. 7*). As mentioned previously, this feature corresponds to the lateral accretion surfaces of the point bar.

The second figure here shows a variogram model based on the experimental data. As you can see, this is a nested structure consisting of three units. The first component has a range of 250 m. The second one has a range of about 3.800 m, while the third has a range of 4.100 m. Most likely, the latter is indicated by the 'smooth' map of the water table surface.

The largest range is almost equal to the length of the point bar, so it may be related to the large-scale process that forms the point bar sedimentary body. The second largest range is quite similar to the previous one and may be related to the effect of a bend in the river channel going in a SE direction. But the smallest range (250 m) may not be caused by hydrological effects at all, but by sedimentological effects. This may be the result of internal heterogeneity of the point bar affecting the surface of the water table. Hence it is the heterogeneity which was really the object of this study.

Fig. 10a depicts the spatial continuity outlined above, while the second figure shows the variogram surface obtained from the variogram model (Panattier, 1996). The similarity is obvious here.

Realizations and simulation uncertainties

From the SGS, 100 equally probable realizations were generated. *Fig. 11* shows 3 of the resulting one hundred images. As can be seen, there are regions where the realizations are not too different. This is caused by the locally low uncertainty of the lateral interpolation (Journel, 1993).

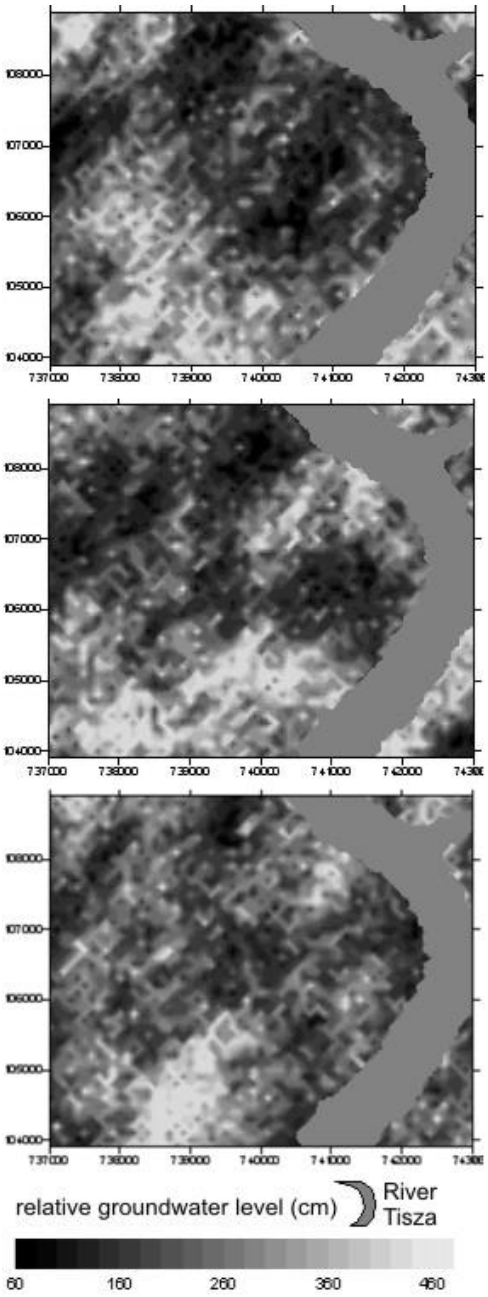

Fig. 11 Stochastic realizations showing equally probable position of the water table

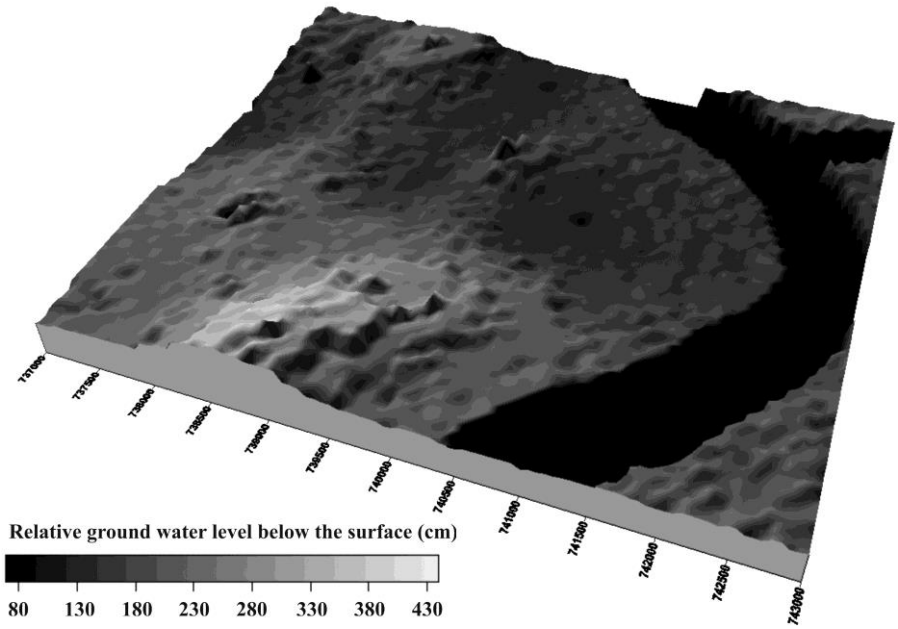

Fig. 12 E-type estimation from the two-hundred stochastic realizations of the relative water table position

The one hundred realizations provide one hundred values estimated for each grid node. This number is quite sufficient to compute the cumulative distribution around an infinitesimally small neighbourhood of each grid point. That is, there is a possibility of estimating not just the expected value, but also the lower and upper bounds of the confidence interval for each grid node. Moreover, we have a way of explicitly answering questions like "How can we calculate the lateral distribution of probabilities associated with the water table level at 72 cm below the surface?" and "Which regions with a water table of 85 cm have a probability value of 0.8?".

Fig. 12 shows the predicted value map of the relative water surface (i.e. its depth below the surface), while *Fig. 13* shows the surface of the water table above the Baltic Sea. The 'smooth surface' obtained by traditional kriging and the one obtained by the E-type estimates (expected values) of the SGS are compared in *Fig. 14a and Fig. 14b*, respectively.

Fig. 14b highlights the local effects of underground flow systems. The advantages of this approach in the three-phase flow simulation were described earlier (see, for instance, Geiger and Komlosi, 1996). Their observations confirmed that these approaches make the flow simulations more effective (than earlier approaches?).

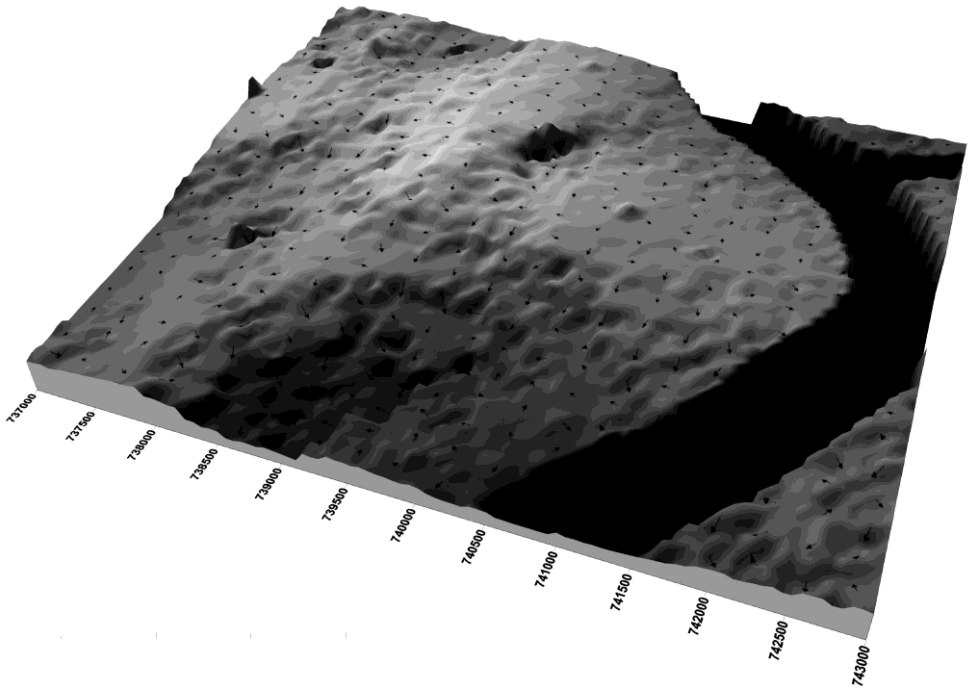

Fig. 13 E-type estimation from the two-hundred stochastic realizations of the absolute water table position. The black arrows are proportional with the hydraulic potential

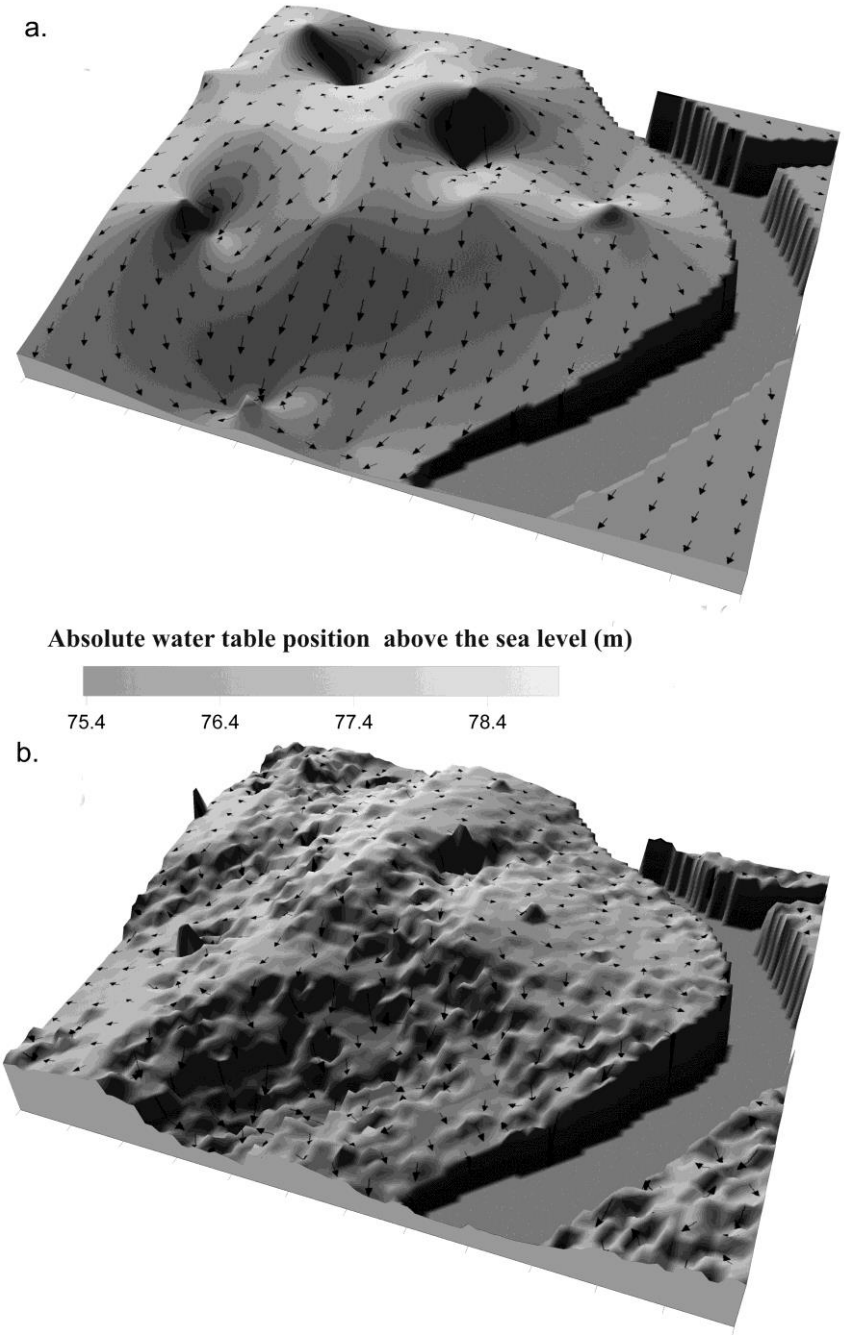

Fig. 14 Comparison of the results coming partly from kriging (a) and partly from E-type estimation of SGS (b)

CONCLUSION

Within the area surveyed, 100 or even 1000 km long oil and gas plant pipeline networks have been installed below the surface. The spatial-temporal analysis of the surface of chemically aggressive groundwater helped one pinpoint the most probable location of a natural pipeline leak. Originally the monitoring system consisted of 25 wells. Since they are located in a cluster, the original monitoring system was supplied with 17 new wells whose locations were calculated with geostatistical analysis. The ground water level was measured monthly in these wells and Sequential Gaussian Simulation was used to demonstrate a mapping process of the groundwater level that is in consistent with small and medium scale sedimentological heterogeneity. A map of absolute position of a ground water level fixed the water table in the real spatial position. The developed map was a plot of a three-variable function, which gave an estimate of the real position, or more precisely one realization of the several existing estimates. The analysis of the spatial continuity of water table was aided by variography. A variogram surface was used for the visual examination of continuity directions. This method identified a principal direction of NE-SW. The smallest continuity was identified in the NW-SE direction. These directions appear on the smooth surface of the water table as well In variograms, the longest range was derived

from the large-scale sedimentological heterogeneity of the point-bar, the medium range was in accordance with the radius of the meander and its direction coincided with the depositional strike of the meander, while the shortest range corresponded to the lateral heterogeneity of the deposits where the ground water level was measured. The similarities and differences of the realizations of SGS expressed the uncertainty of the map representation of the ground water surface. The E-type estimates of 100 equiprobable realizations resulted a very detailed surface. The hydraulic gradient map obtained from the E-type estimates determined the local flow characteristics. The subsurface contamination can spread along these pathways, so it can get far distance from its source.

References

Balderacchi, M. ,Benoit, P., Cambier, P Ekloc O. M., Garginid, A., Gemitzi, A., Gurelf, M., Kløve, B, Nakich, Z., Predaai E., Ruzicic S., Wachniewj, P., Trevisana M. (2013). Groundwater. Pollution and Quality Monitoring Approaches at the European Level. *Critical Reviews in Environmental Science and Technology* 43, 323–408.

Brooker, P. 1979. Kriging. *Engineering and Mining Journal* 1980 9, 148–153.

Brunner, D.S.Endres, A.L.Sudicky, E.A. 2001. Detailed ground-penetrating radar survey of a point-bar, Whiteman's Creek, Ontario for use in a new fully integrated 3D surface/ subsurface flow model. – Geological Society of America Annual Meeting, November 5-8, 2001. Boston, Massachusetts.

Carr, J.R Myers, D.E., 1985. COSIM: A Fortran IV program for Conditional Simulations.—Computer and Geosciences v.11, 675–705.

N. Cressie 1991. Statistics for Spatial Data. John Wiley & Sons, Inc. New York, 892p.

Deutsch C.V. 2002. Geostatistical Reservoir Modelling, Oxford University Press.

Deutsch, C.V., Journel, A. 1998. GSLIB. Geostatistical Software Library and User's Guide. – Oxford University Press, New York, 369p.

Geiger, J. Komlósi, J. 1996. Szedimentológiai geomatematikai 3-D modellező rendszer törmelékes CH-tárolókban (Sedimentological, geomatematical 3D modelling system in turbiditic CH reservoirs) *Kőolaj és Földgáz* 2, 53–81.

Journel, A. 1987. Geostatistics for the environmental sciences. – EPA Project no. Cr 811893. Technical report. U.S. EPA, EMS Lab., Las Vegas, NV

Journel, A, 1993. Modelling uncertainty: Some conceptual thoughts. In: Dimitrakopoulos, R.(ed): Geostatistics for the Next Century, Kluwer, Dordrecht, 30–43.

Miall, A.D. 1996. The Geology of Fluvial Deposits. Sedimentary Facies, Basin Analysis, and Petroleum Geology. – Springer Verlag, New York, 582 p.

Mucsi, L. 2001. Characterisation of oil-industrial contamination using aerial and thermal images - EARSeL Symposium, Drezda. In: Buchroithner (ed:) A Decade of Trans-European Remote Sensing Cooperation, Balkema, Rotterdam, 373–377.

Mucsi, L., Kiss, R., Szatmári, J., Bódis, K., Kántor, Z., Dabis, G., Dzsupin, M. 2004. Felszín alatti vezetékek környezetszennyező hatásainak felmérése távérzékeléses technológiával (Invesgtigation of possible environmental pollution of subsurface pipelines using remote sensing technologies). *Geodézia és Kartográfia* 56 (4) 3–8.

Pryor, W.A. 1987. Permeability, porosity patterns and variations in some Holocene sand bodies. In: Beaumont, E.A., Foster, N.H. (ed) Reservoirs II. Sandstones. AAPGD Treatise of Petroleum Geology Reprint Series. No.4, 127–154.

Theodossiou, N. 1999. Evaluation of the distribution of hydraulic head in an aquifer using the Kriging method. – Scientific Journal of Hellenic Hydrotechnical Association. *Hydrotechnika* 9, 3–14.

Theodossiou, N., Latinopoulos, P. 2006. Evaluation and optimization of groundwater observation network using the Kriging methodology. *Environmental Modelling & Software* 21, 991–1000.

Vanloocke, R., De Borger, R., Voets J. P. . Verstraete W 2010. Soil and groundwater contamination by oil spills; problems and remedies International Journal of Environmental Studies 8 (1-4), 99-111.

Webster, R., Oliver, M. A. (2001): Geostatistics for Environmental Scientists, John Wiley & Sons.

JOURNAL OF ENVIRONMENTAL GEOGRAPHY
Journal of Environmental Geography 6 (3–4), 49–54.
DOI: 10.2478/jengeo-2013-0006
ISSN: 2060-467X

COMPARISON OF PIPETTE AND LASER DIFFRACTION METHODS IN DETERMINING THE GRANULOMETRIC CONTENT OF FLUVIAL SEDIMENT SAMPLES

Ágnes Kun, Orsolya Katona*, György Sipos, Károly Barta

Department of Physical Geography and Geoinformatics, University of Szeged, Egyetem u. 2-6, H-6722 Szeged, Hungary
*Corresponding author, e-mail: k.orsi@geo.u-szeged.hu

Research article, received 25 August 2013, accepted 13 October 2013

Abstract

Nowadays there is a growing demand for rapid and accurate determination of grain size distribution. The conventional pipette method is time-consuming and provides less detailed data compared to recently introduced methods. However, in Hungarian practice the pipette method is still considered to be the standard one, as there are a long series of measurements, and grain size thresholds used in sedimentology and soil sciences are based on this approach. The aim of our research was to determine the comparability of the laser diffraction method (LDM) with the conventional pipette method (PM), in order to investigate the controversial question on the interchangeability of the two methods. Based on our measurements on some representative fluvial sediment samples, we found that the largest difference in results can be expected in the silty grain size range. However if the main fractions (clay, silt, sand) are considered the methods provided similar very results, and correlation factors were above 0.92. In all, the LDM has a clear advantage because of its speed, reproducibility and fewer possibilities for operator failure.

Keywords: laser diffraction method, pipette method, fluvial sediments, grain size distribution

INTRODUCTION

Grain size distribution is a fundamental physical parameter in soil and sediment related researches. Physical and chemical conditions of the sediment and soil samples are mostly determined by the main grain size fractions, which contain the majority of the particles. Grain size classes are determined by almost each research field differently (Blott and Pye, 2012). Grain size distribution can be determined in several ways, however in most research applications a fast and unified method is demanded, which offers reproducible and automated grain size measurements.

In the past few decades, several researches have dealt with the methods of grain size distribution (Konert and Vandenberghe, 1997; Buurman et al., 1997; Beuselnick, 1998; Goossens, 2008; Di Stefano et al., 2010; Hernádi et al., 2008 stb.). A controversial question has been which method is the most proper for different applications. The aim of our research was to examine at what extent the conventional pipette method (PM) and the laser diffraction method (LDM) are interchangeable in terms of unsorted fluvial samples.

The PM is internationally accepted for grain size distribution analysis, hence it was used as the basis during the comparison of the two methods. The PM is based on the Stokes law, i.e. sedimentation rate is depending on particle size. There are however some conditions of its applicability: grains are presumed to be spherical and smooth, sedimentation rate must be constant, the density of particles equals to that of quartz (2.65g/cm^3), particle-to-particle interference and boundary effects from the walls of the sedimentation column are negligible and particles have no impact on the viscosity of the suspension (Di Gleira el al. 1957; Konert and Vandenberghe, 1997; Di Stefano et al., 2010). For example, if the first condition is not met the resulted clay content will be highly influenced by the shape of the particles. The settling velocity of the non-spherical grains in the fine fraction can lead to the underestimation or overestimation of the clay content depending on the shape of the particle. Platy shape grains lead to fine fraction overestimation while disc or rod shape grains result the underestimation in the range of 0.1 μm to 100 μm (Di Stefano et al., 2010).

LDM is based on the dispersion and diffraction of a laser beam that is let through the suspension. The dispersion of light creates special diffraction rings on the sensor and the grain size distribution is determined by the position, size and distance between rings. The application of LDM has also got certain conditions (Konert and Vandenberghe, 1998), namely grains are spherical and particle orientation is random throughout the measurement time. However the flow of the measurement medium will likely to determine the orientation of non-spherical particles (De Vos, 2001).

The accuracy of the measurement also depends on the color of the suspension, the mineral composition of particles, the organic material and carbonate content of the sample and the applied measurement theory.

In general two measurement approaches are applied for the LDM, the so called Fraunhofer and Mie theories. The Fraunhofer theory is operating with the portion of light deflection that occurs as a result of diffraction. One major advantage of Fraunhofer theory is lies on the fact that no knowledge of the optical properties of the examined material is required. However, the Fraunhofer diffraction model provides inaccurate result if the size of the particles is less than 10 λ (wavelength of the laser light) (Loizeau et al., 1994; Xu and Di Guida, 2003; Di Stefano et al., 2010). For particles with diameters not significantly larger than the wavelength of the light used, the Mie theory is applied usually for the analysis, in this case, however, the refraction index and the absorption index of the sample must be known. According to Konert and Vandenberghe (1997) the Fraunhofer theory is well suited for non-spherical clay particles and the same conclusion was established by Di Stefano et al. (2010).

Measured grain size distribution is greatly affected by the applied pre-treatment method. The necessity of the removal of organic matter and carbonate content are strongly controversial. Several authors justify the pre-treatment on sediment samples with high organic matter content (7-8%) (e.g. Murray, 2002). According to his study, only pre-treatment with hydrochloric acid and hydrogen-peroxide could provide any degree of reproducibility. Beuselnick et al. (1998) also investigated the effect of organic matter content, and found that the pretreatment with acids was unnecessary in case of samples with low organic matter content, and in spite of the different pretreatment procedures the results had a strong correlation in the 3 main fractions (clay, silt, sand). A similar statement was made by Ryzak and Bieganowski (2011), namely physical (ultrasonic) dispersion can be equivalent to chemical dispersion methods.

MATERIALS AND METHODS

In order to determine the applicability of the LDM method, several authors have performed measurements on soil samples, loess- and marine sediments (Konert and Vandenberghe, 1998; Di Stefano et al. 2010; Ryzak and Bieganowski 2011; Madarász et al., 2012). However unsorted fluvial samples are very rarely studied (Buurman et al., 2001). Consequently, the analysis was performed on sediments obtained from point bars and swales of a Maros River paleochannel, near Sannicolau Mare, Romania. Samples were derived from 5 boreholes from depths of 30, 50, 70, 90 and 110 cm. In all 25 samples were analysed.

Samples were dried on 105 ˚C and sieved at a 2mm mesh size. The organic matter and carbonate content of sediments were also measured. Carbonate content was under the measurement threshold (Scheibler calcimeter) in case of 15 samples, while 10 samples had carbonate content between 0.42% and 3.35%. Organic matter content was between 0.32% and 2.01 %. Due to the low organic matter and carbonate content, and since the Hungarian standard of the PM (MSZ-08 0206/1-78) does not contain orders of pre-treatment, we considered the removal of these components unnecessary in case of the investigated samples.

The dispersion of the particles was enhanced using sodium pyrophosphate and shaking: 25 g of sample was weighted for the PM analysis, 0.5 g sodium pyrophosphate and 400 ml distilled water was added, then samples were placed in a shaking machine for 6 hours in order to disperse the aggregates into primary particles.

After this pretreatment the suspensions were poured to 1000 ml sedimentation cylinders, which were then filled up with additional distilled water. Based on the schedule of the Khön's table, 10 ml suspension was pipetted and put into a known-mass evaporating vessel, and the following grain size classes were determined <2 μm, 2-5 μm, 5-10 μm, 10-20 μm, 20-50 μm, >50 μm.

For the LDM measurements a Fritsch Analysette 22 MicroTec instrument was applied. Its measurement range is 0.08-2000 μm and it is equipped with 2 linearly polarized lasers: green (λ=532 nm, P=7 mW) and infra-red (λ=940 nm, P=9 mw). During the measurement, samples were homogenized with ultrasonic treatment (f=36 kHz, P=60 W) for 3 min. The grain size distribution was determined at 108 channels. Samples were measured sequentially for 3 times, during the measurement the ultrasonic dispersion was continuous. The difference of the distributions between the 3 measurements was at maximum 3-4% (*Fig. 1*), hence the third measurement was considered as the primary grain size distribution. In order to compare the results of the two methods, intervals of the pipette method were generated out of the continuous distribution curve yielded by the LDM measurements. Grain size distribution analysis was performed by Statgraphics software.

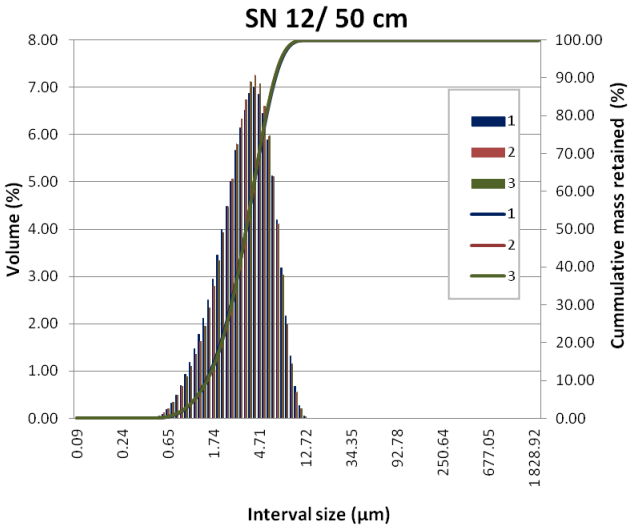

Fig. 1 Differences between three consecutive LDM measurements on the same sample

RESULTS

The texture of the samples was different, but similar attributes characterized the samples along the boreholes (regardless of depth). The highest clay content was measured in borehole SN5, where nearly identical sand content was measured with the two methods. In the meantime borehole SN11 showed the lowest clay content, while these samples had the highest sand contents. Beyond texture analysis, median diameter (D50) and cumulative distribution with 10, 25, 75, 90% values (D10, D25, D75, D90) were also measured. Differences and ratio of the resulted values derived by the two methods were used for the comparative analysis (*Fig. 2*).

Samples of borehole SN11 – with the lowest clay and highest sand contents – showed the greatest differences of cumulative distribution values (D25, D50, D75, D90) obtained by the LDM and the PM. The sources of the dissimilarity have been searched in the differences of sand contents. During the PM, removal of sand content was performed after sedimentation; therefore presence of sand grains could have disturbed the sedimentation speed of grains of other fractions. Moreover, borehole SN12 contained a large amount of sand, D75 and D90 values were also high.

Differences between D values were the lowest in the samples of boreholes SN3, SN4 and SN5. These samples have the lowest sand content, and amount of sand grains was roughly the same after the measurements of the two methods.

Based on the D values, samples can be divided into two groups: SN3, SN4, SN5 and SN11, SN12. Classification is also confirmed by the spatial distribution of the samples, as the samples of the first group is originated from the point bars and swales of the Aranka river, while SN11 and SN12 were obtained from a 6.1±1.1 ka old, meandering riverbed (Kiss et al., 2012). Measured organic matter content also reflects this difference of sample groups. The first group (SN3, SN4, SN5) has an average organic matter content of 2.1%, while the second has an average of only 0.8%. Dissimilarities of samples in grain size distribution and organic matter reflects to the river dynamics of the formerly accumulating river. The samples of the first group belong to the clayey and organic matter rich landforms of a meander with a low discharge, while samples of the second group reflects to a considerably large meandering river (Kiss et al., 2012). Since cumulative and differential size distributions of the samples were similar in each group, distributions will be represented by one sample per group.

Comparison of the two methods can be performed by examining the distribution curves. In the case of sample SN3, the shape of distribution curves derived by the two methods are very similar (*Fig. 3*). Results of the LDM were evaluated using the defined fraction intervals of the Hungarian Standard. Curves are bimodal and their main modus is equivalent, however the secondary modus of the LDM curve is displacing towards the coarser fractions. The peak of the LDM curve is at a larger particle size compared to the PM curve.

The differences between the measurements have occurred at different fractions that depend on the proportion of the fractions. The samples SN5 with high clay content shows significant difference in clay proportion, regardless that difference between D values are the lowest in this borehole (*Fig. 4*). The largest difference can be identified in clay contents, confirmed by former statements as the increase of clay content is also increasing the error and probability of underestimations during LDM (Beuselick et al., 1998; Konert and Vandenberghe, 1998).

In case of high clay content the LDM underestimates the clay fraction in favor of the silt fraction. However the PM overestimates the fine fraction because of the non-spherical shape of the clay particles. Underestimation of clay content with LDM was also

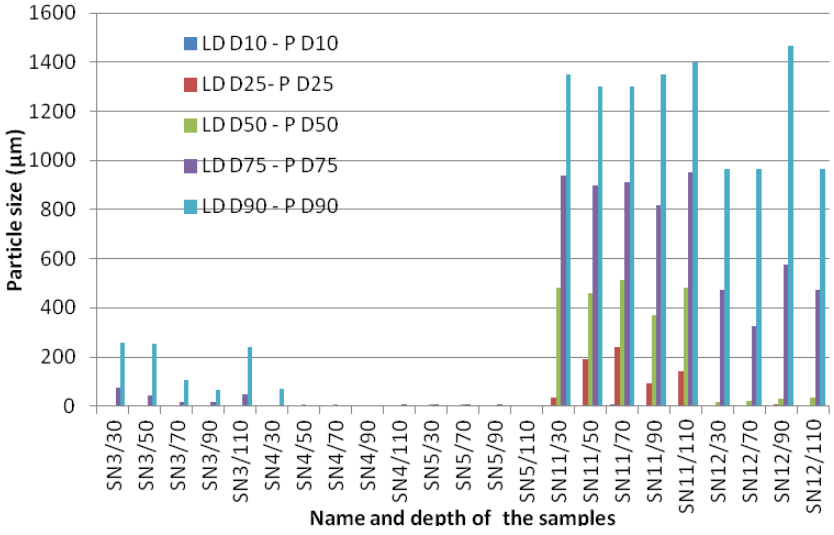

Fig. 2 Difference between the D values derived by PM and LDM

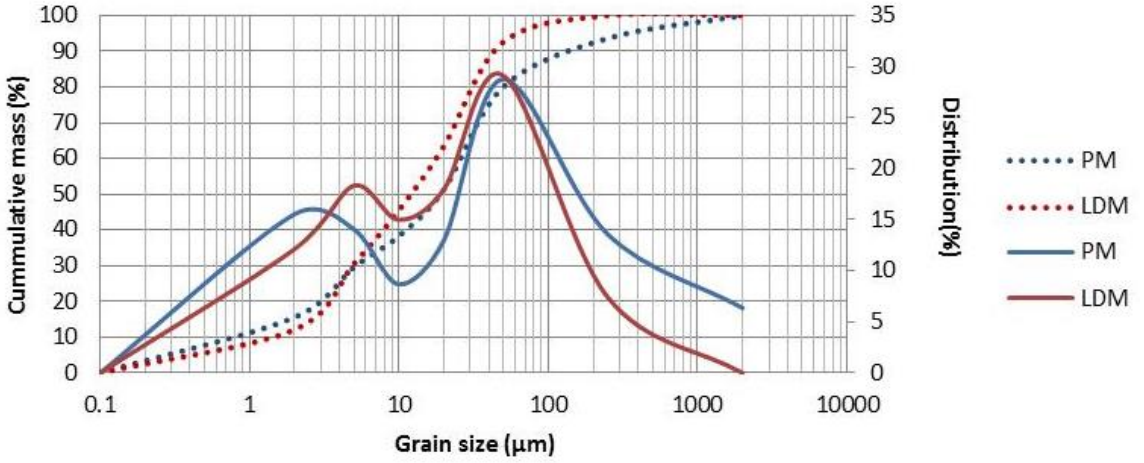

Fig. 3 PM and LDM grain size distribution and cumulative curves of sample SN3/70

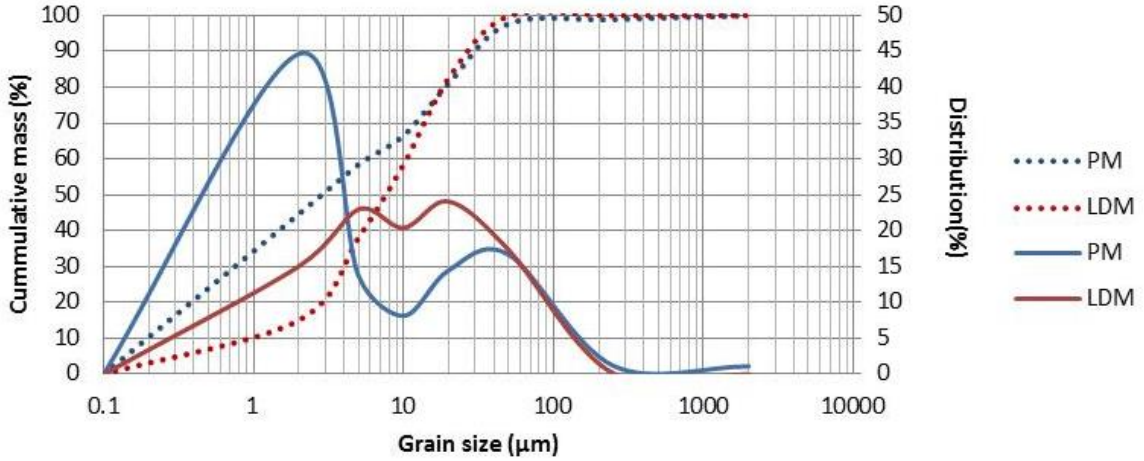

Fig. 4 PM and LDM grain size distribution and cumulative curves of sample SN5/110

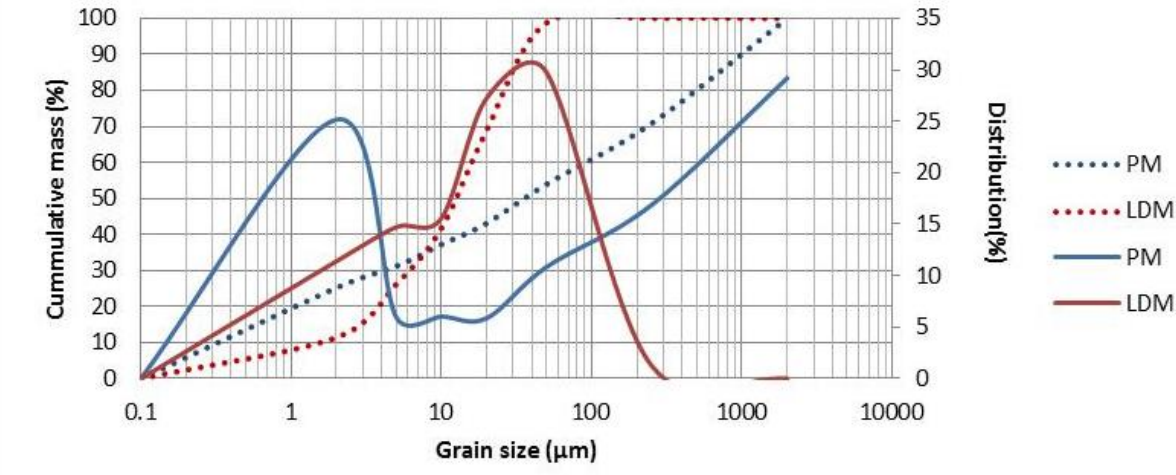

Fig. 5 PM and LDM grain size distribution and cumulative curves of sample SN12/90

typical in other samples of the group. Differences between the LDM and PM are also visible on SN11 and SN12 samples (*Fig. 5*), where the LDM measured lower sand content that can be related to the methodology of sedimentation processes formerly described. Errors during sand content calculations can be explained with the rough surface of grains that leads to the underestimation of sand and therefore overestimation of silt.

Analyzing the results of samples the distribution curves can be very different in certain cases, hence we analysed the result with another approach as well. For every sample we determined the amount of particles in the main fractions (clay, silt, sand) with the two methods, and then we examined the correlation between them. Taking the sediment categories into account, a high correlation was found between the LDM and PM sand, silt and clay content.

Table 1 Correlation of the main fractions determined by different methods

Size Class (µm)	Texture	Correlation factor	Linear regression
<2	Clay	0.928	Y=0.179·X+6.764
2-5	Silt	0.934	Y=1.036·X+16.841
5-10			
10-20			
>20	Sand	0.951	Y=0.482·X+28.663

Table 1 shows the linear function that is calculated by the amount of particles in the main fractions. Figure 6, 7, 8 shows how the values fit on the linear function per each main interval. There is no case where the values are outside of the confidence interval (95%). The correlation factor is significantly high concerning all main fractions, despite the difference between the dispersion curves based on the two methods. For exploring this difference, we examined the correlation as well in each interval (*Table 2*). The lowest correlation factors were experienced in case of coarse silt (10-20 µm) and the fine sand (20-50 µm) fractions. Based on linear regression, separation of the particles with 10-50 µm diameter is problematic. Several author found the results of this fraction doubtful, hence they expressed the silt fraction mathematically as a function of the known clay and silt fraction (Beuselnick, 1998; Buurman et al., 2001; Ferro and Mirabile, 2009; Di Stefano et al., 2010). The modification of the silt fraction's limit is suggested by Konert and Vandenberghe (1997) in order to correct the underestimated clay fraction.

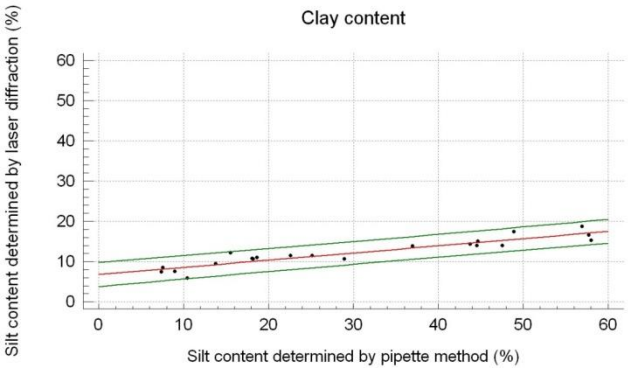

Fig. 6 Correlation between clay content determined by the two methods

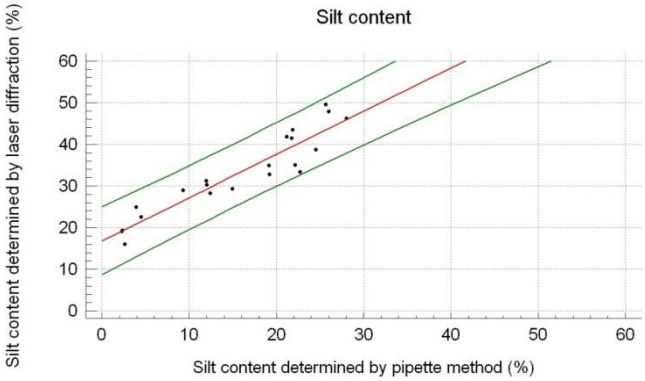

Fig. 7 Correlation between silt content determined by the two methods

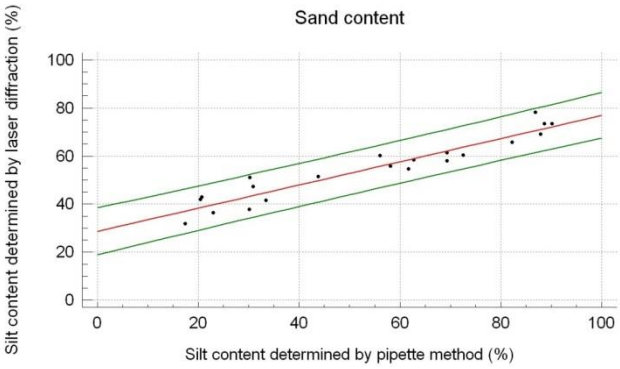

Fig. 8 Correlation between sand content determined by the two methods

CONCLUSION

In our research we examined the interchangeability of two different grain size measurement methods in case of unsorted fluvial samples. During the investigation we compared the cumulative and distribution

Table 2 Correlation between results received for different grain size classes

Size Class (µm)	Correlation factor	Linear regression
<2	0.929	Y=0.180·X+6.,667
2-5	0.921	Y=1.014·X+8.992
5-10	0.899	Y=0.974·X+8.336
10-20	0.676	Y=0.566·X+15.124
20-50	0.567	Y=0.447·X+16.871
>50	0.951	Y=0.483·X-3.551

curves produced by the two methods, studied the effect of clay, silt and sand abundance on distribution difference, and determined the correlation between results received for the main fractions (clay, silt, sand).

In case of high clay content, the LDM seems to underestimate the clay content in favor of the silt fraction. In the meantime the PM seems to overestimate clay and therefore the proportion of the silt fraction is significantly lower. The PM systematically overestimates the sand fraction compared to the LDM results. The LDM underestimates the sand fraction for the benefit of silt fraction because of the rough surface of the sand particles.

The interchangeability of the two methods in terms of the silt fraction is doubtful if distribution curves are considered. However, if the bulk values are calculated for the main fractions, differences are not significant. The lowest correlation factors were found in case of coarse silt (10-20 μm) and fine sand (20-50 μm). Therefore, the comparative analysis of particles with a 10-50 μm diameter is problematic.

Acknowledgement

The research was supported by the HU-RO/0901/266/2.2.2 project.

References

Beuselinck, L., Govers, G., Poesen, J., Degraer, G., Froyen, L. 1998. Grain-size analysis by lase diffractiometry: comparison with the sieve-pipette method. *Catena* 32, 193–208.

Blott, S.J., Pye, K. 2012. Particle size scales and classification of sediment types based on particle size distributions: review and recommended procedures. *Sedimentology* 59, 2071–2096.

Bork, H.R. 1989. Soil erosion during the past millennium in central Europe and its significance within the geomorphodynamics of the Holocene. *Catena Supplement* 15, 121–131.

Buurman, P., Pape, Th., Reijneveld, J.A., De Jong, F., Van Gelder, E. 2001. Laser-diffraction and pipette-method grain sizing of Dutch sediments: correlations for fine fractions of marine, fluvial and loess samples. *Netherlands Journal of Geosciences* 80 (2), 49–57.

De Vos, B.V. 2001. Relationship between soil textural fractions determined by sieve-pipette method and laser diffratiometry. *Wetenschappelijke Instelling van de Vlaamse Gemeenschap, Instituut voor Bosbouw en Wildbeheer*

Di Stefano, C., Ferro, V., Mirabile, S. 2010. Comparison between grain size analyses using laser diffraction and sedimentation methods. *Biosystems Engineering* 106, 205–215.

Ferro, V., Mirabile, S. 2009. Comparing particle size disturbation analysis by sedimentation and laser diffraction method. *Journal of Agricultural Engineering* 2, 35–43.

Fritsch 2009. Particle sizing - laser diffraction, *http://www.benelux-scientific.be/fileadmin/user_files/pdf/poederkarakterisatie/laserd/LASER_DIFFRACTION.pdf, available 2012–08-31*

Goossens, D. 2008. Techniques to measure grain-size distributions of loamy sediments: comparative study of ten instruments for wet analysis. *Sedimentology* 55, 65–96.

Hernadi, H., Makó, A., Kucsera, S., Szabóné Kele, G., Sisák, I. 2008. A talaj mechanikai összetételének meghatározása különböző módszerekkel (Determination of soil mechanical composition by different methods). *Talajvédelmi különszám*

Konert, M., Vandenberghe, J. 1997. Comparation of laser grain size analysis with pipette and sieve analysis: a solution for underestimation of the clay fraction. *Sedimentology* 44, 523–535.

Loizeau, J.L., Arbouille, D., Santiago, S., Vernet J.P. 1994. Evaluation of wide range laser diffraction grain size analyser for use with sediments. *Sedimentology* 41, 353–361.

Madarász, B., Jakab, G., Szalai, Z., Juhos, K. 2012. Lézeres szemcseösszetétel elemzés néhány előkészítő eljárásának vizsgálata nagy szervesanyag-tartalmú talajokon (Examination of sample preparation methods for the laser grain size analysis of soils with high organic matter content). *Agrokémia és talajtan* 61 (2), 381–398.

McCave, I.N., Bryant, R.J., Cool, H.F., Coughanowr, C.A. 1986. Evaluation of laser-diffraction-size analyser for use with natural sediments. *Journal of Sedimentary Petrology* 56, 561–564.

Murray, M.R. 2002. Is laser particle size determination possible for carbonate-rich lake sediments? *J. Paleolimnol.* 27, 173–183.

Ryzak, M., Bieganowski, A. 2011. Methodological aspects of determining soil particle-size distribution using the laser diffraction method. *Journal of Plant Nutrition and Soil Science* 17, 624–633.

Xu, R., Di Guida, O.A. 2003. Comparison of sizing small particles using different technologies. Powder. *Technology* 132, 145–153.